

**ESTABLISHING THE ROLE OF *PEA3*, AN ETS FAMILY TRANSCRIPTION
FACTOR, DURING MOUSE EMBRYONIC DEVELOPMENT.**

By

MICHAEL A. LAING, B.Sc.

A Thesis

Submitted to the School of Graduate Studies

in Partial Fulfilment of the Requirements

for the Degree

Doctor of Philosophy

McMaster University

(c) Copyright by Michael A. Laing, October 1998



**National Library
of Canada**

**Acquisitions and
Bibliographic Services**

**395 Wellington Street
Ottawa ON K1A 0N4
Canada**

**Bibliothèque nationale
du Canada**

**Acquisitions et
services bibliographiques**

**395, rue Wellington
Ottawa ON K1A 0N4
Canada**

Your file Votre référence

Our file Notre référence

The author has granted a non-exclusive licence allowing the National Library of Canada to reproduce, loan, distribute or sell copies of this thesis in microform, paper or electronic formats.

The author retains ownership of the copyright in this thesis. Neither the thesis nor substantial extracts from it may be printed or otherwise reproduced without the author's permission.

L'auteur a accordé une licence non exclusive permettant à la Bibliothèque nationale du Canada de reproduire, prêter, distribuer ou vendre des copies de cette thèse sous la forme de microfiche/film, de reproduction sur papier ou sur format électronique.

L'auteur conserve la propriété du droit d'auteur qui protège cette thèse. Ni la thèse ni des extraits substantiels de celle-ci ne doivent être imprimés ou autrement reproduits sans son autorisation.

0-612-50996-6

Canada

**ESTABLISHING THE ROLE OF *PEA3*, AN ETS FAMILY TRANSCRIPTION
FACTOR, DURING MOUSE EMBRYONIC DEVELOPMENT.**

DOCTOR OF PHILOSOPHY (1998)
(Biology)

McMASTER UNIVERSITY
Hamilton, Ontario, Canada

TITLE: Establishing the role of *Pea3*, an ETS family
transcription factor, during mouse embryonic
development.

AUTHOR: Michael A. Laing, B.Sc. (McMaster University)

SUPERVISOR: Professor J.A. Hassell

NUMBER OF PAGES: xix, 273

ABSTRACT

PEA3 is an ETS family transcription factor and the founding member of the PEA3 group which consists of two other PEA3 related proteins, ERM and ER81. They share ~95 % amino acid identity within their DNA binding domains and ~50 % a.a. identity outside of this region. The goal of this study was to identify the role of PEA3 during mouse embryogenesis. In order to achieve this objective, two complementary approaches were employed.

Firstly, the embryonic expression pattern of PEA3 was determined by whole mount *in-situ* hybridization from mid-gastrulation through early organogenesis. The *Pea3* mRNA was detected in tissues derived from all three germ layers. The sites of expression correlated with regions of embryonic induction, a process governing tissue differentiation, morphogenesis and organogenesis. This study revealed that PEA3 was expressed during gastrulation, patterning of the CNS, neural differentiation, craniofacial development, muscle development, kidney development and limb development.

Secondly, we employed a gene knock-out strategy to define the essential functions of PEA3 either during embryogenesis and within the adult mouse. *Pea3* proved dispensable for embryogenesis. Expression analysis of both ERM and ER81 revealed that ERM may have provided redundant functions in *Pea3* null embryos. However, the male null mice were infertile. Furthermore, female null mice exhibited vastly reduced arborization of the ductal tree within the developing mammary gland. Hence, this study revealed that PEA3 was required for male fertility and ductal morphogenesis of the mammary gland.

ACKNOWLEDGMENTS

I would like to thank the members of my committee, Dr. R. Jacobs, Dr. C. Nurse and Dr. J. Hassell for their guidance and support. I would like to extend my thanks to Dr. W. Muller and Dr. M. Rudnicki for their support and their intellectual contributions to this body of work. I would also like to thank Dr. C. Lobe for her assistance with the *in-situ* hybridization experiments. I have had great lab mates in the past and in the present; their intellectual input into this project and their buoyant personalities have made for a great lab atmosphere. A sincere thanks to all of you. Lastly, I would like to thank Dr. A. Dingle for introducing me to the world of embryonic development and his mentorship throughout my days here at McMaster University.

I have had the unconditional respect and support of my father Graham, my mother Elaine, my brother Stephen and my sister Lisa throughout my life. Growing up in that atmosphere has allowed me to become the person that I am today. To all of the members of the large and ever growing Laing and Taylor clans down home, thank-you; all of your support has been instrumental in shaping my life. I am a lucky person in that I have far too many friends to mention here; but rest assured that each and every one of you made a significant contribution to this body of work. I am eternally grateful.

DEDICATION

During my tenure as a graduate student, I lost two people that I loved very dearly. Both of them passed away well before their time. This thesis as well as any future contributions that I may be fortunate enough to make in the field of cancer research are dedicated to their memories:

To my loving mother F. Elaine Laing, and to a wonderful friend

Bryn Miranda.

THE MUSIC

IN MY HEART I BORE

LONG AFTER

IT WAS HEARD NO MORE

-WORDSWORTH

CONTRIBUTIONS BY OTHERS

Figure 1.1 The amino acid sequence alignment was performed by Jane Barrett, a technician in this laboratory. She designed this figure to illustrate the results from the above alignment.

Figure 1.2 This figure was designed by Jane Barrett. It is based upon the data in Smillie, 1993. Exon 1' was identified by Dr. Ji-Hou Xin, a research associate in this laboratory. This exon was not present in the published PEA3.9 cDNA (Xin et al. 1992).

Figure 3.1 A. The Northern blot hybridization shown in this panel was performed by Dr. Malcolm Trimble, a former post-doctoral fellow in this laboratory. I isolated the total RNA samples used in this experiment.

Figure 3.16 A,B,D & E; Figure 3.17. These whole mount *in-situ* hybridizations were performed and photographed by Jane Vetiska, a former summer student in the laboratory. I isolated, fixed and dehydrated the embryos used in these experiments.

Figure 4.1 C. The blastocyst injections of the D.D1 ES cell line were carried out by Lisa Tabek, a former technician in the laboratory of Dr. M.A. Rudnicki. I would also like to acknowledge the blastocyst injection efforts of Dr. M.A. Rudnicki and Rod Hardy.

Figure 4.2 A. The riboprobe vector illustrated in this figure panel was constructed by Dr. Ji-Hou Xin, a research associate in the laboratory.

Figure 4.2 C. The embryonic fibroblasts used in this experiment were derived by Laura Hastings, a technician in this laboratory. The Western blot was performed by Dr. Richard Tozer, a former post-doctoral fellow in this laboratory.

Table 4.5 and Table 4.7. The *in-vitro* fertilization analysis was carried out by our collaborators at the University of Virginia, Dr. Barry T. Hinton, Jaquelyn Labus and Scott Coonrod. They were also responsible for analyzing the blood hormone levels by radio-immuno assay.

Figure 4.7. The observation of the mammary gland branching morphogenesis defect in the D.D1 mouse line was made by Lesley MacNeil, a graduate student in the laboratory. She performed and photographed the whole mount mammary gland analyses shown in this figure.

TABLE OF CONTENTS

Abstract.....	iii
Acknowledgments.....	iv
Dedication.....	v
Contributions of Others.....	vi
Table of Contents.....	viii
List of Figures.....	xvi
List of Tables.....	xix
CHAPTER 1: INTRODUCTION.....	1
1.1 Developmental Biology, 'Molecular Determinants' and Transcription Factors.....	
1.2 Regulation of Transcription Factor Activity.....	6
1.2.1 The Regulation of DNA Binding Activity by Phosphorylation.....	8
1.2.2 The Regulation of Transactivation Potential by Phosphorylation.....	9
1.2.3 The Regulation of Nuclear Localization by Phosphorylation.....	10
1.3 The Basic Mechanisms of Growth Factor Mediated Signal Transduction.....	11
1.3.1 Activation of Growth Factor Receptors.....	12
1.3.2 The RAS Mediated MAP Kinase Signalling Cascade.....	13

1.3.3	The Phosphatidylinositol 3' Kinase (PI3K) Mediated Signalling Cascade....	14
1.3.4	The Phospholipase C- γ (PLC γ) Mediated Signalling Cascade.....	15
1.3.5	Signalling Cascades Mediated by Cytoplasmic Tyrosine Kinases: An Alternative to Receptor Tyrosine Kinase Mediated Signal Transduction....	18
1.4	The Discovery of the <i>ETS</i> Family of Transcription Factors.....	20
1.4.1	The Members of the <i>ETS</i> Family of Transcription Factors.....	21
1.4.2	Mutations Involving <i>ETS</i> Genes are Implicated in Human Cancers.....	22
1.4.3	<i>ETS</i> Genes Play a Role in Regulating Embryonic Development.....	24
1.4.4	The PEA3 Group is a Subfamily within the of <i>ETS</i> Gene Family.....	26
1.4.5	The PEA3 Group Genes are Developmentally Regulated.....	27
1.5	The PEA3 Transcription Factor.....	30
1.5.1	The Molecular Organization and Chromosomal Localization of the <i>Pea3</i> Gene.....	30
1.5.2	PEA3 may be Involved in the Induction and Progression of tumorigenesis.	
1.5.3	PEA3 has been Implicated in Affecting Tumor Cell Invasion and Metastasis.	
1.5.4	Regulation of the Transcriptional Activity of the PEA3 Protein.....	36
1.6	Experimental Rationale.....	39

CHAPTER 2: MATERIALS AND METHODS.

2.1	Preparation of DNA Probes.....	42
2.2	<i>In-Vitro</i> Transcription of Riboprobes for RNase Protection Analysis.....	44
2.3	Southern Blot Analysis.....	45
2.4	Extraction of Total RNA from Tissue.....	47
2.5	Northern Blot Analysis.....	48
2.6	RNase Protection Analysis.....	49
2.7	Restriction Digestion of DNA.....	50
2.8	DNA Cloning Methodology.....	50
2.9	Embryo Dissection and Fixation for Whole Mount <i>In-Situ</i> Hybridizations.....	53
2.10	Construction of PEA3 Specific Riboprobes for use in Whole Mount <i>In-Situ</i> Hybridizations.....	54
2.11	<i>In-Vitro</i> Transcription of Riboprobes for Whole Mount <i>In-Situ</i> Hybridizations...	57
2.12	Whole Mount <i>In-Situ</i> Hybridization.....	58
2.13	Histological Preparation of Post-Whole Mount Embryos.....	61
2.14	Isolation of Genomic PEA3 Clones from an 129/sv Lambda Phage Library.....	62
2.15	Construction of a Targeting Vector Designed to Generate a Null Allele at the <i>Pea3</i> Locus.....	70
2.16	Embryonic Stem Cell Culture.....	78
2.17	Electroporation of Embryonic Stem Cells.....	80
2.18	Blastocyst Injection of Embryonic Stem Cells.....	82

2.19	Genotype Analysis of Mouse Tail DNA.....	83
2.20	Histological Preparation of Organs and Tissues.....	84
2.22	<i>In-Vitro</i> Fertilization Analysis.....	85
2.22	<i>In-Vivo</i> Fertilization Analysis.....	86
2.23	Betagalactosidase Assays for Epididymis Whole Mounts.....	87
2.24	Determination of Hormone Concentrations by Radio Immuno-Assay (RIA).....	87
2.25	Expression of PEA3 in Various Embryonic Fibroblast Cell Lines.....	88
2.26	Whole Mount Mammary Gland Preparations.....	89

**CHAPTER 3: EXPRESSION PATTERN OF THE PEA3 GROUP mRNAs
DURING MOUSE EMBRYONIC DEVELOPMENT.**

3.1	Introduction.....	90
3.2	Results.	
3.2.1	PEA3 mRNA is Expressed Throughout the Post Implantation Stages Mouse Embryonic Development.....	93
3.2.2	PEA3 Expression Pattern in the Gastrulating Embryo (~ 7.0 to 7.5 d.p.c.).....	94
3.2.3	PEA3 Expression Pattern in the 8.0 d.p.c.(3-5 somite pairs) Embryo.	
3.2.4	PEA3 Expression Pattern in the 9.0 and 9.5 d.p.c. Embryo....	100
3.2.5	PEA3 Expression Pattern in the 10 and 10.5 d.p.c. Embryo.....	105
3.2.6	PEA3 Expression Pattern in the 11.0 and 11.5 d.p.c. Embryo.....	111
3.2.7	PEA3 Expression Pattern in the 12.0 through 12.75 d.p.c. Embryo.	
3.2.8	PEA3 Expression Pattern in the 13.0 d.p.c. Embryo.....	115
3.2.9	Expression pattern of ERM and ER81 in the gastrulating embryo (~ 7.0 to 7.5 d.p.c.).....	118
3.2.10	Expression Pattern of ERM and ER81 in the 8.5 d.p.c. Embryo.	
3.2.11	Expression Pattern of ERM and ER81 in the 9.0 d.p.c. Embryo.	
3.2.12	Expression Pattern of ERM and ER81 in the 10.5 d.p.c. Embryo.	
3.2.13	Expression Pattern of ERM and ER81 in the 11.5 d.p.c. Embryo.	

3.2.14	Expression Pattern of ERM and ER81 in the 12 d.p.c. Embryo.	
3.2.15	Expression Pattern of ERM and ER81 in the 13 d.p.c. Embryo.	
3.3	Discussion.	
3.3.1	PEA3 expression during the pre-implantation stages of mouse development.....	141
3.3.2	PEA3 and ERM may play a role in effecting gastrulation.....	145
3.3.3	The PEA3 group members are expressed in branchial arch mesenchyme and may contribute to craniofacial development.....	150
3.3.4	PEA3 and ERM are expressed in the neural ectoderm of the mesencephalon-metencephalon (mes-met) boundary.....	153
3.3.5	PEA3 is expressed in somatic motor neurons that innervate the limb muscles.....	155
3.3.6	PEA3 and ERM are expressed in the somites and may play a role in affecting skeletal muscle development.....	158
3.3.7	PEA3 and ERM may play a role in affecting the early morphogenesis of the urogenital system.....	162
3.3.8	PEA3 and ERM are expressed in the developing limb.....	165

CHAPTER 4: GENETIC ANALYSIS OF PEA3 FUNCTION.

4.1	Introduction.....	171
4.2	Results.	
4.2.1	Generation and Isolation of Heterozygous Embryonic Stem (ES) Cell Clones Harbouring a Deletion at the <i>Pea3</i> Genomic Locus.....	175
4.2.2	Establishing a <i>Pea3</i> Knock Out Mouse Line.....	176
4.2.3	PEA3 +/- and -/- Mice Harbour the Predicted Deletion Mutation at both the RNA and Protein Levels.....	179
4.2.4	<i>Pea3</i> is not Essential for Embryonic Development.....	180
4.2.5	Male <i>Pea3</i> null Mice are Infertile.....	185
4.2.6	PEA3 mRNA is Expressed in both the Testes and Epididymides Prior to Sexual Maturity.....	185
4.2.7	Histology of the Testes and Epididymides from <i>Pea3</i> Null Mice Appears Normal.....	188
4.2.8	Sperm Derived from <i>Pea3</i> Null Males is Functional <i>In-Vitro</i>	198
4.2.9	<i>In-Vivo</i> Fertilization Analysis.....	198
4.2.10	<i>Pea3</i> null mice exhibit a defect in the branching morphogenesis of the developing mammary gland.....	203
4.2.11	Expression Pattern of the ERM mRNA in <i>Pea3</i> null Embryos....	208

4.3	Discussion.	
4.3.1	<i>Pea3</i> is not required for embryonic development.....	211
4.3.2	<i>Pea3</i> is required for male fertility.....	212
4.3.3	PEA3 affects ductal morphogenesis within the developing mammary gland.....	221
CHAPTER 5:	REFERENCES.....	228

LIST OF FIGURES

CHAPTER 1

Figure 1.1 Alignment of the amino acid sequences of the PEA3 group proteins.

Figure 1.2 The molecular organization of the *Pea3* gene, the *Pea3* mRNA, and the PEA3 protein.

CHAPTER 2

Figure 2.1 Construction of PEA3 specific riboprobes for use in whole mount *in-situ* hybridizations.

Figure 2.2 Mapping the PEA3 positive lambda phage genomic inserts to the *Pea3* Gene.

Figure 2.3 Construction of the plasmid pBSN93, containing the left flank of a targeting construct for the *Pea3* Gene.

Figure 2.4 Construction of the plasmid pSLSN31, containing the right flank of a targeting construct for the *Pea3* Gene.

Figure 2.5 Ligation strategy used to construct the targeting vector pBSneo9331, designed to generate a null allele at the *Pea3* locus.

CHAPTER 3

- Figure 3.1** Analysis of PEA3 mRNA expression during the post-implantation stages of murine embryonic development.
- Figure 3.2** Expression pattern of the PEA3 mRNA in the 7/7.5 d.p.c. embryo.
- Figure 3.3** Expression pattern of the PEA3 mRNA in the 7.5 d.p.c. embryo.
- Figure 3.4** Expression pattern of the PEA3 mRNA in the 8.0 d.p.c. (3-5 somite pairs) embryo.
- Figure 3.5** Expression pattern of the PEA3 mRNA in the 9.0 d.p.c. embryo.
- Figure 3.6** Expression pattern of the PEA3 mRNA in the 9.5 d.p.c. embryo.
- Figure 3.7** Expression pattern of the PEA3 mRNA from 10.0 through 11.5 d.p.c.
- Figure 3.8** Expression pattern of the PEA3 mRNA from 12.0 through 12.75 d.p.c.
- Figure 3.9** Expression pattern of the PEA3 mRNA in the 13.0 d.p.c. embryo.
- Figure 3.10** Expression pattern of the ERM and ER81 mRNAs in the 7.0 d.p.c embryo.
- Figure 3.11** Expression pattern of the ERM and ER81 mRNAs in the 7.5/8.0 d.p.c. embryo.
- Figure 3.12** Expression pattern of the ERM and ER81 mRNAs in the 8.5 d.p.c. embryo.
- Figure 3.13** Expression pattern of the ERM and ER81 mRNAs in the 9.0 d.p.c. embryo.
- Figure 3.14** Expression pattern of the ERM and ER81 mRNAs in the 10.5 d.p.c. embryo.
- Figure 3.15** Expression pattern of the ERM and ER81 mRNAs in the 11.5 d.p.c. embryo.

Figure 3.16 Expression pattern of the ERM and ER81 mRNAs in the 12.5 d.p.c. embryo.

Figure 3.17 Expression pattern of the ERM and ER81 mRNAs in the 13 d.p.c. embryo.

Figure 3.18 Development of the murine inner cell mass (ICM) and blastocyst.

CHAPTER 4

Figure 4.1 Generation of ES cell lines and a mouse line targeted at the *Pea3* genomic locus.

Figure 4.2 Molecular characterization of the *Pea3* null allele.

Figure 4.3 RNase protection analysis of various organs from juvenile mice and the major regions of the adult epididymis.

Figure 4.4 Histology of the testes from *+/+* and *-/-* mice.

Figure 4.5 Whole mount β -galactosidase staining of *+/+* and *-/-* epididymides.

Figure 4.6 Histology of the epididymides from *+/+* and *-/-* mice.

Figure 4.7 Whole mount mammary gland preparations from 6 week old virgin females from the D.D1 mouse line.

Figure 4.8 Expression pattern of the ERM mRNA in *Pea3* null embryos.

LIST OF TABLES

CHAPTER 4

- Table 4.1 Analysis of Genotype Frequencies.
- Table 4.2 Comparison of average mass of $+/+$ vs $-/-$ mice by difference of means.
- Table 4.3 Fertility of the outbred D.D1 PEA3 mouse line.
- Table 4.4 Fertility of the inbred D.D1/sv PEA3 mouse line.
- Table 4.5 *In-vitro* fertilization analysis.
- Table 4.6 *In-vivo* fertilization analysis.
- Table 4.7 Mean hormone concentrations for the mice used in the *in-vitro* fertilization analysis.

CHAPTER 1

INTRODUCTION

1.1 Developmental biology, 'molecular determinants' and transcription factors.

Developmental biologists have been attempting to define the basic mechanisms that regulate fertilization, embryogenesis and the growth of an organism. How does a single cell, the zygote, initiate cell division and then reorganize itself to allow for pattern formation, cellular differentiation and organogenesis to give rise to a multicellular organism? August Weismann was the first to state that the ovum and the spermatozoa each contributed one half of an organism's 'inherited traits'. He put forth the idea that as a cell divided, its two daughter cells acquired a different array of 'nuclear determinants' which in turn governed a cell's phenotype. This was one of the earliest theories of cellular differentiation (Weismann, 1892; 1893; reviewed by Gilbert, 1988).

Subsequently, Sven Horstadius performed a classic series of experiments using the sea urchin embryo as an experimental system. The eight cell morula consisted of four animal pole blastomeres sitting on top of four vegetal pole blastomeres. The morula was first divided equatorially into one group of four animal cells and one group of four vegetal cells. These groups were then allowed to further develop. The animal cell clusters formed ciliated balls of epidermal cells; the vegetal cell clusters developed into complete embryos but with enlarged gut structures. Hence, animal cells and vegetal cells did not demonstrate

equal developmental potential. This finding suggested that embryos developed by a mosaic mechanism: As cells divide, they acquire different fates to give rise to the specific cell types that form the adult organism.

The morula was then divided meridionally into two groups, each consisting of two animal and two vegetal cells. In this case, each group developed into normal sea urchins. Hence, these two cell groups demonstrated an equal developmental potential. This result suggested that embryos developed by a regulative mechanism where cells constantly communicated with each other during embryogenesis to insure the complete development of the adult organism. Horstadius demonstrated that two morphogenetic gradients existed in the sea urchin morula. One gradient ran from the animal pole to the vegetal pole while the other ran in the opposite direction. He believed that these gradients established the animal-vegetal (AV) axis in the early morula and that development then proceeded around this axis guiding embryogenesis (Horstadius, 1939; reviewed by Gilbert, 1988).

The theories of Weismann and Horstadius provided the foundation for modern developmental biology: morphogenetic determinants were organized into gradients within a developing embryo establishing the early embryonic axes. These axes then provided the spatial framework around which the rest of the developmental program proceeded. The existence of 'nuclear determinants' or morphogens has been confirmed. Furthermore, specific determinants do set up gradients within the early embryo to establish the early body axes. These findings are best illustrated in the following example.

Bicoid is a specific embryonic mutation observed in the fruit fly *Drosophila melanogaster*. The embryo lacks a head and thorax while displaying a duplicated telson,

a posterior structure, at either end of the embryo. This phenotype resulted from a mutation in a specific gene named *bicoid*. Cytoplasm taken from the anterior region of a wild-type embryo was microinjected into one end of a *bicoid* embryo and subsequently rescued the mutant phenotype (Frohnhofer and Nusslein-Volhard, 1986). *In-situ* hybridization studies revealed that the *bicoid* mRNA was expressed in the nurse cells surrounding the oocyte and subsequently transported into the future anterior region of the oocyte (Berleth et al. 1988). The fact that this mRNA was imparted to the embryo by the mother characterized *bicoid* as a **Maternal Effect Gene**.

It was later demonstrated that the *bicoid* mRNA was translated during early embryonic cleavage. Furthermore, the *bicoid* protein established a concentration gradient. It was highly concentrated in the anterior end of the syncytium and became more diffuse towards the posterior end (Driever and Nusslein-Volhard, 1988). Anterior structures formed where the concentration of *bicoid* was highest in turn suggesting a function for this protein. These findings characterized the *bicoid* protein as a morphogen.

The *bicoid* protein was shown to possess site specific DNA binding activity. This activity was imparted to the protein by a region conserved throughout evolution referred to as the homeodomain or homeobox. Furthermore, once bound to DNA, the protein was able to activate the transcription of a target gene (reviewed by St. Johnston and Nusslein-Volhard, 1992). Hence, the *bicoid* protein was also a **transcription factor** capable of directly effecting the mRNA expression (transcription) of other genes.

Similar studies carried out on many different embryonic mutations in *Drosophila* led to the discovery of a complex genetic regulatory hierarchy. This

hierarchy regulated the establishment of the early embryonic axes and controlled the segmentation of the embryonic body along these defined axes. Furthermore, it regulated the definition of the morphological identities of each characteristic segment.

The first tier in this hierarchy is represented by the **maternal effect genes**. They function to polarize the oocyte and in turn the early embryo. Furthermore, they regulate the expression of specific genes within the next hierarchical tier. The following three tiers control the segmentation of the embryo along the AP axis. The **gap genes** affect the expression of the **pair rule genes** which in turn affect the expression of the **segment polarity genes**. This leads to the expression of the genes within the final tier in the hierarchy, the **homeotic selector genes**. Each hierarchical tier consists of a number of genes. Specific genes within each tier can then activate or repress the expression of selected genes within the other tiers (reviewed by Gaul and Jackle, 1990; Gurdon, 1992).

Many of the genes within this hierarchy were characterized as site specific DNA binding proteins that directly regulated the transcription of other genes within the hierarchy. These transcription factors all harboured a conserved homeobox DNA binding domain (Scott and Weiner, 1984). The conserved sequences within the homeodomain allowed for the jump from the fruit fly as a model embryonic system to the mouse. Using the *Drosophila* homeodomain sequences as probes, a family of murine homeobox containing genes, the *Hox* genes, was identified (McGinnis and Krumlauf, 1992).

The *Hox* genes have been mapped to four multigene clusters, the *HoxA*, *HoxB*, *HoxC* and *HoxD* clusters. Interestingly, their genomic organization was found to be conserved with that of their *Drosophila* ancestors (Graham et al. 1989). Furthermore, studies demonstrated that the *Hox* proteins were also site specific DNA binding proteins which activated and/or repressed the transcription of other *Hox* genes within the four clusters as well as other target genes.

In-situ hybridization studies in mouse embryos revealed that the *Hox* genes were expressed in the brain and neural tube with overlapping patterns in the posterior regions of the embryo; however, they exhibited gene specific rostral boundaries (Kessel and Gruss, 1990; McGinnis and Krumlauf, 1992). It now appears that the *Hox* genes define the AP axis of the early mouse embryo from the hindbrain to caudal regions. Furthermore, they define the AP axis of smaller developmental fields, such as the limb field, in the later stages of development (Johnson and Tabin, 1997).

The embryonic mutations in the fruit fly provided a powerful means of identifying and cloning developmentally regulated genes in both the invertebrate and mammalian systems. Studies in both systems have identified an essential role for transcription factors in the regulation of embryonic development. Transcription factors regulate gene expression by binding to their cognate DNA binding sites present in the enhancer and proximal promoter elements of their target genes. At this point, they can either activate or repress the transcription of a given target gene (Hoey and Levine, 1988; Han et al. 1989; Driever and Nusslein-Volhard, 1989; Mitchell and Tjian, 1989; Levine and Manley, 1989).

The expression of a defined group of transcription factors within a cell would then affect the transcription of a defined group of target genes within that cell. Daughter cells expressing different transcription factor arrays would then differentiate from one another. Hence, transcription factors appear to function as Weismann's 'nuclear determinants' or Horstadius' morphogens. One is now faced with the following question: If transcription factors guide embryogenesis by regulating target gene expression, then by what means are the activities of these transcription factors regulated ?

1.2 Regulation of transcription factor activity.

Transcription factors are proteins that bind to specific DNA sequences within the regulatory regions of target genes and subsequently activate or repress their transcription. The DNA binding activity and the transactivation activity often reside in separate domains within the protein. Therefore a transcription factor harbours two activities, a sequence specific DNA binding activity and a transactivation activity (Keegan et al. 1986; Ptashne, 1988).

Transcription factor families are generally defined by the presence of a conserved DNA binding domain as is the case with the *Hox* genes. Many types of DNA binding domains have now been identified including the helix-loop-helix (HLH), the helix-turn-helix (HTH), the zinc finger, the basic leucine zipper (bZIP), the homeodomain, and the steroid receptor DNA binding domain (reviewed by Pabo and Sauer, 1992).

Transcriptional activation domains are not well conserved; however, there are features that characterize these domains. They are often rich in particular amino acid (a.a.) residues including acidic regions containing glutamic and aspartic acid, glutamine rich regions and proline rich regions (Ptashne, 1988). Transactivation domains are thought to function by associating either directly or indirectly with proteins in the transcription initiation complex.

These interactions are believed to affect the dissociation of the RNA polymerase from the initiation complex to initiate RNA elongation (Ptashne and Gann, 1990; Lewin, 1990; Greenblatt, 1991). Recent studies demonstrated that specific transcription factors were capable of associating directly or indirectly with the TATA box binding protein (TBP), a protein present in the transcription initiation complex (Stringer et al. 1990; Crowley et al. 1993; Ruppert et al. 1993; Emili et al. 1994; Xiao et al. 1994).

Transcription factors, like all proteins, are translated in the cell cytoplasm. The mechanism by which they activate target gene transcription requires that they be translocated to the cell nucleus in order that they can bind to their cognate DNA binding sequences. Hence, transcription factor proteins have a third biological property, nuclear localization. All three of their biological activities represent potential targets whereby transcription factor activity may be regulated.

The expression of genes in response to various extracellular stimuli does not require *de novo* protein synthesis. Hence, the primary response transcription factors are likely regulated by a post-translational mechanism. Many of the stimuli that induce target gene expression to affect a particular cellular response also activate intracellular

protein kinase activity. Kinases are enzymes that catalyze the addition of a phosphate group to particular amino acid side chains on target proteins. Recent studies have confirmed that transcription factor activity is regulated by phosphorylation. Furthermore, this covalent modification can affect their ability to bind DNA, activate transcription, and translocate to the nucleus (Hunter and Karin, 1992, Hunter, 1997).

1.2.1 The regulation of DNA binding activity by phosphorylation.

The DNA binding activity of transcription factors can be regulated either positively or negatively by phosphorylation. Studies to date indicate that the later effect is more common. A transcription factor may harbour phosphorylation consensus sites either close to or within its DNA binding domain. Phosphorylation may effectively mask the amino acid side chains that are responsible for making base specific contacts within the DNA binding site. The phosphate groups may also contribute to electrostatic repulsion between the DNA binding domain and the phosphate backbone of the DNA binding site.

Alternatively, phosphorylation may affect a conformational change within the protein such that the DNA binding domain becomes masked either by another region within the protein or by an associated protein. Examples of transcription factors that are negatively regulated by the above mechanisms include c-Jun, c-Myb, Oct-1, Pit-1, Myogenin and MyoD. Stimulation of DNA binding activity by phosphorylation is rare; however, serum response factor (SRF) is one transcription factor regulated in this manner (reviewed by Hunter and Karin, 1992).

1.2.2 The regulation of the transactivation potential by phosphorylation.

The transactivation potential of a transcription factor can also be regulated either positively or negatively by phosphorylation. In this case, the former effect is more predominant. Regulation may be affected by a number of different mechanisms. Firstly, phosphorylation may increase the affinity of an activation domain for its target protein present in the transcriptional initiation complex. Secondly, phosphorylation may increase the domains affinity for a specific bridging protein or co-factor that in turn contacts a target protein in the initiation complex.

Thirdly, phosphorylation may affect the dissociation of a negative regulatory protein from the activation domain in turn allowing the domain access to its targets. Lastly, phosphorylation may relieve intramolecular repression to affect transactivation. The above mechanisms are not mutually exclusive. Studies have revealed that individual transcription factors can be regulated by any one of the above mechanisms. A number of transcription factors exhibit positive regulation of their transactivation potential as a result of phosphorylation including CREB, c-Jun, C/EBP β and c-Myc. A limited number of factors are negatively regulated in this manner such as the yeast transcription factor ADR1. In this case, phosphorylation of the transactivation domain inhibits its association with its target protein in the initiation complex (reviewed by Hunter and Karin, 1992).

1.2.3 The regulation of nuclear localization by phosphorylation.

All nuclear proteins, including transcription factors, are first translated in the cytoplasm and then translocated to the nucleus. Two general mechanisms are employed to affect nuclear translocation. Firstly, many proteins destined for the nucleus harbour a small domain rich in lysine and arginine residues that functions as a nuclear localization signal (NLS) (reviewed by Garoff, 1985). The NLS was first characterized in the SV40 large T antigen (LTA), a protein involved in viral DNA replication (Kalderon et al. 1984). When the SV40 LTA NLS was attached to a heterologous cytoplasmic protein, the NLS affected its translocation to the nucleus (Richardson et al. 1986).

Hence, phosphorylation of consensus sites near or within the NLS of a given protein may affect its ability to function. Phosphorylation at a consensus Cdc2 site near the NLS of the yeast transcription factor *SWI5* prevented its translocation to the nucleus. In this case a phosphatase would be required to effect nuclear translocation of *SWI5*. Interestingly, phosphorylation of a casein kinase II (CKII) site near the SV40 LTA NLS increased its rate of translocation to the nucleus (reviewed by Hunter and Karin, 1992).

Secondly, phosphorylation can regulate the association of inhibitory proteins with the NLS regions of transcription factors. Studies demonstrated that the transcription factors NF- κ B and c-Rel were retained in the cytoplasm in unstimulated cells, but were subsequently translocated to the nucleus upon TPA stimulation

(Baeuerle and Baltimore, 1988). Later studies demonstrated that the NLS of both NF- κ B and c-Rel were targets for a regulatory protein I κ B/MAD3.

When these transcription factors were complexed with I κ B, they were retained in the cytoplasm but upon stimulation, the complexes dissociated and the proteins translocated to the nucleus (Beg et al. 1992; Zabel et al. 1993). The investigators proposed a model whereby phosphorylation of I κ B by either protein kinase C (PKC) or protein kinase A (PKA) affected its dissociation from these transcription factors and exposed their NLSs (reviewed by Hunter and Karin, 1992).

1.3 The basic mechanisms of growth factor mediated signal transduction.

Genetic regulatory hierarchies govern axes determination, segmentation, pattern formation, proliferation and differentiation during embryogenesis. They consist of transcription factors that regulate the expression of specific target genes which in turn effect the desired morphogenetic responses. The activity of a transcription factor can be regulated by a number of mechanisms. Firstly, it can be regulated at the level of transcription. In this case, once its mRNA is produced, the protein will be translated and subsequently translocated to the nucleus where it will become active. Secondly, their activity can be regulated by phosphorylation (section 1.2). Lastly, they can be regulated by a combination of these two mechanisms. The important point is that a transcription factor must be located within the nucleus in order to regulate the transcription of its target genes.

However, the signals that influence transcription factor activity within the nucleus are initially extracellular. The question then arises as to how an extracellular signal can travel to the appropriate transcription factor in the nucleus to elicit a specific response. The signalling pathways that link extracellular signals with the appropriate effector proteins in the nucleus are referred to as signal transduction pathways. In this section, I will outline the basic pathways used by secreted or membrane bound growth factors to regulate transcription factor activity.

1.3.1 Activation of growth factor receptors.

The initial signal or growth factor can be secreted or membrane bound. Growth factors have specific receptors located within the plasma membrane of the target cell. Generally, growth factor receptors are members of large families of related receptors. They are composed of three domains, the extracellular domain, the transmembrane domain and the cytoplasmic domain. The extracellular domain is a growth factor specific binding domain. Upon ligand binding, the receptors either homodimerize or heterodimerize with related receptors through their transmembrane domains.

This complex is thought to effect a conformational change within the receptors cytoplasmic domain. The cytoplasmic region of many growth factor receptors contains a tyrosine kinase catalytic domain. Receptor dimerization activates the kinase which results in the phosphorylation of specific tyrosine residues on the cytoplasmic tails of the receptors (Carraway and Cantley, 1994; Hynes and Stern, 1994). Hence, the first stage in signalling includes the formation of a ligand/receptor complex which leads to

the phosphorylation of specific tyrosine residues on the receptor's cytoplasmic tail. In this form, the receptor is said to be activated.

At this stage, a number of cytoplasmic proteins and enzymes are recruited to and bind with the receptor's cytoplasmic domain. Importantly, these proteins bind to the phosphotyrosines on the activated receptor. Proteins that bind phosphotyrosine do so through a conserved region, the src homology 2 (SH2) domain (Pawson and Gish, 1992). Variability in the amino acid sequence surrounding a phosphotyrosine as well as within a given SH2 domain provides sequence specificity for this interaction (Fantl et al. 1992; Pawson and Gish, 1992). Hence, specific SH2 containing proteins bind with specific phosphotyrosines on the receptors' cytoplasmic tail. Each receptor bound SH2 protein can now initiate an individual signalling cascade to elicit a specific response in the nucleus. Although there is significant cross-talk between these cascades, they will be outlined separately.

1.3.2 The RAS mediated MAP kinase signalling cascade.

The Ras superfamily of proteins are small membrane bound molecules with a weak intrinsic GTPase activity. There are many Ras-like GTPase proteins but there are only four 'true' Ras proteins encoded by *H-ras*, *N-ras*, *K-rasA* and *K-rasB*. Historically, Ras function has largely been associated with affecting cellular proliferation. Activating mutations within *Ras* genes are among the most prevalent in human cancers and therefore they comprise a very important group of signalling molecules. Furthermore, recent research has revealed that Ras proteins also affect

embryonic inductions, cell migration, and differentiation. Hence, they regulate many cellular functions aside from proliferation (Boguski and McCormick, 1993).

Ras proteins do not bind directly with activated receptors. There are two SH2 containing proteins that link Ras to the receptor, SHC and GRB-2 (Pawson and Gish, 1992; Margolis, 1992). GRB-2 binds to the rasGEF enzyme recruiting it to the receptor. RasGEF is a GTP Exchange Factor which binds to Ras-GDP and converts it to Ras-GTP, the activated form. Activated Ras then binds directly with members of the Raf or MEKK kinase families and affects their phosphorylation. This event activates the serine/threonine kinase activity of the Rafs and MEKKs (Duam et al. 1994).

The activated Rafs and MEKKs directly phosphorylate MEK kinases on serine and threonine residues thereby activating their kinase activity. The MEKs are dual specificity kinases that can phosphorylate their substrates on both tyrosine and/or threonine. MEKs directly phosphorylate members of the MAP kinase families such as ERK1, ERK2 and the SAPKs. The activated MAPKs then translocate to the nucleus where they directly phosphorylate many transcription factors and hence regulate their activity (Herskowitz, 1995; Hunter, 1997; Wilkinson and Millar, 1998). Therefore, an extracellular growth factor can transduce its signal to the nucleus by a Ras mediated MAP kinase signalling cascade.

1.3.3 The phosphatidylinositol 3' kinase (PI3K) mediated signalling pathway.

PI3K is a kinase that is composed of two subunits, a p85 regulatory subunit, and a p110 catalytic subunit (Margolis, 1992). p85 contains two SH2 domains and

binds phosphotyrosines on the cytoplasmic tails of activated receptors (Pawson and Gish, 1992). p85 can then associate with p110 thus recruiting its catalytic activity to the receptor. PI3K catalyzes the phosphorylation of the inositol ring of phosphatidylinositol at the 3' position to generate phosphatidyl-inositol-3-phosphate (PI3P), PI3,4P₂, and PI3,4,5P₃. These phospho-inositides are thought to function as second messengers within the cytoplasm (Margolis, 1992; Pawson and Gish, 1992; Hunter, 1997).

Proteins that harbour a pleckstrin homology (PH) domain are capable of binding to phosphoinositides via this region. The c-Akt protein is a serine kinase that contains a PH domain. Its catalytic activity is stimulated by activated PI3K, likely via the second messenger PI3,4P₂. The direct targets of c-Akt have yet to be identified; however, it is believed to activate the 70K S6 kinase (S6K). S6K regulates the translation of cytoplasmic mRNAs through the eIF-4E translation initiation factor. Hence the PI3K pathway, although largely incomplete, reveals how a growth factor signal may regulate the expression of proteins that would be required to elicit specific cellular responses. The potential target mRNAs may encode transcription factors and/or enzymes that regulate their activity (reviewed by Hunter, 1997).

1.3.4 The phospholipase C- γ (PLC γ) mediated signalling pathway.

Phospholipases are important enzymes that are involved in fatty acid and lipid metabolism. There are many isoforms including A₁, A₂, C and D. The phospholipases are esterases; they cleave ester bonds present within phospholipid molecules to aid in

many processes including digestion. However, they also generate active lipid molecules within the cell cytoplasm that act as second messengers in signal transduction pathways. Interestingly, Phospholipase-C- γ (PLC γ) was the only isoform identified that contained SH2 domains (Margolis, 1992; Pawson and Gish, 1992).

PLC γ has been shown to bind to a number of activated growth factor receptor tyrosine kinases including PDGFR, EGFR and FGFR1 (Burgess et al. 1990; Margolis, 1992; Valius and Kazlauskas, 1993). This event leads to tyrosine phosphorylation of PLC γ which in turn activates its catalytic activity. Activated PLC γ then becomes localized to the plasma membrane where it acts as a lipid phosphodiesterase. PLC γ converts phosphatidylinositol-4,5 bis-phosphate into diacylglycerol (DAG) and inositol triphosphate (IP₃). Both of these molecules then act as second messengers within the cell cytoplasm.

PLC γ induces a proliferative response in newly formed zygotes. This response depends on both independent and interdependent signals generated from both DAG and IP₃. The sperm head contains membrane bound ligands at its tip. These ligands have specific receptors on the oocyte plasma membrane. Furthermore, the oocyte is surrounded by a tightly adherent outer membrane or vitelline membrane. Hence, when a sperm binds to an oocyte through its cognate receptor, the oocyte receptor becomes activated and recruits PLC to its cytoplasmic tail. Activated PLC then converts PI_{4,5}P₂ to DAG and IP₃.

IP₃ acts to open calcium channels in the membrane of the endoplasmic reticulum (ER) and affects an influx of Ca⁺⁺ ions into the eggs' cytoplasm. The rise in the

intracellular $[Ca^{++}]$ leads to the fusion of cortical granules with the plasma membrane. This event releases the enzyme hyaluronidase into the space between the egg plasma membrane and the vitelline membrane. The vitelline membrane subsequently raises off of the plasma membrane such that the egg becomes surrounded by a clear membrane or zona pellucida. The zona pellucida prevents polyspermic fertilization of the oocyte. Furthermore, many enzymes that activate DNA replication are dependent on the presence of high intracellular $[Ca^{++}]$ and hence IP_3 also contributes to the proliferative response.

DAG acts as a second messenger by binding to and activating a serine/threonine kinase, protein kinase C (PKC). Interestingly, PKC activity also requires a Ca^{++} ion; hence the IP_3 response also helps to activate PKC. Activated PKC phosphorylates and activates a Na^+/H^+ antiport pump within the egg plasma membrane. This pump imports Na^+ and exports H^+ which leads to an increase in the intracellular pH. Elevated intracellular $[Ca^{++}]$ and pH alone initiate a proliferative response by activating the expression of the immediate early transcription factors *c-fos* and *c-myc*. Furthermore, PKC can directly phosphorylate transcription factors and thus regulate their activity (reviewed by Gilbert, 1988). Hence, prevention of polyspermy and activation of cell division within the zygote is dependent upon a ligand/receptor complex that signals to the nucleus through the $PLC\gamma$ enzyme.

1.3.5 Signalling pathways mediated by cytoplasmic tyrosine kinases: an alternative to receptor tyrosine kinase mediated signal transduction.

Thus far, we have examined signalling pathways involving the activation of the catalytic tyrosine kinase domain on the cytoplasmic tail of an activated receptor. However, there exist many receptors that do not possess a tyrosine kinase catalytic domain but when activated, still induce tyrosine phosphorylation of cytoplasmic proteins. This indirect mechanism is employed in lymphocyte signalling where B and T cells are triggered to mount an immune response by the formation of a specific antigen/antigen receptor complex. Hence, how do receptors that do not possess a catalytic kinase domain affect the tyrosine phosphorylation of their cytoplasmic targets (Mustelin and Burn, 1993) ?

There exists a family of membrane associated cytoplasmic protein tyrosine kinases that do not possess a ligand binding or transmembrane domain. This family of kinases is referred to as the *Src* family, named after its founding member pp60^{src}. This family also includes *c-yes*, *fyn*, *lyn*, *lck*, *hck* and *blk*. Interestingly, these kinases all possess an SH2 domain; this domain, the src homology 2 domain was originally identified in pp60^{src} (Mustelin and Burn, 1993).

Lymphocyte receptors are activated when they bind with their cognate antigens. Formation of this complex transduces a conformational change in the cytoplasmic domain of the receptor. This event allows members of the *Src* family to associate with the activated receptor. However, this association is not mediated through phosphotyrosines on the receptor's cytoplasmic tail binding to the SH2 domains within

the Src proteins. The Src proteins bind the receptor via a unique region that lies outside of its SH2 and SH3 domains (Cantley et al. 1991; Mustelin and Burn, 1993). These findings demonstrated how an activated lymphocytic receptor associated with a protein possessing tyrosine kinase activity. Hence, in this manner, activated antigen receptor signalling is similar to growth factor receptor tyrosine kinase mediated signalling.

Interestingly, Src proteins are not activated by binding to an antigen receptor but are regulated by a unique intramolecular mechanism. All Src proteins contain a conserved tyrosine near their carboxyl terminus. Src proteins are phosphorylated on this tyrosine by a family of non-membrane bound cytoplasmic tyrosine kinases, an example being pp50^{src}. This phosphotyrosine binds to the SH2 domain within the same molecule which in turns represses the catalytic activity of the kinase (Cantley et al. 1991).

Receptor-like transmembrane protein tyrosine phosphatases (PTPases) and small intracellular PTPases dephosphorylate Src proteins at this terminal tyrosine. This prevents intramolecular binding and leads to the activation of their tyrosine kinase activity (Cantley et al. 1991; Mustelin and Burn, 1993). Hence Src family catalytic activity is regulated by a balance between the activities of intracellular PTPases and tyrosine kinases that target specific members. Src proteins are also phosphorylated on serine, threonine and other tyrosine residues; however, it is not yet clear if these events contribute to the regulation of their catalytic activity.

Activated Src tyrosine kinases effect the phosphorylation of downstream target proteins to transduce a signal to the nucleus. Interestingly, Src family members can

activate many of the signalling pathways already outlined, including PI3K, PLC γ and Ras. Furthermore, pp60^{src} can associate with the activated PDGFR, a receptor tyrosine kinase. Therefore, *Src* genes may provide an independent means of feeding into the signalling pathways that are directly activated by the receptor tyrosine kinases (reviewed by Cantley et al. 1991; Margolis, 1992, Mustelin and Burn, 1993).

1.4 The discovery of the *ETS* family of transcription factors.

The *ETS* gene family was first identified by the presence of *v-ets* sequences within the gag-myb-ets chimeric oncogene transduced by the Avian Erythroblastosis virus E26 (Leprince et al. 1983; Nunn et al. 1983; Nunn et al. 1984). Subsequent studies identified the *v-ets* region as necessary for both the erythroid and myeloid transforming activity of this fusion protein (Golay et al. 1988; Graf et al. 1992; Kraut et al. 1994). Probes derived from the *v-ets* sequences were used to clone *c-ets* from both human and chicken sources (Chen 1985; Watson et al. 1985; Gegonne et al. 1986; Gegonne et al. 1987; Boulukos et al. 1988; Watson et al. 1988; Fujiwara et al. 1988).

Furthermore, the region of sequence similarity shared between *v-ets* and *c-ets* conferred sequence specific DNA binding activity upon these proteins (Boulukos et al. 1989; Shyam et al. 1990; Nye et al. 1992) and was subsequently termed the ETS domain. The structure of the ETS domain belongs to a unique class of helix-turn-helix DNA binding domains that has been conserved throughout prokaryotic and metazoan evolution (Lautenberger et al. 1992; Degnan et al. 1993; Liang et al. 1994; Donaldson et al. 1996).

1.4.1 The members of the ETS family of transcription factors.

The ETS family includes *c-ets-1*, *c-ets-2* (Chen 1985; Watson et al. 1985; Gegonne et al. 1986; Gegonne et al. 1987; Boulukos et al. 1988; Watson et al. 1988; Fujiwara et al. 1988), *spi-1/PU.1* (Moreau-Gachelin et al. 1988; Klemz et al. 1990; Paul et al. 1991), *elk1*, *elk2* (Rao et al. 1989), *elf-1* (Thompson et al. 1992), *erg1*, *erg2* (Rao et al. 1987; Reddy et al. 1987), *Sap1*, *Sap2* (Dalton and Triesman 1992), *Gabp- α* (Lamarco et al. 1991), *ERGB/Fli-1* (Watson et al. 1992), *spi-B* (Ray et al. 1992), *PEA3* (*E1A-F*, *ETV4*) (Xin et al. 1992; Higashino et al. 1993; Isobe et al. 1995), *ER71*, *ER81* (*ETV-1*) (Brown and McKnight 1992; Monte et al. 1995), *ERM* (Monte et al. 1994; Chotteau-Lelievre et al. 1997), *TEL* (*ETV6*) (Golub et al. 1994), *NERF* (Oettgen et al. 1996), *MEF* (Miyazaki et al. 1999), *ERF* (*PE-2*) (Liu et al. 1997; de Castro et al. 1997), *E4TF1* (Watanabe et al. 1993), *NET* (Giovane et al. 1994), *ERP* (Lopez et al. 1994), *PE-1* (Klemz et al. 1994), *ELF3* (Tymms et al. 1997), *ESX* (Chang et al. 1997), and *Pet-1* (Fyodorov et al. 1998). Many of these proteins have been characterized as sequence specific DNA binding proteins that are capable of either activating or repressing transcription from their target gene promoters. The ETS proteins bind to DNA through the core cis element 5'-GGAA/T-3'.

1.4.2 Mutations involving *ETS* genes are implicated in human cancers.

Evidence suggests that many members of the *ETS* family play a role in affecting cellular immortalization and/or transformation. The transcriptional activity of ETS-1, ETS-2 (Yang et al. 1996), ELK-1 (Marais et al. 1993), NET (Giovane et al. 1994), SAP1a (Janknecht et al. 1995), ERM (Janknecht et al. 1996), ER81 (Janknecht, 1996) and PEA3 (O'Hagan et al. 1996; Brown et al. 1998) is regulated by the classical RAS/RAF/MAPK signal transduction pathway. Recently, *Fli-1* (Delattre et al. 1992), *ERG* (Shimizu et al. 1993; Sorensen et al. 1994; Ichikawa et al. 1994), *ETV-1* (*ER81*) (Jeon et al. 1994), *TEL* (Golub et al. 1994) and *E1A-F* (*PEA3*) (Kaneko et al. 1995; Urano et al. 1996) have been found in chromosomal translocations associated with Ewing's sarcoma, several forms of myeloid leukemia and primitive neuroectodermal tumors (PNETs).

Approximately 85% of Ewing's sarcomas and PNETs contained a t(11;22) (q24;q12) chromosomal translocation. This rearrangement fused the 5' glutamine rich region of the *EWS* gene in frame with the 3' DNA binding region of *FLI1*. These translocations resulted in the expression of chimeric EWS/FLI1 proteins which acted as strong transcriptional activators with *FLI1* target gene specificity (Delattre et al. 1992; Bailly et al. 1994; Lesnick et al. 1994).

EWS encodes a ubiquitously expressed protein of unknown function, although it displays limited homology to RNA binding proteins. The 5' glutamine rich domain of EWS may act as a potent transactivation domain (Ptashne, 1988; Mitchell and Tijan,

1989). EWS/FLI1 expression was ubiquitous as its expression was governed by the EWS promoter (Delattre et al. 1992). Hence, these studies implicated FLI1 target genes as potential transforming genes within restricted cell populations.

Furthermore, two unique cancer associated translocations were identified involving *ERG*. A t(16;21) (p11;q22) translocation was found in several different types of myeloid leukemia (Shimizu et al. 1993). This rearrangement resulted in the fusion of the 5' region of *TLS/FUS*, an EWS related RNA binding protein, with the DNA binding region of *ERG* (Ichkawa et al. 1994). Sequence analysis predicted that this rearrangement would produce a chimeric protein similar to that found in the EWS/FLI1 fusion.

The translocation t(21;22) (q24;q12) was found in approximately 10-15% of Ewing's sarcomas and PNETs. This rearrangement again fused the 5' glutamine rich region of *EWS* with the 3' DNA binding domain of *ERG*. Furthermore, the chimeric protein was expressed in cell lines derived from the tumors although its ability to transactivate remains to be tested (Sorensen et al. 1994). It would likely act via a similar mechanism to that of EWS/FLI1 but with *ERG* target gene specificity.

The chromosomal translocation that involved *TEL* was found in a subgroup of patients that presented with chronic myelomonocytic leukemia (CMML). They harboured a t(5;12)(q33;p13) translocation which was unlike the others involving *ETS* genes. This rearrangement resulted in the fusion of the 5' helix-loop-helix domain of *TEL* which excluded the ETS domain, with the transmembrane and tyrosine kinase domains of PDGFR β . Hence, this chimeric protein would not behave as a transcription

factor with *TEL* target gene specificity. However, it provides another example of a mutation at an *ETS* locus that has been associated with the development of leukemia (Golub et al. 1994).

1.4.3 *ETS* genes play a role in regulating embryonic development.

Many *ETS* genes are developmentally regulated and in most cases their role in affecting tumorigenesis, invasion and metastasis reflects upon their developmental functions. *Ets-1* is expressed throughout embryogenesis in the hindbrain, neural tube, neural crest, branchial arch mesoderm, limb bud mesoderm, tooth primordia, the developing vascular network, heart, kidney, gut, skin, lung and meninges. *Ets-1* expression is restricted to the thymus gland in the adult mouse and is essential for the development and maintenance of both B and T cell populations (Bories et al. 1995; Muthusamy et al. 1995).

Ets-1 has also been implicated in the induction of cellular invasion and migration. ETS-1 was shown to regulate angiogenesis by stimulating the invasion and migration of vascular endothelial cells in response to the growth factors FGF1, FGF2, VEGF and EGF. Furthermore, the endothelial response to ETS1 expression was dependant on the induced expression of urokinase-type plasminogen activator and MMP-1 (Iwasaka et al. 1996). This finding was supported by a later study showing that ETS-1 was expressed in the endothelial cells of the extravillous trophoblast during the first trimester of human pregnancy. These cells are responsible for invading the uterine vessels to establish placental integrity (Luton et al. 1997).

Ets-2 was expressed in the limbud mesoderm, tailbud, bone and tooth primordia, epithelium of the gut, thymus, spleen and skin (Bhat et al. 1987; Bhat et al. 1989; Vandebunder et al. 1989; Kola et al. 1993; Queva et al. 1993; Maroulakou et al. 1994). *Ets-2* was found to be over-expressed in trisomy 21. A transgenic mouse model over-expressing *Ets-2* resulted in disrupted bone morphogenesis producing a Down's Syndrome-like phenotype (Sumarsono et al. 1996). Hence, ETS-2 appeared to play an important role in bone development.

The *Ets-2* null genotype resulted in early embryonic lethality. This was attributed to defects within the extraembryonic tissues that formed the placenta. The ectoplacental cone was surrounded by a persistent extracellular matrix and displayed a vastly reduced mitotic index. Interestingly, these defects were attributed to the reduced expression of MMP-9. However, *Ets-2* null mice were viable after tetraploid rescue. The null mice displayed wavy hair and whiskers, a similar phenotype to mice harbouring mutations in *Egfr* (reviewed by Hynes and Stern, 1994).

Furthermore, FGF failed to induce MMP-3 and MMP-13 expression in *Ets-2* null fibroblasts. Hence, this study showed that *Ets-2* was required for proper placentation, hair follicle development, and for inducing the expression of specific MMPs (Yamamoto et al. 1998). Defective placentation could not have resulted solely from decreased expression of MMP-9 as *Mmp-9* null mice were viable and did not display placental defects. However, it was required for proper skeletal development (Vu et al. 1998).

The expression pattern of *Spi-1/PU.1* implicated this gene in hematopoiesis and myelopoiesis (Schuetze et al. 1993; Voso et al. 1994). The *PU.1* knockout mouse was devoid of these cell lineages (Scott et al. 1994). The *Fli-1/ERGB* knockout mice displayed thymic hypocellularity confirming its role in T cell development (Melet et al. 1996). The *TEL* knockout proved to be embryonic lethal due to a defect in yolk sac angiogenesis (Wang et al. 1997).

Hence, the developmental functions of many *ETS* genes involve angiogenesis, hematopoiesis and/or myelopoiesis and may explain why this family affects many different forms of leukemia. Furthermore, the *ETS* genes play a significant role in regulating the expression of the *Mmp* gene family. This fact may explain their ability to affect cellular invasion and migration during embryogenesis. Hence, the above studies implicate the *Ets* gene family in initiating tumorigenesis and promoting tumor cell invasion and metastasis.

1.4.4 The PEA3 group is a subfamily within the *ETS* gene family.

The *ETS* genes have been grouped into subfamilies based upon three criteria, i) the degree of sequence identity within the ETS domain, ii) the position of the ETS domain within a given cDNA and iii) the presence of conserved regions that lie outside of the ETS domain (reviewed in Wasylk et al. 1993; Janknecht and Nordheim, 1993). *Pea3* is the founding member of one such subfamily, the PEA3 group (Xin et al. 1992). This subfamily also includes *ER81* and *ERM*. These proteins share ~ 95 % a.a.

identity within the ETS domain, ~ 85 % a.a. identity within the 5' acidic region and an overall a.a. identity of ~ 50 % (figure 1.1) (de Launoit et al. 1997; Monte et al. 1995).

1.4.5 The PEA3 group genes are developmentally regulated.

A recent study reported the developmental expression patterns for *Pea3*, *Erm* and *Er81* from 10.5 d.p.c. through to 17.0 d.p.c. All three genes were expressed in ectodermal derivatives (CNS, neural crest), mesodermal derivatives (kidney, dermamyotome, limb bud, skeletal muscle) and endodermal derivatives (endothelium lining the digestive tract) (Chotteau-Lelievre et al. 1997). The authors concluded that their expression patterns correlated with regions of cellular proliferation and migration within the embryo. Furthermore, they were expressed in tissues and organs undergoing branching morphogenesis and in mobile neural crest and mesodermal derivatives. These observations correlate with their potential role in affecting tumor cell invasion and metastasis.

Interestingly, a subset of these observations were also made for the zebrafish homologue of PEA3. zPEA3 was expressed in the developing somites, the CNS and neural crest cells (Brown et al. 1998). However, it was also expressed in the dorsal neural tube, a location not seen in mouse embryogenesis (Chotteau-Lelievre et al. 1997; Brown et al. 1998; chapter 3). This may reflect a unique functional adaptation specific for embryonic development in the class *Osteichthyes*.

Figure 1.1 Alignment of the amino acid sequences of the PEA3 group proteins.

This is an alignment of the amino acid sequences of the mouse and human homologues of each of the three PEA3 group proteins. The light aqua shading highlights conserved amino acid residues.

1.5 The PEA3 transcription factor.

PEA3 (Polyoma Enhancer Activator 3) was originally described as a site specific DNA binding activity protecting the 5'-AGGAAG-3' motif located in the α -enhancer element of the Polyoma virus (PyV) in DNaseI footprinting analysis (Martin et al. 1988). Previous studies illustrated the importance of this motif in affecting PyV DNA replication and transcription (Veldman et al. 1985; Hassell et al. 1986). Our laboratory isolated the cDNAs encoding the PEA3 protein by screening a lambda gt-11 expression library using the radioactively labelled multimerized binding motif as a probe (Xin et al. 1992).

The initial study revealed that *Pea3* expression was restricted to the brain and epididymis in the adult mouse. Furthermore, the expression levels of its transcript were down regulated in F9 and P19 cells that were induced to differentiate by retinoic acid. These findings suggested that *Pea3* was developmentally regulated (Xin et al. 1992), a fact that was confirmed in recent expression studies in the mouse and zebrafish (Chotteau-Lelievre et al. 1997; Brown et al. 1998).

1.5.1 The molecular organization and chromosomal localization of the *Pea3* gene.

In order to characterize the murine *Pea3* genomic locus, a mouse NIH3T3 cosmid library was screened using the full length PEA3.9 cDNA as a probe (Smillie, 1993; Xin et al. 1992). CosIgPEA3 was the largest PEA3 positive clone that was isolated; it spanned ~35 kbp. Overlapping restriction fragments were ligated into plasmids and subjected to sequence analysis. The *Pea3* gene was encoded by 13 exons

separated by 12 introns spanning 17.6 kbp (figure 1.2). The sequences of all the splice donor and splice acceptor sites shared extensive homology with the previously defined consensus sites (Smillie, 1993; Green, 1986).

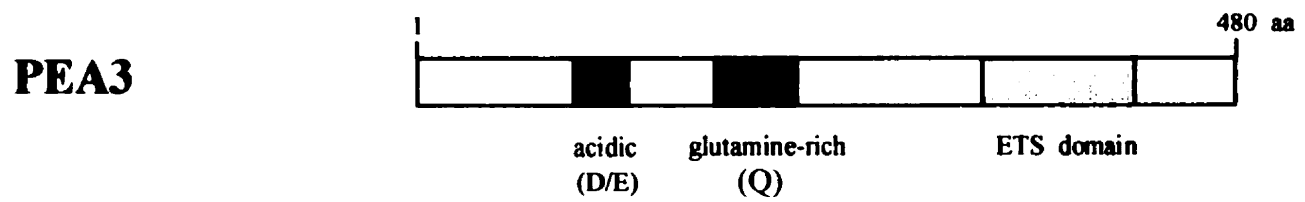
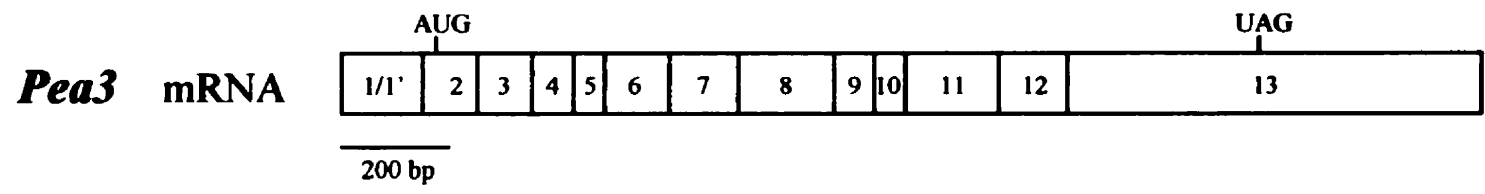
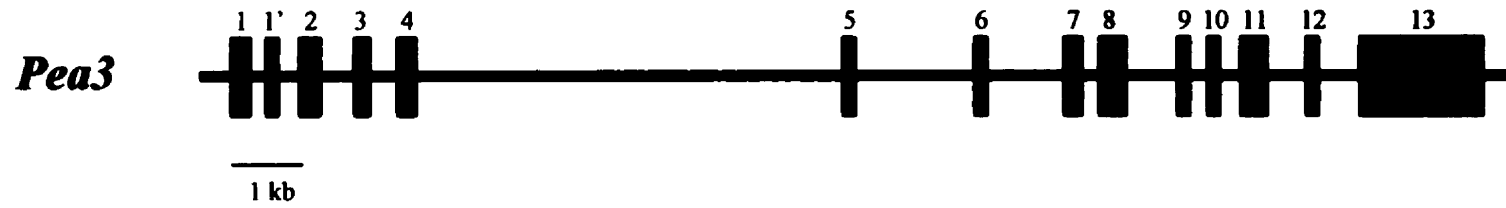
The *Pea3* locus was mapped by fluorescence *in-situ* hybridization (FISH) to mouse chromosome 11, band D. Concurrently, *E1A-F* (*PEA3*, *ETV4*) was mapped to human chromosome 17q21.3 by FISH (Barrett and Hassell, unpublished data, Isobe et al. 1995). Human chromosome 17q21 is syntenic with mouse chromosome 11 D (Copeland et al. 1993). Interestingly, two candidate breast cancer susceptibility genes have also been localized to 17q21, *HER2* and *BRCA1* (Coussens et al. 1985; Miki et al. 1994; Futreal et al. 1994).

1.5.2 PEA3 may be involved in the induction and progression of tumorigenesis.

PEA3 was found to be overexpressed in human metastatic mammary adenocarcinomas. Furthermore, its overexpression correlated with the overexpression of *HER2* (*ErbB2*, *c-neu*), a member of the EGF receptor family (Benz et al. 1997). Interestingly, *PEA3* was also overexpressed in two transgenic mouse models for this disease (Guy et al. 1992a; Guy et al. 1992b; Trimble et al. 1993). One of these transgenic lines was engineered to overexpress *c-neu* in the mouse mammary epithelium and hence was in accordance with the findings in the human study (Guy et al. 1992b; Benz et al. 1997). The question then arises as to how *PEA3* and *HER2* may interact to influence the development and progression of this disease. Two mechanisms that need not be considered mutually exclusive are currently being tested.

Figure 1.2 The molecular organization of the *Pea3* gene, the *Pea3* mRNA and the PEA3 protein.

The *Pea3* gene is encoded by 13 exons (red boxes) that span ~ 17.6 kbp of DNA. The *Pea3* mRNA contains a translation start sequence in exon 2 (AUG) and a translation stop sequence in the middle of exon 13 (UAG). The PEA3 protein is aligned with the above mRNA. The acid rich region (blue box) is encoded by exons 5 and 6 while the glutamine rich region is encoded by exons 7 and 8. The ETS DNA binding domain (yellow box) is encoded in exons 11, 12 and 13. This figure is based on the data from Smillie, 1993.



HER2 is a member of the EGFR family of receptor tyrosine kinases including *Egfr* (*ErbB*), *ErbB3* and *Erb4* (Carraway and Cantley, 1994). *HER2* is overexpressed by gene amplification in approximately 30% of human mammary adenocarcinomas (Hynes and Stern, 1994). The *HER-2* promoter contains a functional PEA3 cis element, 5'-AGGAAG-3' (Scott et al. 1994). In cases where the *HER2* locus has been amplified, the same may also be true of *PEA3* (*E1A-F*) due to their close proximity on human chromosome 17q21 (Coussens et al. 1985; Isobe et al. 1995; Barrett and Hassell, unpublished data).

Hence, high levels of PEA3 in these cells may lead directly to the overexpression of *HER2* and result in tumor induction or progression. This model was consistent with an *in-vitro* study showing that PEA3 could transactivate its own promoter and that of *HER2* (Benz et al. 1997). Furthermore, recent data from our lab revealed that PEA3 was a downstream target of *HER2* (O'Hagan and Hassell, 1998). Therefore, the initial amplification and activation of *HER2* may initiate tumorigenesis and concurrently lead to the activation of PEA3. PEA3 could then form a positive feedback loop with the *HER2* promoter and influence tumor induction and progression.

However, PEA3's potential role in initiating tumorigenesis is not limited solely to breast cancer. Recent studies showed that both *E1A-F* (*PEA3*) and *ETV-1* (*ER81*) were translocated to the *EWS* locus in human PNETs and Ewing's sarcomas (Jeon et al. 1994; Kaneko et al. 1996; Urano et al. 1996). These translocations likely resulted in chimeric EWS-ETS proteins that may function as highly active transcription factors

with PEA3 group target gene specificity (Bailly et al. 1994; Braun et al. 1995). Our lab is currently testing the ability of these chimeric proteins to induce tumors *in-vivo* (Cirnac, 1997; Sheppard and Hassell, unpublished data).

1.5.3 PEA3 has been implicated in the processes of tumor cell invasion and metastasis.

Members of the PEA3 group, and specifically PEA3, have also been implicated in the process of tumor invasion and metastasis. The PEA3 cis element, 5'-AGGAAG-3', appears within the promoters of numerous genes belonging to the matrix metalloproteinase (MMP) family and their inhibitors (TIMPs). These proteases are thought to play a critical role in tumor invasion and metastasis. The MMPs are also expressed during embryonic development where they likely affect extracellular matrix and tissue remodelling (Birkedal-Hansen 1995; Roskelley et al. 1995; Coussens and Werb 1996). PEA3 (E1A-F) can directly transactivate the promoters of TIMP1 (Edwards et al. 1992), stromelysin (MMP-3), type I collagenase (MMP-1), and type IV collagenase (MMP-9/ gelatinase B) (Higashino et al. 1995).

A recent study demonstrated that *PEA3 (E1A-F)* was capable of conferring an invasive phenotype upon a human breast cancer cell line (MCF-7 cells) *in-vitro* and *in vivo*. Furthermore, this phenotype correlated with elevated levels of the MMP-9 transcript, a putative PEA3 target gene. PEA3 expression also stimulated the motile activity of MCF-7 cells. PEA3 expression did not however induce the expression of either MMP-1 or MMP-3 in the invasive cells. Hence, the authors concluded that

PEA3 was capable of inducing an invasive phenotype by specifically up-regulating MMP-9 (Kaya et al. 1996).

In support of the above study, another group introduced an antisense *PEA3* (*EIAF*) expressing construct into a human oral squamous cell-derived carcinoma cell line (HSC3). The parental cell line was highly invasive and expressed high endogenous levels of *PEA3*, *MMP-1*, *MMP-3*, and *MMP-9*. Transfection of the antisense *PEA3* construct resulted in the reduction of both the mRNA and protein levels of all three MMPs. Furthermore, the antisense *PEA3* expressing cell lines exhibited reduced invasive potential *in vitro* and *in vivo* (Hida et al. 1997).

However, one should not assume that *PEA3*'s functions are linked exclusively to the regulation of MMP family members. *PEA3* was also capable of transactivating the Vimentin promoter in mammary epithelial and tumor cells. The Vimentin gene encodes an intermediate filament protein that is associated with cell motility (Chen et al. 1996). *PEA3* was also found to transactivate the β -enolase promoter. β -enolase encodes a muscle specific gene that is expressed in proliferating myoblasts from adult skeletal muscle (Taylor et al. 1997). More recently, two studies showed that *PEA3* and *PEA3* group proteins could transactivate the promoters of two different cell adhesion molecules, VE-cadherin and ICAM-1 (Gory et al. 1998; de Launoit et al. 1998)

1.5.4 Regulation of the transcriptional activity of the *PEA3* protein.

As previously discussed, transcription factor activity and/or expression is often regulated by extracellular signals, many of which are members of growth factor

families (section 1.2 & 1.3). These ligands bind to their transmembrane receptors at the cell surface and affect a conformational change in the receptor's cytoplasmic domain. This signal is transduced to the nucleus by various kinase cascades (section 1.3). Finally, the terminal kinases regulate transcription factor activity by phosphorylation (reviewed by Hunter and Karin, 1992; Hunter, 1997).

Recent studies revealed that the transcriptional activities of the PEA3 group proteins were potentiated by Ras (Janknecht et al. 1996; Janknecht, 1996; O'Hagan et al. 1996). Members of the *Ras* superfamily of genes are membrane associated proteins with GTPase catalytic activity (section 1.3.2). These proteins are activated when bound to GTP and they affect the phosphorylation of other downstream kinases (Boguski and McCormick, 1993). Many of the growth factor receptors that regulate cellular proliferation, differentiation and embryonic inductions transduce their signals through the RAS family proteins (Hunter, 1997).

Studies in our lab showed that PEA3 transcriptional activity was stimulated eight fold over its basal activity in the presence of activated Ras. Furthermore, dominant negative Raf and Rac-1 independently reduced this effect by two fold. These results indicated that Ras stimulated PEA3 activity through two distinct downstream kinase cascades, the Ras/Raf/Erk cascade, and the Rac/Mekk/Sek/SapK cascade. This model was further supported by co-transfection experiments that used activated and dominant negative downstream effector molecules within each of these cascades to assay their effects on PEA3 transcriptional activity (O'Hagan et al. 1996). These studies were consistent with previous studies that showed PEA3 activity was regulated

by various mitogens, growth factors, and oncogenes that were known to signal through Ras mediated pathways.

PEA3 was found to be phosphorylated largely on serine residues. The protein contains eight proline directed serines, the target sequence preferred by the Erks and SapKs (O'Hagan et al. 1996). Furthermore, PEA3 was phosphorylated *in-vitro* by recombinant Erk and SapK (Cox and Hassell, unpublished observations). This data is consistent with the findings of the above studies. Hence, there is strong evidence supporting the model that PEA3 transcriptional activity is regulated by Ras through both the Erk and SapK pathways. The mechanism by which phosphorylation of PEA3 increases its transactivation potential has yet to be determined.

A previous study from our lab also revealed that *HER2 (ErbB2)*, like activated Ras, stimulated the transcriptional activity of PEA3. *HER2* was characterized as a receptor tyrosine kinase that transduced extracellular signals through Ras mediated signalling pathways (Hynes and Stern, 1994). Various dominant negative molecules that inhibited Ras signalling through the ERK cascade or the SAPK/JNK cascade were capable of inhibiting *HER2* mediated stimulation of PEA3 transactivation.

This study showed that *HER2* stimulated PEA3 activity through a Ras mediated pathway. Furthermore, Ras regulated PEA3 activity through both the Raf/Mek/Erk and the Rac/Mekk/Sek/SapK cascades (O'Hagan and Hassell, 1998). When combined, the above evidence indicates that PEA3 activity may be regulated by growth factor receptor tyrosine kinases through the classical Ras/Mekk/Mek/MapK signalling cascade

(reviewed by Herskowitz, 1995). Hence, PEA3 may be a downstream target for many different receptor tyrosine kinases.

1.6 Experimental rationale.

PEA3 is a transcription factor that belongs to the *ETS* superfamily of transcription factors. It is the founding member of an *ETS* subfamily, the PEA3 group, which consists of two other PEA3 related proteins, ERM and ER81. The members of this subfamily share ~95% a.a. identity within their *ETS* DNA binding domains and an overall a.a. identity of ~50% (de Launoit et al. 1997). This fact implies that these proteins are capable of regulating overlapping sets of target genes and therefore may serve redundant functions during embryogenesis and tumorigenesis.

Members of the matrix metalloproteinase (MMP) family of secreted proteases represent a subset of the target genes for both the PEA3 group genes and other *ETS* genes (section 1.4.3; 1.5.2). Hence, members of the PEA3 group may potentiate cell invasion and migration during embryonic development by activating the expression of specific MMPs. Furthermore, these proteins may contribute to the invasive and metastatic potential of cancer cells in a recapitulation of their embryonic functions.

PEA3 was found to be overexpressed in HER2 overexpressing human breast cancers. The overexpression of these two genes correlated with a poor prognosis for the patient as their cancers were highly invasive and metastatic (Benz et al. 1997). This phenotype may be due to the fact that PEA3 is a downstream effector in the HER2 signalling pathway (section 1.5.1; 1.5.3). Together, their combined activities may

ultimately lead to the overexpression of specific MMPs. The MMPs could then contribute to a cancer's metastatic potential by degrading the ECM surrounding a tumor and/or reducing the cell adhesive properties within the tumor.

There is now a significant body of evidence supporting this molecular model (section 1.5.1; 1.5.2). Furthermore, the MMTV-*neu* transgenic mouse model for metastatic mammary adenocarcinoma overexpressed PEA3 (Trimble et al. 1993; Guy et al. 1992b). Hence, this provided a mouse model that could be used to test the above hypothesis. It was the information concerning PEA3's role in affecting human mammary cancer that provided the scientific rationale for undertaking the experiments that are outlined in this thesis.

Firstly, we identified the PEA3 expression pattern during murine embryonic development from early post-implantation through to mid-organogenesis. Histological analysis of many childhood and adult tumors reveals that cancer cells often possess an embryonic or stem cell phenotype. From a developmental perspective, this observation makes good sense. Stem cell populations within a developing embryo are genetically programmed to proliferate, invade, migrate, differentiate and even die upon receiving the appropriate signals that regulate these processes. Therefore, at the molecular level, many cancers arise or are influenced by genetic mutations that affect developmentally regulated signalling pathways.

Recent data has revealed that PEA3 may be a downstream target of the HER2 signalling pathway (Benz et al. 1997; O'Hagan et al. 1998; section 1.5.1; 1.5.3). However, their expression patterns during normal mammary gland development are not

consistent with this being the case in normal cells. Hence, we have undertaken a detailed study to identify the embryonic expression pattern of *Pea3* during mouse embryogenesis. This study will allow us to identify which cell types express PEA3 during embryonic development. Furthermore, we will be able to identify any common biological properties between the different cell types that normally express PEA3. Lastly, we will be able to correlate the PEA3 expression profile with those of the members of other receptor tyrosine kinase signalling pathways. This information will help to identify the signalling pathways that normally regulate PEA3 expression and/or transcriptional activity.

Secondly, we employed a classical reverse genetics approach in order to determine the essential functions of PEA3. A mouse line was generated that lacked the *Pea3* gene. The resulting phenotypes would allow us to assess which of its potential functions were essential during embryogenesis or adult life. Furthermore, provided that the *Pea3* null mouse was viable, we could test the HER2/PEA3 breast cancer model at the genetic level by mating the MMTV-*neu* transgene into the *Pea3* null genetic background and assessing the effects upon the induction and progression of the disease.

CHAPTER 2

MATERIALS AND METHODS

2.1 Preparation of Radiolabelled DNA Probes.

DNA probes were labelled to high specific activity by the method of primer extension (Feinberg and Vogelstein, 1983). The DNA probe fragments were excised from their plasmid backbones using the appropriate restriction enzymes (section 2.7). The DNA fragments were then separated from the plasmid backbone by horizontal agarose gel electrophoresis. Briefly, the restriction digest reaction was electrophoresed through a 1% agarose gel containing 0.5 $\mu\text{g/ml}$ ethidium bromide (EtBr) in 1 X TAE buffer (0.04 M Tris-acetate, 0.001 M EDTA) @ 100 volts for 1 to 3 hrs. The DNA fragments were then visualized by UV illumination (UVP White/UV Transilluminator, DiaMed).

The appropriate fragments were then excised from the gel using a sterile scalpel. The weight of the gel slice was ~ 150-200 mg. The DNA was then purified from the agarose using the QIAquick Gel Extraction Kit[™] (QIAGEN) according to the manufacturer's specifications with the following modifications: the 0.75 ml PE buffer wash step was increased from a 1 min to a 5 min incubation prior to centrifugation; the DNA was eluted from the spin column in 50 μl of dH_2O such that the final [DNA] = ~ 40-50 $\text{ng}/\mu\text{l}$.

The radiolabelling reaction was carried out in a 20 μ l volume. 100-200 ng of probe DNA (5 μ l vol.) was mixed with 5 μ l of random primers (resuspended in dH₂O @ 20 OD 260 units/ ml; Pharmacia) in a 1.5 ml tube and boiled for 5 min. The tube was then quenched on ice for 1 min and centrifuged @ 12000 rpm for 1 min. At this point one added 2 μ l of 20 mM dithiothreitol (DTT), 2 μ l of 5 mM dGTP/ dATP/ dTTP (Pharmacia), 2 μ l of 10 X random primer buffer (900mM HEPES pH 6.6, 100 mM MgCl₂), 5 μ l of [α -P³²] dCTP (3000 Ci/ mmole; Amersham) and 1 μ l (6-10 units) of Large Fragment of DNA Polymerase (BRL). The reaction was incubated @ 37°C for 2 hrs.

The percentage incorporation of [α -P³²] dCTP was calculated for each probe reaction using the method of adsorption to DE-81 cellulose filters (Sambrook et al. 1989, E.19). 1 μ l of the probe reaction was mixed with 9 μ l of dH₂O. 5 μ l aliquots were then placed onto two separate DE-81 cellulose filters (Whatman). One filter was washed with 0.5 M Na₂HPO₄ (pH 7.0), rinsed with dH₂O and dried with a 100% ethanol rinse. The two filters were then subjected to scintillation counting (Beckman LS 6800, Beckman). The percentage incorporation was calculated by dividing the total counts on the washed filter by the total counts on the unwashed filter. Probes were generally labelled to a specific activity of $\geq 10^8$ cpm/ μ g.

Radiolabelled DNA probes were separated from unincorporated [α -P³²] dCTP by spun-column chromatography through Sephadex-G-50 (Pharmacia) (Sambrook et al., 1989, E.37-38). A 1 ml tuberculin syringe was plugged with glass wool and filled with 1 ml of Sephadex-G-50 equilibrated in spun-column buffer (10mM Tris-Cl pH 8.0, 1 mM EDTA pH 8.0, 0.1% SDS). The column was inserted into a 14 ml tube (#2057, Falcon) and

centrifuged @ 1000 rpm for 5 min (Sorvall RT6000 B, Dupont). The column was washed with 500 μ l of spun-column buffer and centrifuged as before. Prior to loading the probe onto the column, 180 μ l of column buffer was added to the probe reaction and incubated @ 37°C for 10 min to stop the klenow reaction. This 200 μ l volume was then loaded onto the Sephadex G-50 column and the probe collected in a 1.5 ml tube by centrifugation as above. Probes were denatured by boiling for 5 min and ice quenched for 1 min prior to use in hybridizations.

2.2 *In-Vitro* Transcription of Riboprobes for RNase Protection Analysis.

For the plasmid map and construction of the riboprobe PEA3 5' KPN, please refer to section 3.2.1. The pSP64 PGK-1 plasmid was provided by Dr. Michael Rudnicki. Template DNA was prepared by digesting 20 μ g of the template plasmid with 20 units of the appropriate restriction enzyme for 4 hrs in a 50 μ l volume. The reaction was heat inactivated @ 85°C for 20 mins, quenched on ice for 1 min and brought up to a 100 μ l volume with sterile dH₂O. The reactions were extracted with 100 μ l of phenol-chloroform (equilibrated in TE pH 8.0; 10 mM Tris-Cl, 1 mM EDTA). The aqueous phase was transferred to a sterile 1.5 ml tube and the DNA precipitated @ -80°C for 1 hr by the addition of 10 μ l of 3M NaAcetate (pH 5.2) and 300 μ l of 100% ethanol. The precipitated DNA was centrifuged for 15 min @ 12000 rpm @ 4°C. The DNA pellet was resuspended in 20 μ l of diethyl-pyrocabonate (DEPC) treated dH₂O at [template] = 1 μ g/ μ l.

The *in-vitro* transcription reaction was carried out in a 20 μ l volume in a 1.5 ml tube. The reaction contained 4 μ l of 5 X T7/T3 transcription buffer (250 mM NaCl, 200

mM Tris-Cl pH 8.0, 40 mM MgCl₂, 10 mM spermidine) (BRL), 1 μ l 200 mM DTT, 1 μ l of a 10 mM ATP/CTP/GTP mix (Pharmacia), 1 μ l 0.2 mM UTP (Pharmacia), 1 μ l (~ 1 μ g) template DNA, 1 μ l RNAGuard™ (BRL), 1 μ l dH₂O, 9 μ l [α -P³²] UTP (3000 Ci/mmole, Amersham). The reaction was incubated for 2 hrs @ 37°C. After 2 hrs, 10 μ g of y_tRNA (5mg/ml) and 3 μ l of DNaseI (RNase free, Pharmacia) were added to the reaction and incubated a further 10 min @ 37°C. The volume was brought up to 100 μ l with DEPC dH₂O and extracted with an equal volume of phenol-chloroform. The aqueous phase was precipitated three times with 33 μ l of 7.5 M NH₄ Acetate and 500 μ l of 100% ethanol @ -80°C for 30 min to remove unincorporated [α -P³²] UTP. Riboprobes were resuspended in 100 μ l of DEPC dH₂O; 1 μ l was precipitated onto DE-81 cellulose filters and subjected to scintillation counting (section 2.1). PEA3 riboprobes were resuspended @ 1 X 10⁶ cpm/ μ l; internal control riboprobes were resuspended @ 5 X 10⁴ cpm/ μ l.

2.3 Southern Blot Analysis.

Southern blot analysis was carried out essentially as outlined (Southern, 1975). DNA samples were subjected to restriction digestion (see 2.7) and then subjected to agarose gel electrophoresis in either 1 X TAE (0.04 M Tris-Cl, 0.001 M EDTA) or 1 X TPE (0.09 M Tris-Acetate, 0.002 M EDTA). Gels were then denatured in 1 L of 0.4 N NaOH, 0.6 M NaCl for 45 mins with gentle agitation (Belly Dancer, Stovall Life Sci. Inc.) and then neutralized in 1 L of 1.5 M NaCl, 0.5 M Tris-Cl pH 7.5 for 45 mins. The DNA was transferred to nylon membranes (Genescreen Plus™, Dupont) by capillary blot transfer using 10 X SSC (1.5 M NaCl, 0.15 M Na-Citrate) as the transfer buffer. Prior to

transfer, membranes were prewetted in dH₂O for 10 mins and soaked in 10 X SSC for a minimum of 15 mins. After transfer was complete, the membrane was rinsed 2 X 5 mins in 5X SSC @ room temperature (RT) and the excess liquid wicked off using 3MM paper (Whatman). DNA was covalently cross-linked to the membranes by subjecting them to UV irradiation in a Stratalinker 2400 set on the auto-crosslink function (Stratagene).

Membranes were prehybridized in 5 X SSC, 5 X Denhardt's reagent (50X contains 5 gm Ficoll (Type 400, Pharmacia), 5 gm polyvinylpyrrolidone, 5 gm bovine serum albumin (BSA Fraction V; Sigma) in 500 ml dH₂O), 0.5 % SDS, 100 µg/ml sheared/heat denatured herring sperm DNA (Gibco-BRL) @ 65°C for a minimum of 2 hrs. The standard volume of solution used was 0.2 ml/cm² of membrane. After prehybridization was complete, the appropriate radiolabelled DNA probe (section 2.1) was added directly to the prehybridization solution.

Hybridizations were carried out for a minimum of 8 hrs @ 65°C. After hybridizations were complete, the membrane was washed 2 X 5 mins in 250 ml of 2 X SSC @ RT and a further 3 X 15 mins in 350 ml of 2 X SSC, 1% SDS @ 65°C. Membranes were air dried on Whatman 3MM paper, wrapped in Saran Wrap™ and exposed to X-ray film (Kodak XAR-5) @ -80°C in Lightning Plus X-ray cassettes (Wolf X-ray Corp.). The films were developed using a Kodak M35A X-OMAT Processor (Kodak).

2.4 Extraction of Total RNA from Tissue.

The method used for RNA extraction from tissue was as outlined (Chirwigin et. al. 1979). Freshly dissected tissues were placed in a 1.5 ml tubes and immediately flash frozen in liquid nitrogen. The samples could be stored at -80°C until needed. The samples were then placed in 4 ml of Tissue Guanidinium Solution (5M guanidinium isothiocyanate, 50 mM Tris-Cl pH 7.5, 10 mM EDTA pH 8.0, 5% β -mercaptoethanol) and homogenized with a tissue homogenizer (Model PT 10/35, Brinkman Instruments). The homogenates were then carefully layered onto individual 5 ml 5.7 M CsCl cushions in Ultraclear ultracentrifuge tubes (Beckman). The CsCl solution was prepared by dissolving CsCl in 0.1 M EDTA prepared with DEPC treated dH₂O and then autoclaving it to inactivate the DEPC.

The samples were ultracentrifuged in an SW-41.Ti swinging bucket rotor @ 32000 rpm for 19 hrs @ 22°C. The supernatant was carefully removed from the tubes by aspiration so as not to contaminate the RNA pellet with genomic DNA and protein. The bottoms of the tubes (containing the RNA pellet) were cut off with a sterile scalpel and placed in 50 ml tubes (#2057, Falcon). The samples were resuspended overnight (~ 8 hrs) in 3 ml of Tissue Resuspension Buffer (5mM EDTA, 0.5% N-lauroylsarcosine, 5% β -mercaptoethanol).

The samples were then extracted with an equal volume of phenol/chloroform and precipitated with 1/10 volumes of 3M Na-Acetate pH 5.2 (DEPC treated) and 2.5 volumes of 100% ethanol @ -20°C for 2 to 8 hrs. The samples were then centrifuged at 9000 rpm for 20 min @ 4°C (Sorvall RC-5B refrigerated superspeed centrifuge, SS-34 rotor,

Dupont). Finally, the RNA pellet was resuspended in 200 μ l of DEPC dH₂O and the concentration determined by taking the optical density @ 260/ 280 nm (DU 640 Spectrometer, Beckman).

2.5 Northern Blot Analysis.

Northern blot analysis was carried using the method of formaldehyde RNA denaturation (Rave et al., 1979) with the following modifications. Total RNA (~20 μ g/lane) (section 2.4) was precipitated in a 100 μ l volume of DEPC dH₂O with 33 μ l NH₄-Acetate and 300 μ l 100% ethanol @ -80°C for ~ 1 hr. The samples were then centrifuged @ 12000 rpm @ 4°C for 30 min. Each 20 μ g pellet was resuspended in 4.5 μ l DEPC dH₂O, 2 μ l formaldehyde gel-running buffer (5X stock is 0.1 M 3-(N-morpholino) propanesulfonic acid (MOPS), 40 mM Na-Acetate, 5 mM EDTA pH 8.0), 3.5 μ l 37% formaldehyde (BDH) and 10 μ l deionized formamide. The samples were incubated @ 65°C for 15 min and quenched on ice for 1 min. Finally, 2 μ l of sterile DEPC treated formaldehyde gel-loading buffer (50% glycerol, 1mM EDTA, 0.25% bromophenol blue, 0.25% xylene cyanol FF) was added to each sample.

The samples were electrophoresed through a 1.2% agarose gel in 1 X formaldehyde gel-running buffer (gel and running buffer contained 0.3 M formaldehyde; Tsang et al. 1993). The gels were electrophoresed @ 3-4 Volts/cm. After electrophoresis, the gels were rinsed 3 X 20 mins in 500 ml of DEPC dH₂O and then soaked a further 45 min in DEPC 10 X SSC. At this point the RNA was transferred to Genescreen Plus™ (Dupont) by capillary blotting in 10 X SSC (DEPC treated) for a minimum of 8 hrs. The

membrane was then rinsed 2 X 5 min in 5 X SSC and the RNA covalently UV cross-linked to the membrane (same conditions as in section 2.3). The conditions for prehybridization, hybridization and washing were as previously outlined (section 2.3).

2.6 RNase Protection Analysis.

Each RNA sample (section 2.4) contained: 30 to 40 μg of total RNA; 1×10^6 cpm of the PEA3 5' KPN riboprobe (1 μl vol); 5×10^4 cpm of the pSP6 PGK-1 internal control riboprobe (1 μl vol); in a total volume of 45 μl (brought up to vol. with DEPC dH_2O). These samples were precipitated with 1/10 vol. of 3.0 M Na-Acetate pH 5.2 (DEPC treated) and 3 vol of 100% ethanol. The samples were placed at -80°C for 20 min and then centrifuged @ 12000 rpm @ 4°C in a table top centrifuge. The pellets containing the RNA and riboprobes were then resuspended thoroughly in 30-50 μl of hybridization solution (50% formamide, 40 mM Pipes pH 6.5, 400 mM NaCl, 1 mM EDTA pH 8.0).

The samples were heated to 85°C for 5 min and then incubated @ 50°C for a minimum of 12hrs. After hybridizations were complete, the samples were centrifuged for 30 sec to collect the condensate. 300 μl of RNase T2 digestion buffer (50 mM Na-Acetate pH 4.5, 2 mM EDTA pH 8.0, 30 Units/ml RNase T2) was added to each sample. Digestions were carried out for 45 min @ 30°C . RNase T2 digestion was stopped with the addition of 80 μl of stop buffer (2 M NH_4 -Acetate, 50 mM EDTA pH 8.0, 5.7 $\mu\text{g}/\text{ml}$ yeast tRNA) and 800 μl of 100% ethanol. The samples were then placed @ -80°C for 25 min and then centrifuged @ 12000 rpm for 25 min @ 4°C .

The pellets were aspirated dry and resuspended in formamide loading buffer (80% formamide vol/vol, 1 mM EDTA pH 8.0, 0.1 % bromophenol blue, 0.1 % xylene cyanol FF). The samples were loaded onto standard 8% denaturing sequencing gels and electrophoresed @ 70 Watts for 3 hrs. The gels were backed onto 1MM paper (Whatman), covered with Saran Wrap™ and dried on a gel drier (Model 583; BioRad) @ 80°C for 35 min. The dried gels were lightly dusted with talcum powder and exposed to X-ray film (Kodak XAR-5) @ -80°C for a minimum of 24 hrs in Lightning Plus X-ray cassettes.

2.7 Restriction Digestion of DNA.

All DNA restriction enzymes were purchased from Gibco-BRL, Pharmacia or New England Biolabs. All digestions were carried out according to the manufacturer's specifications using the commercially supplied 10 X digestion buffers. In all cases where more than one restriction enzyme was used in one reaction where their buffer compositions were incompatible, 10 X One-Phor-All Buffer™ (Pharmacia) was employed at the optimal concentration for both enzymes. Generally, 1-2 units of enzyme were used per 1 µg of DNA.

2.8 DNA Cloning Methodology.

All DNA constructs made within this body of work were generated using the method of DNA cloning from low melting point (LMP) agarose (Strul, 1985; Dharanjaya et al. 1991). However, this protocol was modified in that ligation products were transformed into *E. Coli* by electroporation rather than by the CaCl₂/ heat shock method.

Vector and insert DNA was first digested using the appropriate restriction enzyme(s) (section 2.7). These reactions were heat inactivated @ 85°C for 20 min and equilibrated to RT for 20 min. At this point, 6 X gel-loading buffer III (30% glycerol, 0.25% bromphenol blue, 0.25% xylene cyanol FF) was added to a final concentration of 1 X to the insert DNA samples; they were stored on ice. Concurrently, vector DNA (initially a 20 μ l vol) was dephosphorylated with the addition of 4 μ l 10 X CIAP buffer (Boehringer Mannheim), 20 units of CIAP (Calf Intestinal Alkaline Phosphatase) and 14 μ l of dH₂O. This reaction was incubated @ 37°C for 2-4 hr and then stopped by heat inactivation @ 75°C for 10 min.

The reaction was equilibrated to RT for 20 min and 6 μ l of 6 X gel-loading buffer III added. The vector and insert DNA samples were then electrophoresed through a 1-2 % LMP agarose (BRL) gel in 1 X TAE @ \leq 80 Volts. The vector and insert DNA bands were visualized under UV illumination and excised from the gel with sterile scalpel blades; the gel slices were placed in sterile 1.5 ml tubes. The samples were then melted @ 60°C for 20 min and equilibrated to 37°C. For two part ligations, 5 μ l of molten vector were combined with 35 μ l of molten insert and 40 μ l of 2 X ligase mix containing 50 units T4 DNA Ligase (New England Biolabs, NEB). For three part directional ligations, volumes of molten gel containing equimolar amounts of the DNA fragments were combined in a total volume of 50-60 μ l with the addition of 50-60 μ l of 2 X ligase mix containing 50 units T4 DNA ligase (NEB). Ligation reactions were incubated @ RT for a minimum of 12 hr.

Ligation products were transformed into *E. Coli* by electroporation. Electro-competent bacteria were prepared as follows: 100 ml of Luria Broth (LB) was inoculated with a single bacterial colony and incubated with gentle shaking @ 37°C for 8-10 hr. 1 ml of this culture was used to inoculate another 100 ml LB culture. This secondary culture was incubated with gentle shaking @ 37°C for 3hr (until OD₆₀₀ = ~0.5). At this point the culture was separated into two 50 ml tubes (#2057; Falcon) and chilled on ice for 30 min. The samples were then centrifuged @ 4000 rpm @ 4°C for 15 min (Sorvall GS3 rotor, Dupont). The bacterial pellets were resuspended in ice cold sterile dH₂O and centrifuged as before. The pellets were then resuspended in 20 ml of ice cold sterile 10% glycerol and again centrifuged. Both pellets were resuspended in a final volume of 400 μl ice cold 10% glycerol.

At this point, the ligation reactions were melted @ 60°C for 20 mins and then equilibrated to 37°C. 5 μl of a molten ligation reaction was quickly mixed with 45 μl of electro-competent bacteria in a pre-chilled 1.5 ml tube and transferred to a pre-chilled electroporation cuvette (0.2 cm gap, BioRad). The cuvette was then pulsed @ 2.25 kV, 25 μF, 200 Ω in a GenePulser™ (BioRad). Time constants were between 4.5-5.0 msec. 1 ml of ice cold LB was added immediately after the pulse and the contents transferred to a chilled 1.5 ml tube.

The samples were then incubated @ 37°C for 30 min, centrifuged @ 12000 rpm for 60 sec, resuspended in 200 μl of LB and plated on LB Agar plates containing 80 μg/ml ampicillin (Sigma). The plates were incubated @ 37°C overnight. The resulting colonies were screened for the appropriate plasmid constructions using the standard protocol for

small-scale preparation of plasmid DNA by alkali lysis (Birnboim & Doly, 1979; Ish-Horowicz and Burke, 1981) followed by restriction digestion analysis (section 2.7) and agarose gel electrophoresis. Large scale preparations of the desired constructs were then prepared using a scaled up version of the alkali lysis protocol followed by plasmid purification via ultracentrifugation through CsCl gradients (Sambrook et al. 1989).

2.9 Embryo Dissection and Fixation for Whole Mount *In-Situ* Hybridizations.

Matings were set up with Balb/C males and females. The females were super-ovulated by serial intraperitoneal injections of 5 units of Pregnant Mare's Serum (PMS) (Terochem, Cat # 367222) resuspended in 1 X phosphate buffered saline (PBS) (8 gm NaCl, 0.2 gm KCl, 1.44 gm Na₂HPO₄, 0.24 gm KH₂PO₄ per liter of dH₂O, pH 7.4), and 48 hrs later, with 50 units of human chorionic gonadotropin hormone (hCG) (Sigma, Cat # CG5) resuspended in 1 X PBS. The females were then placed in individual cages with one stud male and left overnight. The next morning the females were separated from the males and examined for the presence of a vaginal plug. Embryonic development was staged at 0.5 days at 12 pm on the day that a plug was detected. Females were sacrificed by cervical dislocation and the embryos dissected from the uterus.

Dissected embryos were placed immediately into DEPC treated 1 X PBS and the extraembryonic membranes removed. The embryos were then fixed in 4% paraformaldehyde (PFA)/ 0.2% glutaraldehyde (GA) (Fisher Scientific) in 1 X PBS for a period of 2-4 hrs for embryos @ 6.5 through 9.5 d.p.c. and ~8 hrs (overnight) for embryos @ 10.5 through 12.5 d.p.c. After fixation, embryos were placed in two changes

of PBT (1 X PBS, 0.1 % Tween-20) for 5min @ 4°C. The embryos were then dehydrated in 25 % methanol (MeOH)/PBT for 5min, 50 % MeOH/PBT for 5min, 75 % MeOH/PBT for 5 min, 100 % MeOH for 5 min and a final change of 100 % MeOH and stored @ -20°C until needed for the whole mount *in-situ* hybridization protocol (section 2.12).

2.10 Construction of PEA3 Specific Riboprobes for use in Whole Mount In-Situ Hybridizations.

The PEA3 group genes share a high degree of DNA sequence identity in two conserved regions, the acidic region (88%), and the ETS DNA binding domain (95%) (de Launoit et al. 1997). The ETS domain spans approximately 81 amino acids or 243 bp. Hence any riboprobe including this domain might cross-hybridize to the transcripts of all three PEA3 group mRNAs in *in-situ* hybridizations. In order to avoid this problem, two similar PEA3 specific riboprobes were constructed for use in the whole mount protocol (figure 2.1). The PEA3.9 cDNA (Xin et al. 1992) was engineered to include a HindIII site at its putative start ATG. This cDNA was ligated as a HindIII-SstI fragment into pGEM7zf(+)™ (Promega) generating the plasmid pGEM7PEA3 (figure 2.1 A) (U. Ashraf, R. O'Hagan and J. Hassell). Two overlapping riboprobes were constructed using this cDNA.

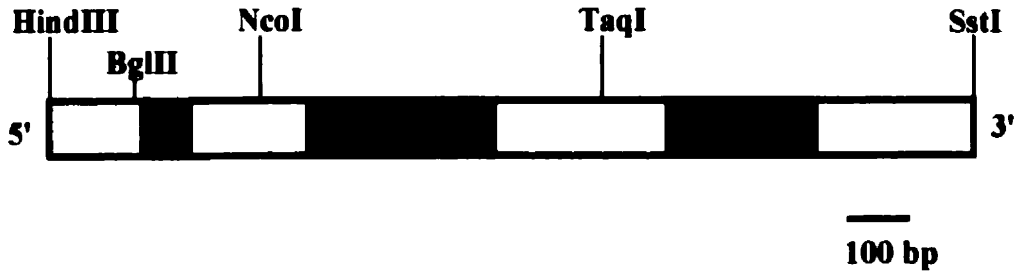
The PEA3 specific riboprobe plasmid pBSPEA3HT892 was constructed by excising an 892 bp HindIII-TaqI fragment from pGEM7PEA3. This fragment was rendered blunt ended and then ligated into the EcoRV site of pBluescript™ (figure 2.1 B). An antisense riboprobe was generated from this plasmid by digesting it with Sall and transcribing in the

Figure 2.1 Construction of PEA3 specific riboprobes for use in whole mount *in-situ* hybridizations.

(A) Schematic diagram of the PEA3 cDNA excised from the plasmid pGEM7 PEA3. The HindIII site was engineered at the start ATG at site 353 bp according to the numbering system described for the PEA3.9 cDNA (Xin et al. 1992). The blue box marks the acidic (D & E) domain, the red box marks the glutamine (Q) rich domain and the green box marks the ETS DNA binding domain. (B) The plasmid pBSPEA3HT892 was constructed by excising the 892 bp HindIII-TaqI fragment from A and ligating the blunt ended fragment into the EcoRV (RV) of the pBluescript™ plasmid. (C) The plasmid pBSPEA3BT744 was constructed by excising the 744 bp BglII-TaqI fragment from A and ligating the blunt ended fragment into the RV site of the pBluescript™ plasmid.

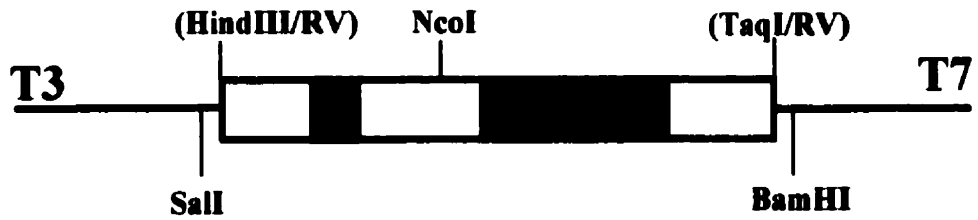
A

PEA3 cDNA



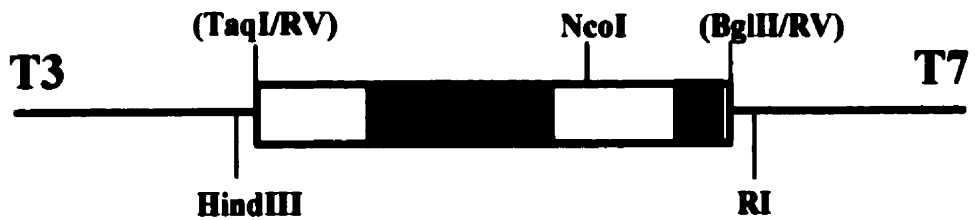
B

pBSPEA3HT892



C

pBSPEA3BT744



presence T7 RNA polymerase. A sense riboprobe was generated from this plasmid by digesting it with BamHI and transcribing in the presence of T3 RNA polymerase. This vector was used in all of the *in-situ* hybridizations carried out in this study. A slightly shorter riboprobe plasmid, pBSPEA3BT744, was also constructed (figure 2.1 C); however, it was not used in the following studies.

2.11 *In-Vitro* Transcription of Riboprobes for Whole Mount *In-Situ* Hybridizations.

For the details concerning the construction of the PEA3 specific riboprobe (pBSPEA3HT892), please refer to section 2.10. The murine ERM riboprobe was provided by Dr. Yvan de Launoit (Institut Pasteur de Lille, Lille France). It contained the first 550 bps of the murine ERM cDNA (Chotteau-Leleivre et al. 1997). It was digested with HindIII; the antisense riboprobe was transcribed with T7 RNA polymerase. The murine ER81 riboprobe was provided by Dr. Thomas Jessell (Columbia University, New York). It consisted of the entire murine ER81 cDNA ligated into pBS[™] (Stratagene). It was linearized by HindIII digestion and the antisense riboprobe transcribed with T7 RNA polymerase. The PEA3 antisense template was digested with Sal I and transcribed with T7 RNA polymerase. The PEA3 sense template was digested with BamHI and transcribed with T3 RNA polymerase.

Riboprobe template DNA was prepared as previously described (section 2.2). The RNA polymerases were purchased from either Boehringer Mannheim or Gibco-BRL. The reaction conditions for transcribing both the antisense and sense riboprobes were as follows: (mixed in a 1.5 ml tube @ RT) 14 μ l dH₂O, 2 μ l 10 X Transcription buffer (400

mM Tris-Cl pH 8.25, 60 mM MgCl₂, 100 mM DTT, 20 mM spermidine, Boehringer Mannheim), 2 μ l DIG RNA Labelling Mix™ (10 mM GTP, ATP, CTP, 6.5 mM UTP, 3.5 mM DIG-UTP, Boehringer Mannheim), 1 μ l (~ 1 μ g) template DNA, 1 μ l (~ 30 units) RNAGuard™ (Pharmacia), 1 μ l RNA polymerase (~ 50 units). The reactions were incubated @ 37°C for 2hrs.

The reactions were stopped with the addition of 2 μ l (~ 20 units) of DNaseI (RNase-Free, Boehringer Mannheim) and incubated a further 15 min @ 37°C. 1 μ l of the original reaction was electrophoresed through a 1% agarose 1XTAE gel to insure the reaction had worked and to estimate the yield of riboprobe via comparison to known amounts of molecular weight standards run in adjacent lanes. After DNaseI digestion, riboprobes were precipitated for 30 min @ -20°C with the addition of 78 μ l DEPC dH₂O, 10 μ l 4M LiCl and 300 μ l 100 % ethanol. The precipitate was centrifuged @ 12000 rpm @ 4°C for 30 mins and resuspended in 100 μ l of DEPC dH₂O (~ 100 ng/ μ l). At this point the riboprobes were ready for use (section 2.12).

2.12 Whole Mount *In-Situ* Hybridizations.

This protocol was communicated to me by Dr. Corrinne Lobe. This protocol originated in the laboratory of Dr. Peter Gruss (Gottingen, Germany). Embryos (section 2.9) were placed in the wells of a 6 well culture dish and treated as follows: (3-4 ml volumes per well) 75% MeOH/PBT for 5min, 50% MeOH/PBT for 5 min, 25% MeOH/PBT for 5 min, PBT for 5 min, PBT for 5 min, 6% H₂O₂/PBT for 1 hr (mixed fresh), 3 changes of PBT for 5 min each, 10 μ g/ml proteinase K/PBT for 15 min @ RT,

2 mg/ml glycine/PBT for 5 min (mixed fresh), 2 changes of PBT for 5 min each, post-fixed in (0.2% GA + 4% PFA)/ PBT for 20 min (mixed fresh), 2 changes of PBT for 5 min each. At this point the embryos were blocked in prehybridization mix (50% formamide, 5X SSC pH 4.5, 1% SDS, 50 μ g/ml yeast tRNA, 50 μ g/ml heparin) for 1 hr @ 70°C. The prehybridization mix was then replaced with 3-4 mls of hybridization mix (Prehyb Mix, 10 μ l/ml (~ 1 μ g/ml) riboprobe) and incubated overnight (\geq 8 hr) @ 70°C.

The embryos were subsequently washed 2 X for 30 min @ 70°C in Solution 1 (50% formamide, 5X SSC pH 4.5, 1% SDS), Solution 1/ Solution 2 (0.5 M NaCl, 10 mM Tris-Cl pH 7.5, 0.1 % Tween-20) (1:1) for 10 min @ 70°C, 3 X 5min washes @ RT in Solution 2, 100 μ g/ml RNaseA/ Solution 2 for 30 min @ 37°C (optional), Solution 2 for 5 min @ RT, Solution 3 (50 % formamide, 2 X SSC pH 4.5) 5 min @ RT, 2 washes in Solution 3 for 30 min each @ 65°C, 3 X 5 min washes @ RT in TBST (10X TBST (100ml) 8 gm NaCl, 0.2 gm KCl, 25 ml 1M Tris-Cl pH 7.5, 10 ml Tween-20, autoclaved, diluted to 1X with DEPC dH₂O, and add levamisole (Sigma) to 2mM (0.48 mg/ml) on day of use).

The embryos were blocked in 10% fetal bovine serum (FBS)/ TBST for 90 min @ RT (FBS was heat inactivated @ 70°C for 30 min prior to use); the embryos were then incubated with 0.5 μ l of Anti-DIG Fab fragments (Boehringer Mannheim) per ml of 1% FBS/TBST at 4°C for \geq 12 hrs. The Anti-DIG Fab fragments first had to be pre-adsorbed to embryo powder prior to incubation with the hybridized embryos. Embryo powder was prepared by homogenizing 13.5 d.p.c. embryos in a minimum volume of

sterile 1XPBS; 4 volumes of ice cold acetone were then added and the mixture incubated on ice for 30 min. The mixture was centrifuged, the pellet washed in ice cold acetone, and again centrifuged. The pellet was spread out on 3MM paper (Whatman) and ground into a fine powder with a spatula. The powder was stored @ 4°C until needed. Pre-adsorption of the antibody was carried out by adding 5 μ l of FBS and 1 μ l of Anti-DIG Fab fragments to 0.5 ml of TBST containing 3 mg of the embryo powder. This mixture was incubated for 1 hr @ 4°C with gentle agitation. The embryo powder was then removed by centrifugation and the volume brought up to 2 ml with the addition of 1.5 ml 1% FBS/TBST. At this point the Fab fragments were ready for use in the above protocol.

Antibody that bound non-specifically was removed with the following series of washes: 3 X 5 min in TBST @ RT, 4 X 1 hr in TBST @ RT and a final wash overnight in TBST @ RT. The Fab fragments were conjugated to the enzyme alkaline phosphatase. At this point the embryos were prepared for the enzymatic colour reaction: embryos were washed 3 X 10 min @ RT in NTMT (100 mM NaCl, 100 mM Tris-Cl pH 9.5, 50 mM MgCl₂, 0.1% Tween-20, 2 mM levamisole); embryos were then incubated in 4.5 μ l of NBT/ml (Boehringer Mannheim) and 3.5 μ l of BCIP/ml (Boehringer Mannheim) in NTMT for 1 hr to overnight (until desired colour intensity was achieved with a good signal to noise ratio). At this point the colour reaction was stopped by incubating the embryos 2 X 15 min @ RT in PBT, 50% glycerol/ PBT for 15-30 min, 80% glycerol/ PBT for a minimum of 8 hr @ 4°C. Embryos were subsequently photographed using a Wild M3C Stereo dissecting microscope mounted with a Wild MPS51 35mm camera and a Wild Photoautomat MPS45 automatic exposure apparatus.

2.13 Histological Preparation and Sectioning of Post-Whole Mount Embryos.

Embryos that were subjected to the whole mount protocol were post-fixed, sectioned and counterstained in order to better define the tissue localization of the hybridized riboprobes. The glycerol was washed out of the embryos with 8 X 20 min washes in PBT @ RT. At this point the embryos were post-fixed overnight in 4% PFA + 0.2% GA/ PBT (Fisher Scientific). The fixative was washed away with 8 X 20 min washes in dH₂O. Embryos \leq 10.5 d.p.c. were embedded in 0.5 % low melting point agarose (GibcoBRL), post-fixed overnight in 10% buffered formalin (Fisher Scientific) and then processed for histological analysis (section 2.18). Embryos \geq 11.0 d.p.c were treated in the same fashion but were not embedded in LMP agarose. The paraffin embedded embryos were then sectioned @ 10-20 μ m on a microtome (Microm, HM330) using disposable stainless steel Feather Microtome Blades (type S35). The sections were floated onto a TissuePrep Flotation Bath set @ 37°C (Fisher Scientific), adhered to glass slides and subsequently placed on a slide warmer (42°C) until the sections were dry (~ 60 min). The slides were then placed in a 37°C incubator overnight.

The sections were then dewaxed and counterstained by the following protocol (all volumes were 250 ml in standard histological staining dishes (Wheaton, Fisher Scientific)): the sections were dewaxed 2 X 10 min in xylenes (BDH), 4 X 5 min in 100% ethanol, rinsed in tap water for 2 min, counterstained for 10-30 sec in a 1/200 dilution of Eosin Y (stock=1% w/v, Fisher Scientific) in tap water, rinsed for 1-10 min in tap water, dehydrated 2 X 5 min in 100% ethanol and equilibrated 2 X 10 min in xylenes. At this point, the sections were mounted with coverslips using Permount™ (Fisher Scientific). The

slides were then placed in a fume hood overnight to let the Permount™ set. The slides were viewed by standard light microscopy and photographed using a Zeiss Axioskop mounted with a Zeiss MC100 35 mm camera (Courtesy of Dr W. J. Muller, McMaster University).

2.14 Isolation and Mapping of Genomic PEA3 Clones from a λ DASH™II Phage Library.

The DNA source used to construct this genomic library was isolated from the J1 embryonic stem (ES) cell line (129/sv mouse strain) and partially digested with the restriction enzyme MboI. DNA fragments within the 14-15 kbp size range were isolated and cloned into the BamHI site of the λ phage vector Lambda DASH™ II (Stratagene). This library was constructed in the laboratory of Dr. R. Jaenish (Whitehead Institute, Boston, MA) and kindly provided by Dr. M. Rudnicki (McMaster University, Hamilton, Ont.). Screening of this genomic phage library was carried out essentially as outlined in the standard protocol provided by Stratagene; however, some minor modifications were made.

50 mls of Terrific Broth (TB) (5 gm NaCl, 10 gm Bactotryptone per litre), supplemented with 0.2% maltose and 10 mM MgSO₄, was inoculated with a single bacterial colony (strain LE392). The culture was incubated overnight (~ 8 hr) with gentle shaking @ 30°C, transferred to a 50 ml tube (#2057, Falcon) and then centrifuged @ 4000 rpm for 10 min (Sorvall RC-3B centrifuge, Dupont). The bacterial pellet was resuspended in 10 mM MgSO₄ to an O.D.₆₀₀ = ~0.5/ml. 600 μ l of this bacterial stock was then inoculated with 5 X 10⁴ pfu (plaque forming units) in a 14 ml tube (#2059, Falcon). The contents of the tubes were mixed with gentle tapping and then incubated @ 37°C for 15

min. At this point, 6.5 ml of top agarose (Luria Broth (10 gm NaCl, 5 gm yeast extract, 10 gm bactotryptone/ litre tap water) supplemented with 0.2% maltose, 10 mM MgSO₄, 0.7% agarose) equilibrated to 48°C was added to each tube and subsequently spread onto a 150 mm LB agar plate (supplemented with 0.2% maltose, 10 mM MgSO₄) pre-warmed to 37°C. The top agarose was allowed to solidify for 10 min @ RT. The plates were then inverted and incubated for ~ 12 hr (until plaque diameter = ~ 1-2mm) @ 37°C. A total of 1 X 10⁶ pfus were screened (20 X 150 mm plates, ~ 5 mouse genomes). The plates were then taken out of the 37°C incubator and chilled @ 4°C overnight.

Two plaque lifts were made from each master plate using 132 mm circular HYBOND™ filters (Amersham). The first lift was carried out for 2 min and the second for 4 min. The orientation of the filters were marked on the plates by puncturing the filter and the LB agar with an 18 gauge needle. As the lifts were completed, the filters were stacked individually between pieces of 3MM paper (Whatman) and the stack wrapped in aluminum foil. The stack was autoclaved for 2 min @ 212°F on a liquid cycle to lyse the phage and allow the DNA to bind with nylon filters.

The DNA was covalently cross-linked to the filters by UV irradiation (section 2.3). The filters were then prehybridized for 4-12 hrs @ 65°C (20 filters/ 30 ml prehybridization solution) as outlined (section 2.3). The radiolabelled probe (section 2.1) was then added directly to the prehybridization solution and incubated a further 12 hr @ 65°C. The probe used for this library screen was an EcoRI fragment containing the full length PEA3.9 cDNA in pGEM7Zf(+)[™] (Promega) (Xin et al., 1992). The filters were washed 2 X 15 min in 2 X SSC @ RT and 3 X 15 min in 0.1 X SSC/ 0.1% SDS @ 65°C. The filters were

then dried on 3MM paper (Whatman) and exposed to x-ray film (Kodak XAR-5) in Lightning-Plus x-ray cassettes @ -80°C for \geq 48 hr.

Plaques were picked based on the presence of over-lapping hybridization signals on both the first and second lift filters. These plaques were then picked into 1 ml of suspension medium (SM, 5.8 gm NaCl, 2.0 gm MgSO₄·7H₂O, 50 ml Tris-Cl pH 7.5, 5 ml 2% gelatin per litre) with one drop of chloroform added and allowed to resuspend overnight @ 4°C. These samples were then subjected to subsequent rounds of the above protocol until the plaques were purified.

Phage DNA was isolated by the following phage mini-preparation protocol provided by Dr. M. Rudnicki. A purified plaque was picked and placed in a 5 ml tube (#2063, Falcon) with one drop from a 50 ml overnight bacterial culture (strain LE392) prepared as above. The phage were adsorbed to the bacteria for 5 min @ RT and then 2 ml of LB (supplemented with 10 mM MgSO₄) was added to the tube. The tube was rotated overnight. The sample was then divided into two 1.5 ml tubes and 100 μ l of chloroform added to each tube and then incubated @ 37°C for 15 min. The bacterial debris was centrifuged @ 4000 rpm for 5 min (Sorvall RC-3B centrifuge, Dupont). The supernatant was removed and stored @ 4°C. This supernatant was considered to be the primary phage culture.

15 μ l of the primary phage culture was adsorbed to 1 ml of the overnight bacterial culture for 5 min @ RT. The 1 ml volume was used to inoculate 50 ml of LB (supplemented with 10 mM MgSO₄) and then incubated overnight @ 37°C with shaking (250 rpm). 500 μ l of chloroform and 1.5 gm of NaCl were then added to the flask and the

NaCl allowed to dissolve by gentle shaking @ 37°C. The 50 ml culture was transferred to a 50 ml tube (#2057, Falcon) and centrifuged @ 4200 rpm @ 4°C for 10 min (Sorvall RC-3B centrifuge, Dupont).

The phage supernatant was added to a fresh 50 ml tube containing 5 gm of polyethylene glycol (PEG) 8000 and inverted until the PEG dissolved. The tube was incubated @ 4°C for 1 hr and then centrifuged as above. The phage pellet was resuspended in 600 μ l of SM (without the 2% gelatin). 2.5 μ l of DNaseI (~ 25 units) was added to the phage suspension and incubated for 1 hr @ 37°C. The DNaseI was inactivated with the addition of 2 μ l of DEPC and the sample split into two 1.5 ml tubes. 600 μ l of 1 M Tris-Cl pH 8.5, 1% SDS, 100mM EDTA was added to each tube and the tubes incubated @ 70°C for 5 min.

300 μ l of 5 M K-Acetate was added to each tube, the tubes chilled on ice for 30 min, and then centrifuged @ 12000 rpm @ 4°C for 15 min. The supernatants were transferred to fresh 1.5 ml tubes, 0.5 volumes of propan-2-ol added to each tube and the tubes mixed by gentle inversion. The precipitated DNA was removed from the solution with a wooden toothpick and transferred into 500 μ l of TE pH 8.0 containing 20 μ g/ml RNaseA. The samples were phenol/chloroform extracted and reprecipitated with the addition of 1/10 vol. 3M Na-Acetate pH 5.2 and 2.5 volumes of 100 % ethanol. The DNA pellet was then resuspended in a final volume (50-200 μ l) of sterile dH₂O containing 20 μ g/ml RNaseA. The phage DNA was now used for restriction digestion analysis and cloning (see sections 2.7 & 2.8).

The first generation of targeting vectors designed for homologous recombination in ES cells produced very low targeting frequencies ($\sim 1/1000$). This low frequency of homologous recombination was attributed to the fact that most of the early targeting vectors were generated from DNA sources that were non-isogenic to the ES cell line that was being targeted. Although the sequence and the organization of the *Pea3* gene had been determined (Smillie, 1993), these studies were carried out using genomic DNA clones that were non-isogenic to the J1 ES cell line that we were to employ in our recombination experiments.

Hence, in order to generate an efficient targeting construct for the *Pea3* locus, three unique and overlapping phage clones, $\lambda 31$, $\lambda 91$ and $\lambda 93$ were isolated from an isogenic phage genomic library. Their genomic DNA inserts were mapped using a combination of restriction digestion and Southern blot analysis. Using the genomic map and sequence data for the *Pea3* gene, a series of genomic DNA fragments derived from *CosI*, a cosmid that contained the entire gene, were used as probes for mapping the phage DNA inserts (Smillie, 1993).

A 2.1 kb *EcoRI* fragment containing exons 7 and 8 was radiolabelled and hybridized to a Southern blot of *EcoRI* digested DNA from the three phage clones. All three phage clones harboured a 2.1 *EcoRI* fragment that hybridized with this probe. Hence all three phage clones contained this region of the *Pea3* gene (figure 2.2 A; panel i). A 4.9 kb *EcoRI-KpnI* fragment containing exons 1 through 4 was radiolabelled and hybridized

to a Southern blot of EcoRI digested phage DNA. Only $\lambda 91$ contained sequences that hybridized with this probe; an 8.0 kb EcoRI fragment (figure 2.2 A; panel ii).

A probe was also generated using a 4.0 kb fragment from the 5' most EcoRI site to the ClaI site. This probe still contained exons 1 through 4 but lacked 1 kb of 3' intron sequence. This probe failed to hybridize to any of the clones (data not shown). Hence $\lambda 91$ contained the 5' most sequences of the three phage isolates but lacked exons 1 through 4.

A 6.0 kb EcoRI fragment containing exons 9 through 13 was radiolabelled and hybridized to a Southern blot of EcoRI digested phage DNA. Both $\lambda 31$ and $\lambda 93$ harboured a 6.0 kb fragment that hybridized with this probe whereas $\lambda 91$ contained a 3.5 kb fragment that hybridized with this probe (figure 2.2 A; panel iii). A probe generated using the 3' most EcoRI fragment as a template hybridized with a ~6.0 kb EcoRI fragment from $\lambda 31$. This probe failed to hybridize with sequences within $\lambda 91$ and $\lambda 93$ (data not shown). Hence, $\lambda 31$ contained the 3' most sequences of the *Pea3* gene.

Finally, a 1.3 kb EcoRI fragment derived from $\lambda 31$ was radiolabelled and hybridized to a Southern blot of EcoRI digested phage DNA. It hybridized to a 1.3 kb fragment in $\lambda 31$ as expected, an 8.0 kb fragment in $\lambda 91$ and a ~7.0 kb fragment in $\lambda 93$ (figure 2.2 A; panel iv). This probe hybridized to the same EcoRI fragment in $\lambda 91$ that the 5' EcoRI-KpnI probe hybridized with. This revealed that the 7.0 kb EcoRI fragment from $\lambda 93$ also contained the 5' regions of the PEA3 gene but that it lacked about 1.0 kb

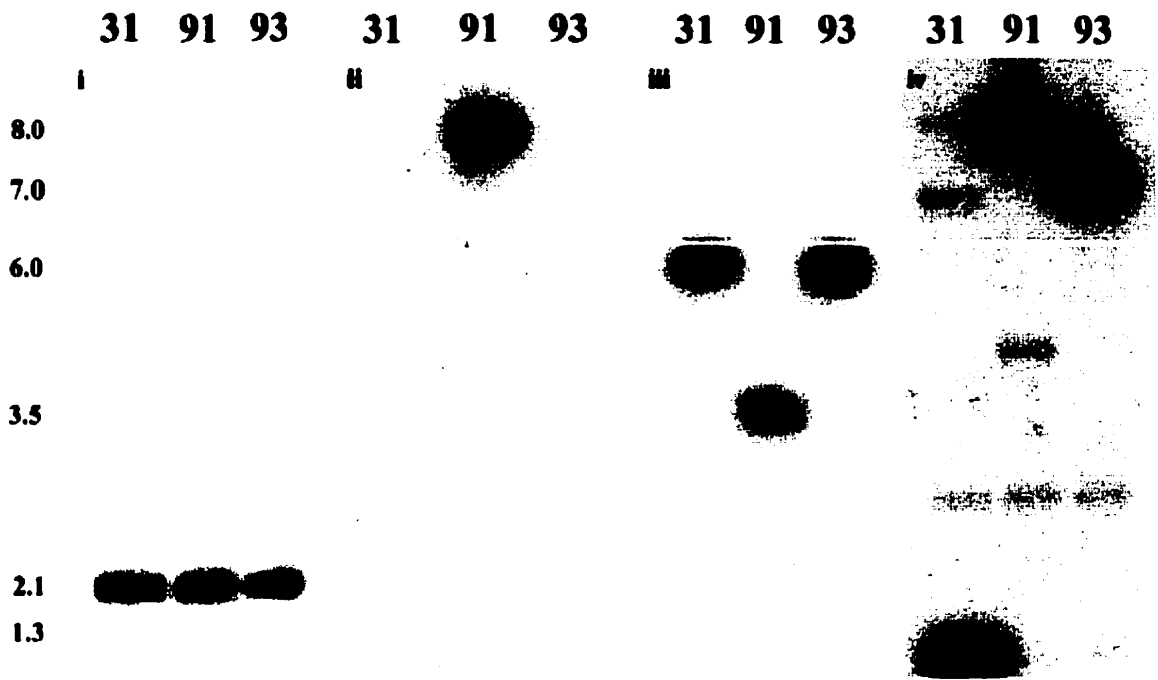
Figure 2.2 Mapping the PEA3 positive lambda phage genomic inserts to the *Pea3* gene.

(A) Southern blot analysis of EcoRI digested DNA from phage clones $\lambda 31$, $\lambda 91$ & $\lambda 93$.

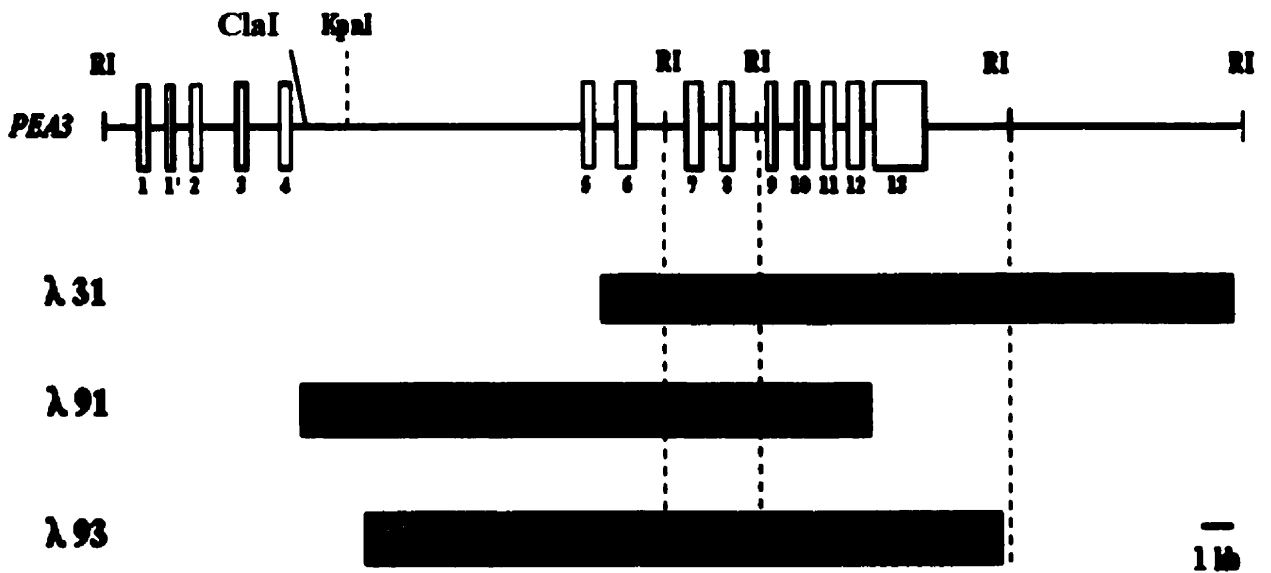
(i) Probe was derived from a cosmid containing the entire *Pea3* locus, CosI (Smillie, 1993); it was a 2.1 kb EcoRI fragment containing exons 7 and 8. **(ii)** Probe was derived from a 5.0 kb EcoRI-KpnI fragment from CosI containing exons 1 through 4. **(iii)** Probe was derived from a 6.0 kb EcoRI fragment from CosI containing exons 9 through 13. **(iv)** Probe was derived from a 1.3 kb EcoRI fragment from $\lambda 31$ containing exon 6. **(B)**

Schematic diagram of the *Pea3* gene with the relevant restriction sites indicated; the grey boxes represent the regions of *Pea3* that were mapped within the individual λ phage genomic inserts using the restriction digest and Southern blot data from A.

A



B



at its 5' end relative to the 8.0 kb fragment from $\lambda 91$ (figure 2.2 A, compare panel ii with panel iv). Furthermore, this revealed that the 5' most sequences of $\lambda 91$ and $\lambda 93$ were both 3' of exon 4. These mapping results allowed for the alignment of the three genomic phage inserts to the map of the *Pea3* gene (figure 2.2 B). Hence, the genomic inserts from $\lambda 31$, $\lambda 91$ and $\lambda 93$ spanned the *Pea3* genomic locus from approximately the 5' KpnI site through to the 3' most EcoRI site and included exons 5 through 13 (figure 2.2 B).

2.15 Construction of a Targeting Vector Designed to Generate a Null Allele at the *Pea3* Locus.

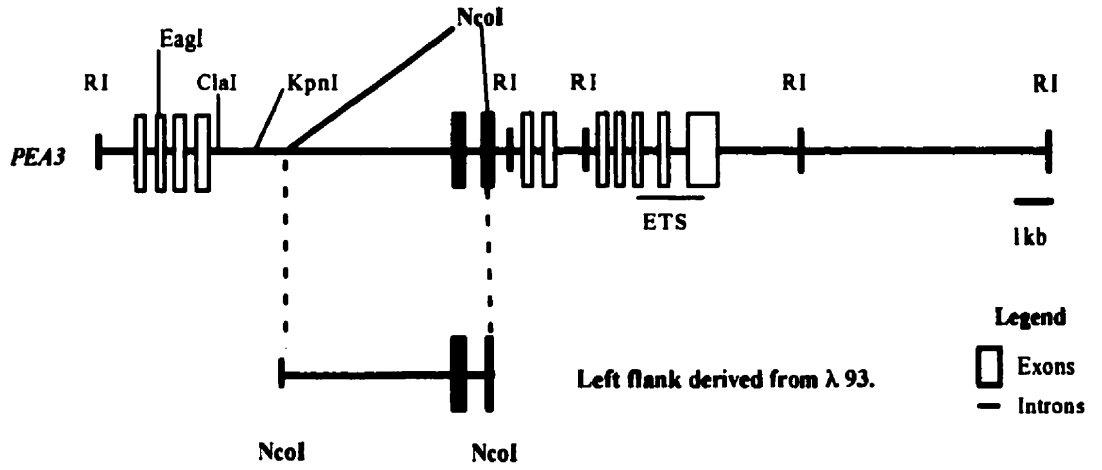
Two lambda phage clones were used to construct a targeting vector designed to knock out the *Pea3* gene. The left flank, an ~ 6.0 kbp NcoI fragment, was derived from $\lambda 93$ (figure 2.2 B). It contained exons 5 and 6 at its 3' border (figure 2.3 A). This NcoI fragment was rendered blunt ended using the Klenow fragment of DNA polymerase. It was then ligated into the vector pBluescript™ (pBS) that had been digested with EcoRV and subsequently dephosphorylated with Calf Intestinal Alkaline Phosphatase (CIAP). This ligation reaction introduced a vector derived EcoRI site into the beginning of exon 6 while destroying the adjacent endogenous NcoI site. This plasmid was referred to as pBSN93 (figure 2.3 B).

The right flank, an ~ 10.8 kbp SnaBI-NotI fragment, was derived from $\lambda 31$ (figure 2.2 B). It contained exons 12 and 13 at its 5' border (figure 2.4 A). This fragment was ligated into the pSL301™ vector (InVitrogen) that was digested with SmaI and NotI and subsequently dephosphorylated with CIAP. This ligation reaction juxtaposed a vector

Figure 2.3 Construction of the plasmid pBSN93, containing the left flank of a targeting construct for the *Pea3* gene.

(A) Schematic diagram of *Pea3* showing the relevant restriction sites. Exons 5 and 6 are marked as green boxes. A 6.0 kb *NcoI* fragment was excised from the λ 93 clone and rendered blunt ended with Klenow fragment. **(B)** The *NcoI* fragment was ligated into the *EcoRV* digested, CIAP treated plasmid pBluescript™. This cloning step juxtaposed the *NcoI* site present in exon 6 to the *EcoRI* site present in the vector's polylinker.

A



B

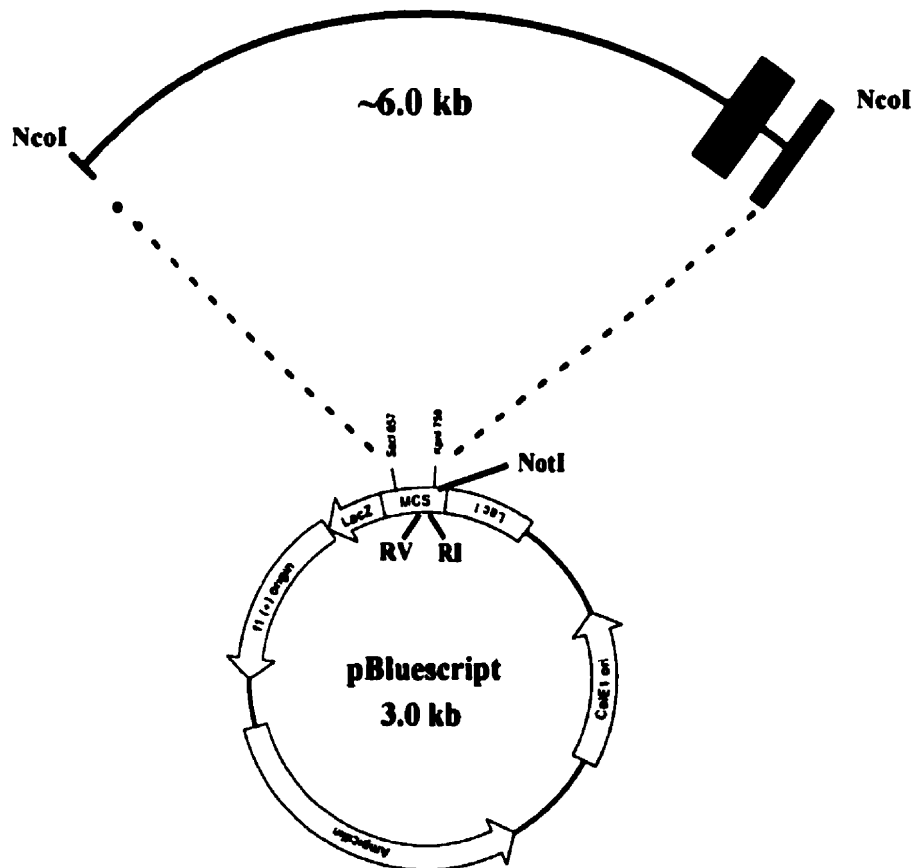


Figure 2.4 Construction of the plasmid pSLSN31, containing the right flank of a targeting construct for the *Pea3* gene.

(A) Schematic diagram of *Pea3* showing the relevant restriction sites. Exons 12 and 13 are marked by blue boxes. A ~ 10.8 kb *Sna*BI-*Not*I fragment was excised from the λ 31 clone. The *Sna*BI site was an endogenous site located between exons 11 and 12; the *Not*I site was derived from the right hand side of the multicloning site in the λ DashII[™] vector. **(B)** The 10.8 kb *Sna*BI-*Not*I fragment was ligated into the *Sma*I/*Not*I digested, CIAP treated plasmid pSL301[™]. This cloning step juxtaposed a vector derived *Sal*I site to the (*Sma*I/*Sna*BI) site immediately 5' to exon 12.

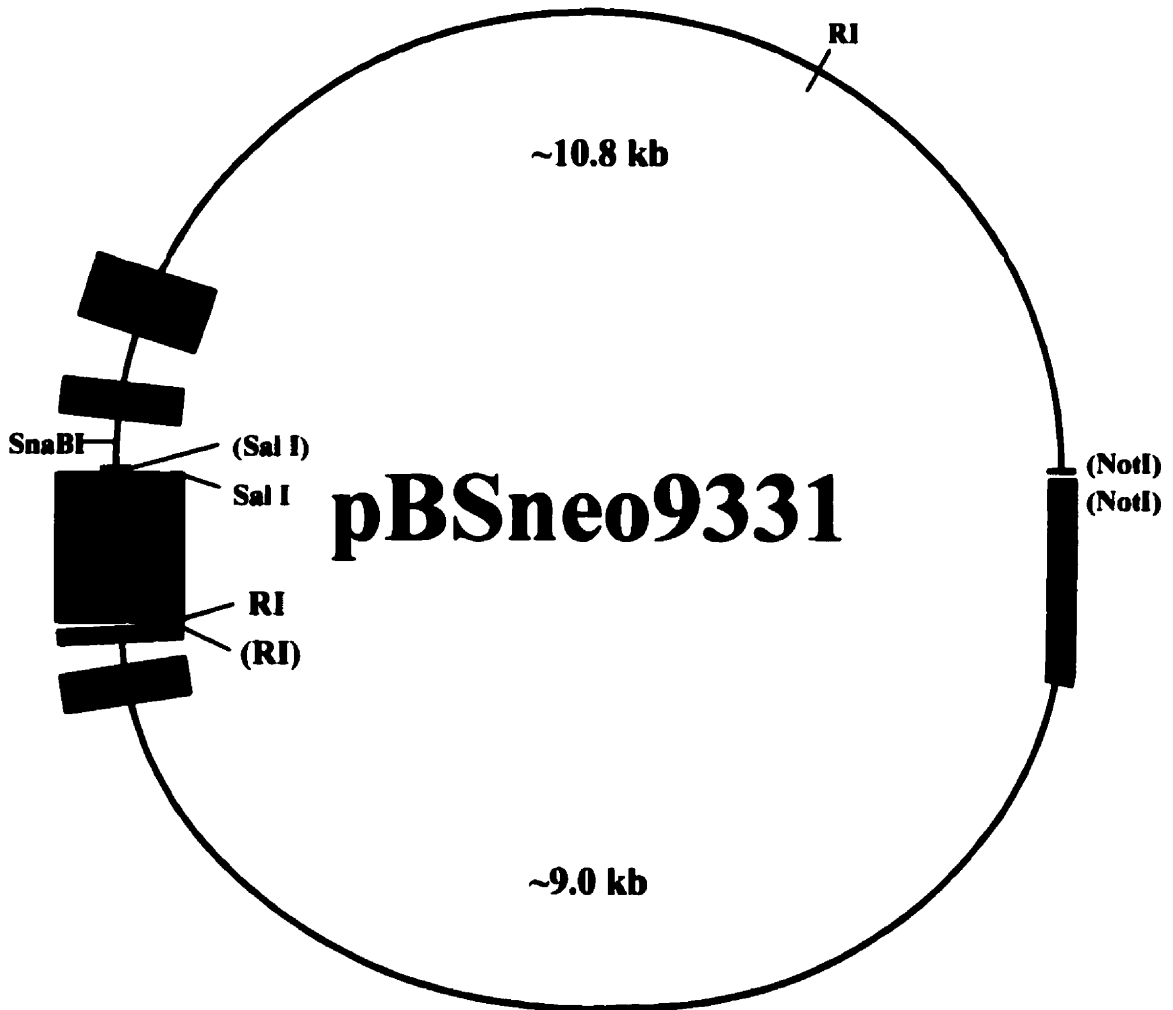
derived *Sall* site to the 5' border of the right flank fragment while maintaining the *NotI* site at its 3' border. This plasmid was referred to as pSLSN31 (figure 2.4 B).

The final knock-out construct was generated by a directional cohesive end triple ligation. pBSN93 was digested with *EcoRI* and *NotI*; this fragment maintained the pBS vector providing the plasmid backbone for the targeting construct as well as its left flank (figure 2.3). pSLSN31 was digested with *Sall* and *NotI*; the 10.8 kb *Sall-NotI* fragment was isolated and used as the right flank of the targeting vector (figure 2.4). The final fragment, the PGKneoPA cassette, was excised from the plasmid pKJ1(*Sall*) as a 1.7 kb *EcoRI-Sall* fragment (McBurney et al. 1991). These three fragments were mixed together in equimolar ratios and ligated. The resulting targeting construct, pBSneo9331, could be linearized by *NotI* restriction digestion (figure 2.5).






A double recombination event at the *Pea3* locus would result in the deletion of exons 7 through 11 (figure 4.1 A). Since the PEA3 ETS DNA binding domain was encoded in exons 11, 12 and 13, this construct would delete the first 38 a.a.s of this domain including two of its essential tryptophan residues. This design would insure that any truncated proteins produced from this locus would not be capable of binding to the PEA3 cis element 5'-AGGAAG-3' (Martin et al. 1988). Hence, the predicted homologous recombination event should yield a null allele.

Figure 2.5 Ligation strategy used to construct the targeting vector pBSneo9331, designed to generate a null allele at the *Pea3* locus.

The plasmid pBSN93 was digested with EcoRI and NotI; this digest retained the pBS vector and the left flank sequences in a single 9.0 kb DNA fragment (exons 5 and 6 = green boxes, pBS sequences = thick black line). The plasmid pKJ1(SalI) (McBurney et al., 1991) was digested with EcoRI and SalI releasing a 1.7 kb fragment containing the PGKneoPA positive selection cassette (red box, direction of transcription marked by black arrow). The plasmid pSLSN31 was digested with SalI and NotI to release the 10.8 kb right flank containing exons 12 and 13 (blue boxes). These three DNA fragments were mixed together in equimolar ratios and ligated in a single reaction to generate the targeting construct pBSneo9331. This construct could then be linearized with NotI.



Legend

-  Exons of left flank
-  Exons of right flank
-  PGK neo PA
-  pBluescript
-  Introns

2.16 Embryonic Stem (ES) Cell Culture.

ES cell culture was carried out according to the basic methods outlined (Robertson, 1989). ES cells and embryonic fibroblasts were incubated @ 37°C under an atmosphere of 5% CO₂ in humidified Water Jacketed™ cell culture incubators (Forma-Scientific). ES cells were cultured on feeder layers derived from G418 resistant primary embryonic fibroblasts in order to maintain their totipotency.

Primary embryonic fibroblasts were generated by the following protocol provided by Dr. M. Rudnicki: β2m male mice (which express the neo positive selection marker in all tissues) were mated with female mice (Balb/C). Pregnant females were sacrificed on day 14 of embryonic development. The uterine horns were dissected from the female using sterile technique and placed in a sterile 10 cm tissue culture dish. The embryos were then dissected away from the uterine tissue and each embryo placed into individual 10 cm tissue culture dishes. Their heads and internal organs were removed and the carcasses rinsed with 10 ml of sterile PBS.

The PBS was removed and 5ml of 0.25% trypsin/ 1mM EDTA added to each plate and the carcasses minced using either watchmaker's forceps (#5's) or a scalpel. The plates were then incubated @ 37°C for 30 min. The tissue was pipetted up and down until it dispersed completely. 5 ml of standard tissue culture medium supplemented with 10% FBS (Gibco-BRL) and 1 X penicillin/ streptomycin (Gibco-BRL) (DMEM/ 10% FBS) was added to each. The samples were transferred to 15 ml tubes and centrifuged @ 1000 rpm for 5 min @ RT (Sorvall RT6000B, Dupont).

The cell pellets were resuspended in DMEM/ 10% FBS and the cells from each carcass plated onto 3 X 10 cm culture dishes. The plates were incubated for ~48 (until they reached confluence). At this point, each plate was treated with 2 ml of 0.25% trypsin/ 1mM EDTA and the cells dispersed by pipetting. The trypsin was inhibited with the addition of 8 ml of DMEM/ 10% FBS and cells collected by centrifugation as above. The cells from individual plates were resuspended in 1.5 mls of cell freezing medium (DMEM/ 20% FBS/ 10% DMSO), placed in 2 ml cryovials (Dow-Corning) and stored @ -80°C or in N₂(l) until needed.

Fibroblast feeder cells were generated from these frozen primary embryonic fibroblasts. Vials were thawed, rinsed in 10 ml of PBS (equilibrated to 37°C), resuspended in DMEM/ 10% FBS and plated out onto 3 X 10 cm culture dishes. The fibroblasts were grown to confluence (~3-4 days) and each 10 cm plate passaged onto 12 X 10 cm plates. When these plates reached confluence (~4-5 days), the culture medium was removed and replaced with 5 ml of DMEM/ 10% FBS supplemented with 1 µg/ml of mitomycin C (Sigma Chemical Co.) and incubated for 2-3 hr. This medium was removed and each plate rinsed 3 X with 5 ml PBS. The plates were trypsinized with 2 ml trypsin/EDTA per plate and the cells collected in DMEM/ 10% FBS. The cells were then counted on a haemocytometer.

The feeder layers were prepared by diluting the cells to 3 X 10⁵ cells/ ml in DMEM/ 10% FBS and plating them onto 10 cm culture dishes at a density of 5 x 10⁴ cells/ cm². However, prior to plating, the 10 cm culture dishes were coated with 0.1% gelatin (Swine Skin type I, Sigma). The feeder layers were then incubated overnight where they

adhered as a monolayer to the bottom of the gelatinized culture dishes. At this point, the mitotically inactivated feeder layers were ready for use.

The J1 ES cell line (derived from mouse strain 129/sv) was used in this study and was provided by Dr. M. Rudnicki. ES cells were cultured in DMEM (high glucose, no pyruvate, low Na-bicarbonate) (Gibco-BRL), 15 % Fetal Bovine Serum (FBS) (Hyclone), supplemented with non-essential amino acids (Gibco-BRL), L-glutamine (Gibco-BRL), penicillin and streptomycin (Gibco-BRL), 3.5 μ l of β -2mercaptoethanol/500ml culture medium, 500 units/ ml of Leukemia Inhibitory Factor (LIF) (ESGRO™, Gibco-BRL) and 250 μ g/ml Geneticin (Gibco-BRL). J1 ES cells were plated out @ 5 X 10⁵ cells/ml per 10 cm tissue culture plate. The media was changed every 24 hr and the cells passaged on every third day maintaining ES cell density @ 5 X 10⁵ cells/ ml per 10 cm plate.

2.17 Electroporation of ES Cells and Isolation of ES Cell Clones Targeted via Homologous Recombination at the *Pea3* Locus.

ES cells were treated with trypsin-EDTA for 5 min @ 37°C (2 ml/10 cm plate), dispersed by pipetting, and then added to a 15 ml tube containing 8 ml of complete ES medium (section 2.14). The cells were counted and then collected by centrifugation @ 1000 rpm for 5 min @ RT (Sorvall™ RT 6000B, Dupont). The cells were resuspended in electroporation buffer (20 mM Hepes pH 7.0, 137 mM NaCl, 5 mM KCl, 0.7 mM Na₂HPO₄, 6 mM D-glucose, 0.1 mM β -mercaptoethanol) at 1.0 X 10⁷ cells/ 0.8 mls.

The 0.8 ml samples (1 X 10⁷ cells) were then mixed with 25 μ g (200 μ l vol. in sterile dH₂O) of pBSneo9331-14 digested with the enzyme NotI (section 2.7). This 1.0 ml

sample was placed into a 0.4 cm gap electroporation cuvette (BioRad) and subjected to electroporation in a Gene Pulser™ (BioRad) set @ 400 Volts and 25 μ F. Immediately after samples were pulsed, they were added to 5 ml of complete ES media (no G418), and then aliquoted onto 6 X 10 cm culture dishes containing feeder layers and 9 mls of complete ES media (no G418) (section 2.14). The post-electroporation ES cells were cultured for 24 hrs without G418 to allow the cells to recover from the electroporation procedure and to allow for the expression of the positive selection cassette (PGKneoPA, section 4.2.2).

After the recovery period was complete, the media was aspirated off the cells and the plates rinsed with PBS (10 ml/10 cm plate). At this point, 10 mls of complete ES media supplemented with 200 μ g/ml Geneticin (Gibco-BRL) was added to each 10 cm plate. The media was changed every day and the ES colonies were allowed to grow to a diameter appropriate for picking (~ 8-12 days). ES cell colonies were picked directly off the 10 cm plates in a 5 μ l vol. using a Gilson™ P-20 pipette aid. Each colony was placed into a single well of a 96 well (U-well) culture dish containing 100 μ l of 0.25% trypsin-EDTA.

The samples were incubated for 5 min @ 37°C and then dispersed by pipetting the samples up and down. 30 μ l of each individual sample was added to individual wells of a 96 well (flat-well) culture dish (gelatinized, containing a feeder layer) containing 170 μ l of complete ES media (no G418). The cells on this 96 well plate were cultured for 24 hrs at which time the media was aspirated off and replaced with complete ES media supplemented with 200 μ g/ml G418 (200 μ l vol/well). The cells were cultured for 3-4 days under selection with daily media changes.

The media was then aspirated off, the cells washed with PBS and 80 μ l of trypsin-EDTA added to each well. The plate was incubated @ 37°C for 7 min. The cells were then dispersed by gentle pipetting using a multichannel pipette aid. 80 μ l of 2X freezing medium (20% DMSO, 20% FBS, DMEM) was added to each sample and each sample overlaid with ~20 μ l of sterile ultr-pure light mineral oil (Sigma). The edges of the 96 well dish were sealed with parafilm™ and the plates stored at -80°C until needed. These plates were used for growing up ES clones that have been genotyped (section 2.17).

The remaining 70 μ l from each original sample was added to individual wells of a 24 well tissue culture dish (gelatinized, no feeder layers) containing 1.5 mls of complete ES medium (no G418). The media was changed every 24 hrs and the cells cultured until each well was confluent (~3-4 days). These cells were used to isolate genomic DNA for genotype analysis (section 2.3 and 2.17) of the colonies frozen on the 96 well plate.

2.18 Generation of Chimeric Mice via Blastocyst Injection.

Chimeric mice were generated by the technique of blastocyst injection essentially as described (Bradley, 1987). Briefly, ES cells harbouring the PEA3 null allele were injected into the blastocoel of 3.5 d.p.c Balb/c blastocysts. These injected blastocysts were then transferred into the uterine horns of pseudo-pregnant BVD females. Recipient females were rendered pseudo-pregnant by mating them with vasectomized stud males; the recipients were then used at 2.5 d.p.c. The resulting male chimera was subsequently mated with Balb/c females generating the outbred mouse line referred to as D.D1 and with 129/sv females generating the inbred mouse line referred to as D.D1/sv.

2.19 Genotype Analysis of ES Cell Clones and Mouse Tail DNA.

Individual ES cell clones were grown to confluence on gelatinized 24 well culture dishes (section 2.15). The media was aspirated from the wells and each monolayer rinsed with 1.5 ml of PBS. 0.5 ml of lysis buffer (100mM Tris-Cl pH 8.5, 5 mM EDTA pH 8.0, 0.2 % SDS, 200 mM NaCl, 100 μ g Proteinase K/ml) was then added to each well. Lysis and digestion were complete after an overnight incubation @ 37°C. Tail DNA samples (0.5 mm biopsy) from individual mice were placed in 1.5 ml tubes and treated in an identical fashion except that overnight incubation was carried out @ 55°C.

The genomic DNA was precipitated by adding 0.5 ml of Propan-2-ol to each sample and subjecting them to gentle agitation. Prior to precipitation, the tail samples were centrifuged at 12000 rpm to remove residue. Genomic DNA was then collected with a toothpick and the DNA resuspended in 100 μ l of sterile dH₂O. The samples were pipetted up and down repeatedly using a P-200 (#115 or #110 yellow tip) until the DNA ran easily through the end of the tip (Laird et al. 1991).

Two separate restriction digests were employed to confirm the presence of a homologous recombination event at the *Pea3* locus. Firstly, a ClaI-EcoRI digest would generate a wild type fragment of ~8.21 kb and a recombinant fragment of ~7.46 kb. These restriction fragments were detected by Southern blot analysis using an 840 bp ClaI/KpnI probe residing just 5' to the left flank of the knock out construct (figure 4.1A). Secondly, exon 2 of genomic PEA3 contains an EagI site. A homologous recombination event would introduce a second EagI site (present in the PGKneoPA cassette) into this locus. Hence, an EagI digest would be expected to generate a ~10 kb recombinant

fragment that could be detected in a Southern blot using the same 840 bp probe (figure 4.1A & B). The *Cla*I/ *Eco*RI digest was carried out in a 30 μ l vol. (3 μ l 10 X Buffer H (Boehringer Mannheim), 40 U *Cla*I (1 μ l vol., Boehringer Mannheim), 50 U *Eco*RI (1 μ l vol., Gibco-BRL), 4 μ l genomic DNA, 21 μ l sterile dH₂O). The reactions were incubated for \geq 12 hrs @ 37°C. The *Eag*I digests were carried out as above using 40 U of *Eag*I (1 μ l vol., NEB) and 3 μ l of the commercially supplied 10 X restriction digestion buffer.

2.20 Histological Preparation of Organs and Tissues.

Dissected organs and tissues were fixed overnight in 4 % PFA/ PBS @ 4°C. After fixation, the samples were dehydrated through a graded series of ethanol baths (3 X 20 min in 50 % EtOH, 3 X 20 min in 70 % EtOH, 3 X 20 min in 95 % EtOH and 3 X 20 min in 100 % EtOH). The samples were then placed in xylenes (4 X 10 min) and then incubated in a 50 % xylenes/ 50 % paraffin wax mixture @ 60°C. This was followed by incubation in molten paraffin (3 X 1 hr @ 60°C). The paraffin impregnated tissues were then oriented and embedded in paraffin blocks for sectioning.

Samples were sectioned on a standard microtome at a thickness of 4.0 μ m to 8.0 μ m. Sections were subsequently counterstained with haematoxylin and eosin. Coverslips were mounted with Permount™ mounting medium (Fischer Scientific). A significant proportion of the histological preparations shown in this thesis were carried out as a service in the anatomical pathology laboratory at the McMaster University Health Sciences Center.

2.21 *In-Vitro* Fertilization Analysis.

In vitro fertilizations were carried out in the laboratory of Dr. Barry Hinton (Dept. of Cell Biology, University of Virginia). The *In-Vitro* fertilization methods employed in this study were essentially as described (Bleil, 1991). Briefly, outbred female ICR mice (Hilltop Breeders) were superovulated by serial intraperitoneal injections of 5 IU of PMSG (Sigma) and 5 IU of hCG (Sigma) 48 hr apart. Males (ICR retired breeders, PEA3 +/+ & PEA3 -/-) were sacrificed 12 hr after hCG injections and their cauda epididymides placed in 250 μ l drops of media (M199 with 4 mg/ml BSA and 3.5 mM sodium pyruvate) covered with paraffin oil.

The epididymides were minced with watchmakers forceps; the sperm were allowed to swim for 15 min @ 37°C. The entire drop, less the epididymal tissue, was placed under 1.5 ml of media in a 12 ml culture tube (Falcon); the sperm was allowed to capacitate for at least 45 min @ 37°C. Capacitated sperm (1×10^6 /ml) was collected from the upper one quarter of the swim-up medium and placed under oil in 100 μ l drops. Cumulus-enclosed egg masses were isolated from the oviducts of sacrificed females 13 hrs post hCG injection. The masses were placed under oil in 200 μ l drops containing M199 with 0.5 mg/ml hyaluronidase (Sigma) for 5 min @ 37°C to remove cumulus cells.

The cumulus-free eggs were then washed 5 X and co-incubated with sperm (15-30 eggs per drop) for 3 hrs. The eggs were then washed 3 X, placed in fresh medium and cultured for 20 hr at 37°C and 5 % CO₂. Following overnight incubation, eggs which had undergone cleavage were scored as fertilized while one celled oocytes were scored as unfertilized. Observations were recorded using an Olympus S-30 dissecting microscope.

2.22 In-Vivo Fertilization Analysis.

Female Balb/c mice (Harlan Laboratories) were superovulated by serial intraperitoneal injections of 5 IU of PMSG (Sigma) and 5 IU of hCG (Sigma) 48 hr apart. Individual females were then paired with individual male mice; the mating pairs were left together overnight. The following morning the female mice were removed and examined for the presence of a copulatory plug. Females were routinely examined for the presence of spermatozoa in their uterine horns and vagina. Briefly, females were sacrificed and their uterine horns and vagina flushed with 300 μ l of 1 X PBS containing dilute haematoxylin. The fluid was placed on glass slides, coverslipped and examined for the presence of spermatozoa using phase contrast microscopy (Leitz Labovert FS).

Pronucleation was scored as follows: Cumulus egg masses were dissected from the oviducts and placed in 3 ml of M2 medium containing 0.5 mg/ml hyaluronidase (Sigma) for 5 min @ RT. The cumulus-free eggs were then washed by transferring them through 3 X 3 ml of M2 medium @ RT and transferred to 3 ml of M19 medium in a 35 mm tissue culture dish. The oocytes were cultured for 24 hrs @ 37°C under 5 % CO₂. Eggs that had undergone cleavage were scored as pronucleated; those that remained single celled were scored as non-pronucleated.

M2 and M19 oocyte culture media were prepared as described (Hogan et al., 1986). M2; 50 ml recipe: (39.0 ml dH₂O, 5.0 ml solution A, 0.8 ml solution B, 0.5 ml solution C, 0.5 ml solution D, 4.2 ml solution E, 0.2 gm BSA (Sigma)). M19; 50 ml recipe: (39.0 ml dH₂O, 5.0 ml solution A, 5.0 ml solution B, 0.5 ml solution C, 0.5 ml solution D, 0.2 gm BSA (Sigma)). Solution A; 100 ml (5.53 gm NaCl, 0.35 gm KCl, 0.16

gm KH_2PO_4 , 0.29 gm $\text{MgSO}_4 \cdot 7\text{H}_2\text{O}$, 4.34 gm Na-Lactate (60% syrup, Sigma), 1.00 gm Glucose, 0.06 gm penicillin, 0.05 gm streptomycin). Solution B; 100 ml (2.10 gm Na-Bicarbonate, 0.01 gm phenol red). Solution C; 10 ml (0.036 gm Na-pyruvate). Solution D; 10 ml (0.25 gm CaCl_2). Solution E; 100 ml (5.95 gm HEPES, 0.01 gm phenol red, pH to 7.4 with NaOH). The above stock solutions are filter sterilized (0.22 μm filters) and stored at 4°C.

2.23 Betagalactosidase Staining of the Epididymides.

The epididymides were dissected from male mice and fixed for 4 hr in 4 % PFA/PBT. After fixation, the samples were washed 3 X 20 min in 5ml PBT and subsequently incubated @ 37°C in X-gal staining solution (1 X PBT containing 1 mg/ml X-gal, 5 mM $\text{KFe}_3(\text{CN})_6$, 5mM $\text{KFe}_4(\text{CN})_6$ and 2 mM MgCl_2) for 1 hr. The samples were then washed 2 X 10 min in 5 ml PBT, cleared in 50 % glycerol/ PBT for 15 min and then stored in 80% glycerol/ PBT @ 4°C. The samples were photographed using a Wild MC3 stereo dissecting microscope mounted with a Wild MPS51 35 mm camera and a Wild MPS45 Photoautomat automatic exposure system.

2.24 Determination of Hormone Concentrations by Radio Immuno-Assay (RIA).

Determination of hormone concentrations in male mice was carried out by the laboratory of Dr. Barry Hinton at the University of Virginia. Blood was collected from each mouse from the inferior vena cava using a 21 G needle attached to a 3 ml syringe containing 0.1 ml heparin. Blood was transferred to a 1.5 ml and centrifuged for 15 min

@ 4°C. Plasma was collected and stored @ -20°C. Levels of Luteinizing hormone (LH) and follicle-stimulating hormone (FSH) in each plasma sample was measured by RIA using reagents provided by the National Hormone and Pituitary program of NIDDDH.

Anti-rat LH (S-11), anti-rat FSH (S-11) and reference preparations RP-3 (LH) and RP-2 (FSH) were used in these assays. The intrassay coefficient of variation for the quality controls ranged from 6.65 to 13.99 % for LH and 6.2 to 14.3 % for FSH. Testosterone concentrations in plasma were measured by RIA using antibody-coated tubes manufactured by ICN Biomedicals (Costa Mesa, CA). The assay had a sensitivity of 0.22 ng/ml and less than 7.8 % reactivity with other relevant hormones including dihydrotestosterone. The intrassay coefficient of variation for the quality controls ranged from 2.5 to 8.2 %.

2.25 Expression of PEA3 in Various Embryonic Fibroblast Cell Lines.

Immortalized embryonic fibroblasts were derived from embryos harvested at day 13.5 d.p.c. by standard methodologies (Todaro and Green. 1963) and were established by Laura Hastings, a research technician in the laboratory of Dr. J.A. Hassell. These cell lines were grown in DMEM and 10% calf serum until ~ 80% confluence on 100mm plates. The monolayers were washed with ice cold PBS and harvested by scraping. The cells were centrifuged and nuclear extracts prepared using the method of Lee et al. 1988. 25 µg of nuclear extract was electrophoresed on a 10% SDS-polyacrylamide gel and transferred to a nylon membrane. The membrane was blocked with 5% skim milk in TBST, incubated with PEA3 specific monoclonal antibodies MP-13 and MP-16, followed by horse radish peroxidase-conjugated goat anti-mouse secondary antibody (Kirkegaard

and Perry Laboratories). The western blots were developed by chemiluminescence (Boehringer Mannheim). The western blot analysis was carried out by Dr. Richard Tozer.

2.26 Whole Mount Preparations of Mammary Glands.

Whole mount mammary gland preparations were carried out as described (Vonderhaar et al. 1979). Briefly, mammary glands were dissected from female mice and the tissue spread out on a glass slides and air dried at room temperature overnight. The glands were then fixed and defatted via an overnight incubation in acetone. The glands were then stained overnight in Harris' modified haematoxylin. The preparations were then destained by incubating them in destain solution (1% HCl in 75% EtOH). The stain was subsequently fixed by incubation in 0.002% NH_4OH for 30 s. The preparations were then dehydrated in 75% EtOH for 5 min and 100% EtOH for several hrs. Lastly, the preparations were cleared by incubation in xylenes overnight and mounted with coverslips using Permount™ mounting medium. The whole mount preparations shown in figure 4.7 were carried out by Lesley MacNeil, a graduate student in the laboratory of Dr. J.A. Hassell.

CHAPTER 3

EXPRESSION PATTERN OF THE PEA3 GROUP mRNAs DURING MOUSE EMBRYONIC DEVELOPMENT

3.1 INTRODUCTION.

Many of the *ETS* genes have proven to be developmentally regulated (section 1.4.3). Furthermore, mutations within many *ETS* genes have been associated with the induction of human malignancies (section 1.4.2). A subset of these transcription factors appear to contribute to the invasive and/or metastatic potential of a given tumor (section 1.4.3). Interestingly, many of the biological properties that *ETS* genes confer upon a tumor appear to recapitulate their normal developmental functions (sections 1.4.2; 1.4.3). Hence, establishing the developmental expression patterns for the *ETS* genes has helped to elucidate their roles in normal embryonic development and in affecting tumor induction, invasion and metastasis.

The *ETS* family has been subdivided into subfamilies based upon the degree of a. a. sequence conservation within the ETS DNA binding domain (section 1.4.4). PEA3 is the founding member of the PEA3 group which also includes ERM and ER81. This group shares ~95% a.a. identity within their ETS domains and an overall a.a. identity of ~50% (de Launoit et al. 1997). This fact implies that all three proteins are capable of transactivating an overlapping set of target genes. Mutations in both *PEA3* (*E1A-F*, *ETV4*)

and *ER81 (ETV1)* have been found in Ewing's sarcomas and PNETs (Kaneko et al. 1995; Urano et al. 1996; Jeon et al. 1994). Both PEA3 and ER81 over-expression has been correlated with human metastatic breast cancer (Benz et al. 1997; reviewed by de Launoit et al. 1997).

Furthermore, the PEA3 group proteins have been linked to tumor cell invasion and metastasis (section 1.5.2). Interestingly, a subset of the PEA3 group target genes are members of the *Mmp* family of secreted proteases. The current body of evidence suggests that the PEA3 group proteins confer invasive or metastatic potential upon a tumor cell by up-regulating the expression of specific *Mmps* (1.5.2; reviewed by de Launoit et al. 1997). However, this hypothesis has been based largely on the fact that their expression correlates with invasive or metastatic potential. Direct evidence has thus far been lacking; however, a recent study has now provided more direct proof that PEA3 is capable of conferring an invasive phenotype upon MCF-7 cells. Furthermore, PEA3 expression in this system was correlated with elevated levels of MMP-9 (Kaya et al. 1996).

The PEA3 group proteins all demonstrated an increased transactivation potential in the presence of activated Ras and/or Erk kinases (Janknecht et al. 1996; O'Hagan et al. 1996). These results implied that the PEA3 group proteins may be regulated by similar if not identical signal transduction pathways (section 1.3). Furthermore, this data suggested that they may be regulated by growth factor receptor tyrosine kinases (section 1.3.1). Activated growth factor receptor tyrosine kinases have been linked to many types of cancer. However, the signal transduction pathways that regulate the activity of the PEA3 group proteins *in-vivo* have yet to be identified. Hence, we do not yet understand the

functional significance of the expression of the PEA3 group proteins, and specifically PEA3, with respect to human breast cancer. Furthermore, we do not yet understand which signalling molecules regulate their activity.

In order to gain more insight into the role of the PEA3 group proteins in affecting tumorigenesis, we elucidated their expression patterns during embryonic development. In this study, I determined the embryonic expression patterns for PEA3, ERM and ER81 from early post-implantation (~ 7.0 d.p.c.) through to organogenesis (13.0 d.p.c.). This information will allow us to identify common biological properties amongst the different cell populations that express the PEA3 group proteins. Furthermore, we will be able to identify some of the potential functions of these proteins during normal embryonic development. This information will be useful in helping to establish their roles in affecting tumorigenesis.

Lastly, we will be able to compare the expression patterns of the PEA3 group members with the expression patterns of different growth factors and growth factor receptors. This analysis will help us identify potential *in-vivo* signalling pathways that regulate the activity of the PEA3 group members during normal development and in the genesis of human cancers.

During the course of carrying out the expression analysis of the PEA3 group genes, a group from France published an expression study of this group (Chotteau-Lelievre et al. 1997). Their study included the stages from 9.5 d.p.c. through 15.5 d.p.c of mouse development. The analysis in this thesis has covered embryonic development from ~ 7.0 d.p.c. through to 13.0 d.p.c. and therefore includes novel information regarding the role

that these genes play in early post-implantation development. Furthermore, at the stages where our studies overlapped, our expression analysis revealed many sites of PEA3 expression that were not reported in the above study. A more recent study also published the developmental expression pattern for the zebrafish homologue of PEA3 (Brown et al. 1998). The results from this distant species provide an opportunity to establish how its expression pattern has changed through the course of evolution. Hence, the expression analysis carried out by myself lends support to the published studies. Furthermore, it has generated novel information concerning the expression patterns of the PEA3 group genes and hence their potential functions during embryonic development.

3.2 RESULTS.

3.2.1 PEA3 is expressed throughout the post-implantation stages of murine embryonic development.

Total embryonic RNA was isolated from mouse embryos from 7.0 days post coitus (d.p.c.) through 15 d.p.c. and analyzed for expression of the PEA3 mRNA. Northern blot analysis revealed that PEA3 was expressed from 8 d.p.c. through 15 d.p.c. (figure 3.1 A, upper panel, lanes 3-10). RNA extracted from FM3A cells served as a positive control for the presence of the PEA3 message (figure 3.1 A, upper panel, lane 1). It was difficult to discern if there was a PEA3 specific signal present at 7 d.p.c. (figure 3.1 A, upper panel, lane 2). PEA3 expression levels appeared to be stable throughout development as illustrated by the levels of β -actin RNA in the samples (figure 3.1 A, lower panel). The

higher level of PEA3 RNA detected in the 13 d.p.c. sample was a result of overloading as indicated by the β -actin internal control (figure 3.1 A, lane 8).

RNAse protection analysis was performed using the same RNA samples. It confirmed that PEA3 was expressed from 8 d.p.c. through 15 d.p.c. (figure 3.1 B, lanes 3-10). Furthermore, this analysis revealed that PEA3 was expressed at 7 d.p.c. (figure 3.1 B, lane 2). Again, FM3A RNA served as a positive control for PEA3 expression in this experiment (figure 3.1 B, lane 1). An antisense riboprobe directed against the ribosomal pseudogene *rp/32* served as an internal control in these hybridizations (figure 3.1 B, lower panel) (Dudov et al. 1984). Hence, PEA3 was expressed from mid-gastrulation (~7 d.p.c.) through to organogenesis (15 d.p.c.) during murine embryonic development. In order to define the tissue specificity of PEA3 expression, we subjected embryos from ~7/7.5 d.p.c. through 13 d.p.c. to the whole mount *in-situ* hybridization protocol.

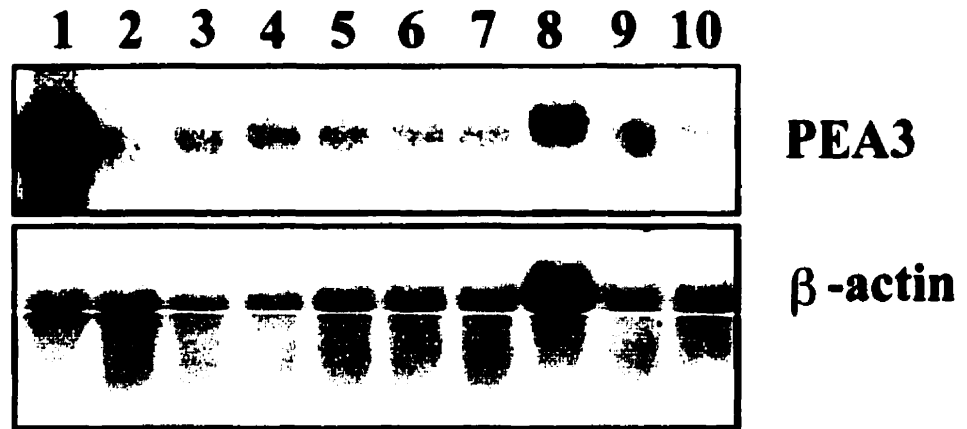
3.2.2 PEA3 expression in the gastrulating embryo (~7.0-7.5 d.p.c.).

Northern blot and RNAse protection analysis revealed that PEA3 was expressed during the gastrulation stages of embryonic development (~7.0-7.5 d.p.c.). Whole mount *in-situ* hybridizations were carried out on 7.0 d.p.c. and 7.5 d.p.c. embryos using the above PEA3 riboprobe. PEA3 was expressed in the posterior half of early to mid-primitive streak stage embryos (~7.0/7.5 d.p.c.) caudal to the node (figure 3.2 A, yellow arrow). A posterior view of this embryo revealed that PEA3 was expressed in a bilateral pattern along the entire length of the proximal-distal (PD) axis (figure 3.2 B, yellow arrow). Serial transverse sections through this embryo revealed that the PEA3 expression signal was

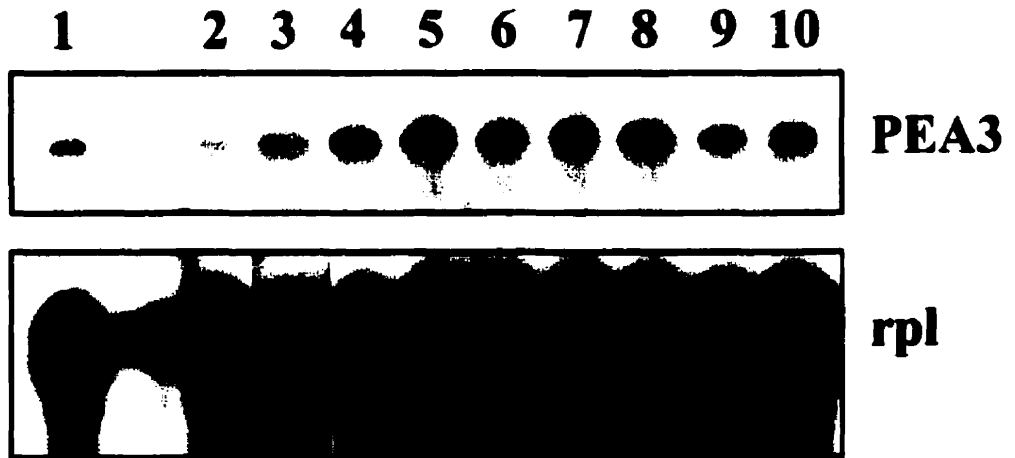
Figure 3.1 Analysis of PEA3 mRNA expression during the post-implantation stages of murine embryonic development.

(A) Northern blot of total embryonic RNA hybridized with a full length PEA3 cDNA probe (upper panel). This blot was stripped and rehybridized with a mouse β -actin probe to control for loading (lower panel). Each lane contains 20 μ g of total RNA. (B) RNase protection of total embryonic RNA with an antisense PEA3 riboprobe (upper panel). These samples were concurrently hybridized with an internal control riboprobe generated from the ribosomal pseudogene *rp132* (lower panel). Each lane contains 30 μ g of total RNA. For both A and B, lane 1 = FM3A cells; lane 2 = 7 d.p.c.; lane 3 = 8 d.p.c.; lane 4 = 9 d.p.c.; lane 5 = 10 d.p.c.; lane 6 = 11 d.p.c.; lane 7 = 12 d.p.c.; lane 8 = 13 d.p.c.; lane 9 = 14 d.p.c.; lane 10 = 15 d.p.c.

A



B



restricted to the epiblast or primitive streak ectoderm along the length of the PD axis (figure 3.2 C to F, yellow arrows). Furthermore, its signal was not detected in ectodermal derivatives rostral to the node or in the mesoderm (figure 3.2 C to F, blue & light green arrows respectively).

This observation also held true in the mid to late primitive streak stages of gastrulation (~7.5 d.p.c.) just prior to the onset of the segmentation of the paraxial mesoderm. PEA3 expression was again confined to the posterior half of the embryo caudal to the node (figure 3.3 A & C, yellow arrows). Serial transverse sections through this embryo confirmed that PEA3 expression was restricted to the primitive streak ectoderm along the length of the PD axis (figure 3.3 to G, yellow arrows). Furthermore, PEA3 was not expressed in the rostral most regions of the posterior neural folds (figure 3.3 H & I, yellow arrows). Hence, PEA3 appeared to be expressed in epiblast cells that were being recruited to the primitive streak during gastrulation. Again, PEA3 was not detected in the rostral neural ectoderm, head mesenchyme or the mesendodermal cells that had ingressed through the primitive streak (figure 3.3 to G, blue & light green arrows respectively).

3.2.3 PEA3 expression pattern in the 8.0 d.p.c. (3-5 somite pairs) embryo.

PEA3 expression was detected in four distinct cell populations derived from all three germ layers within the 8.0 d.p.c. embryo (figure 3.4). Both side and posterior views of this embryo showed that PEA3 was expressed at in the rostral half of the embryo in a region just behind the developing heart (figure 3.4 A & B, blue arrows). PEA3 was

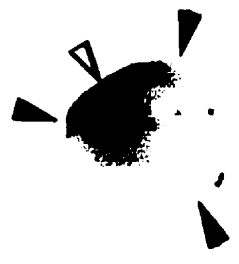
Figure 3.2 Expression pattern of the Pea3 mRNA in the 7/7.5 d.p.c. embryo.

(A) Side view of a whole mount embryo hybridized with antisense PEA3. (B) Posterior view of embryo in A. (C through F) Serial transverse sections of the embryo from A; the schematic next to (A) shows the position of each section from C through F in lower case. (red arrow = the rostral headfold region of the embryo; dark green arrow = caudal end of the embryo; yellow arrow = the ectoderm of the primitive streak, the site of PEA3 expression; black arrow = the approximate position of the node; white arrow = primitive streak; blue arrow = headfold ectoderm; light green arrow = headfold mesoderm). original magnification of A & B was 25X, the bar in B = 800 μm ; original magnification of C-F was 200X, the bar in F = 100 μm .

c
d
e
f

A musical staff with five horizontal lines. The letters 'c', 'd', 'e', and 'f' are written below the lines. A solid black shape is positioned above the lines, partially overlapping them.

A



B



C



D



E



F



detected at much higher levels in the posterior half of the embryo caudal to the newly formed somites within the lordotic region (figure 3.4 A & B, yellow arrows). The posterior expression pattern was again bilateral along the length of the primitive streak (figure 3.4 B, yellow arrow). Serial frontal sections through this embryo revealed that the rostral-most signal resulted from expression in the dorsal mesentery (mesocardium) of the developing heart (figure 3.4 C, white arrow), the mesenchyme of the rudimentary first branchial arch (figure 3.4 C & D, red arrows), and the endoderm lining the developing foregut (figure 3.4 D, blue arrow). PEA3 expression was not detected in the somites at this stage (figure 3.4 F, orange arrows). PEA3 expression in the posterior region of the embryo was again restricted to the ectodermal cells along the length of the primitive streak caudal to the node (figure 3.4 G & H, yellow arrows).

3.2.4 PEA3 expression pattern in the 9.0 and 9.5 d.p.c. embryo.

At 9.0 d.p.c., PEA3 was again detected in derivatives of all three germ layers. It was expressed in two locations within the CNS, the rostral tip of the prosencephalon (figure 3.5 A, B & F, dark green arrows) and in the region of the mesencephalon-rhombencephalon boundary (figure 3.5 A; light green arrow). The later signal was not detected in transverse sections through this region of the embryo; hence it could have resulted from expression in either the neural ectoderm or the head mesenchyme. PEA3 was expressed in the mesenchyme of the first and second branchial arches (figure 3.5 A to D, red arrows) and in the mesenchyme of the rudiments of the third pair of branchial arches (figure 3.5 F & G, red arrows).

Figure 3.3 Expression pattern of the PEA3 mRNA in the 7.5 d.p.c. embryo.

(A) Side view of a whole mount embryo hybridized with antisense PEA3. (B) Posterior view of the embryo in A. (C) Dorsal view of the embryo in A. (D through I) Serial transverse sections of the embryo in A; the schematic next to (A) shows the position of each section from D through I in lower case. (red arrow = the rostral headfold region of the embryo; dark green arrow = caudal end of the embryo; yellow arrow = the ectoderm of the primitive streak, the site of PEA3 expression; white arrow = primitive streak; blue arrow = headfold ectoderm; light green arrow = headfold mesoderm). Original magnification of A & B was 25X, the bar in C = 800 μm ; original magnification of D-I was 200X, the bar in I = 100 μm .

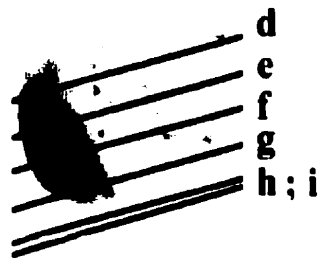
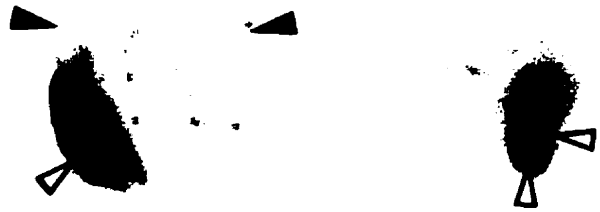
A**B****C****D****E****F****G****H****I**

Figure 3.4 Expression pattern of the PEA3 mRNA in the 8.0 d.p.c. (3-5 somite pairs) embryo.

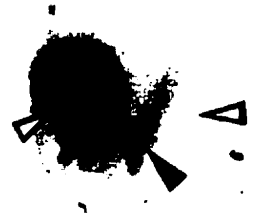
(A) Side view of a whole mount embryo hybridized with antisense PEA3. **(B)** Posterior view of the embryo in A. **(C through H)** Serial frontal sections through the embryo in A; schematic next to (A) shows the position of each section in C-H in lower case. (red arrow = the rostral end of the embryo in A, branchial arch mesenchyme in C and D; dark green arrow = caudal end of the embryo; yellow arrow = the ectoderm of the primitive streak; black arrow = the approximate position of the node; white arrow = heart; blue arrow = endoderm lining the gut; orange arrow = somites). Original magnification of A & B was 25X, the bar in B = 800 μm ; original magnification of C-H was 200X, the bar in H = 100 μm .



A



B



C



D



E



F



G



H



PEA3 was also detected in the first and second branchial membranes of the first and second pharyngeal pouches (figure 3.5 E, light blue arrows). PEA3 expression was detected in the forelimb bud mesenchyme just as they were initiating outgrowth along their PD axis (figure 3.5 A & C, pink arrows). Lastly, PEA3 was detected in bilateral stripes which had rostral borders at the caudal ends of the forelimb buds and continued caudally into the tailbud of the embryo (figure 3.5 A & C, white arrows). Transverse section revealed that these structures were the developing pronephric tubules (figure 3.5 F, G & H, white arrows). PEA3 was not expressed at detectable levels in the somites at this stage of development (figure 3.5 H, orange arrows).

The expression pattern at 9.5 d.p.c. was essentially identical to the pattern detected at 9.0 d.p.c. (compare figures 3.5 A & 3.6 A). However, at 9.5 d.p.c., PEA3 expression was detected in a bilateral segmental pattern along the rostral half of the neural tube (figure 3.6 A & C; orange arrows). Transverse sections localized this low signal to the sub-ectodermal regions of the dermamyotomes of the rostral somites (figure 3.6 F & G, orange arrows). Furthermore, expression was still detected in the rostral regions of the developing kidney (figure 3.6 A & H, white arrows) but had become more 'patchy' in its caudal regions (figure 3.6 A & I, white arrows).

3.2.5 PEA3 expression pattern in the 10.0 and 10.5 d.p.c. embryo.

PEA3 expression was still present in the region of the midbrain-hindbrain junction in both 10.0 and 10.5 d.p.c. embryos (figure 3.7 A & B, light green arrows). It appeared to be expressed equally on both sides of this boundary. PEA3 was also detected in both

Figure 3.5 Expression pattern of the PEA3 mRNA in the 9.0 d.p.c. embryo.

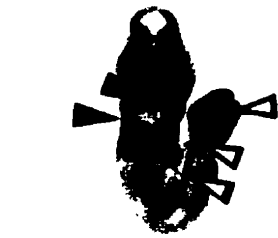
(A) Side view of a whole mount embryo hybridized with antisense PEA3. **(B)** Ventral view of the embryo in A. **(C)** Dorsal view of embryo in A. **(D through H)** Serial transverse sections through embryo in A; schematic next to (A) shows the position of each section in D-H in lower case. (red arrow = branchial arch mesenchyme; dark green arrow = prosencephalon; yellow arrow = tailbud; white arrow = pronephric tubules; blue arrow = endoderm lining the gut; orange arrow = somites; pink arrow = limb bud mesenchyme). Original magnification of A, B & C was 25X, the bar in C = 1000 μm ; original magnification of D-H was 100X, the bar in H = 250 μm .



A



B



C



D



E



F



G

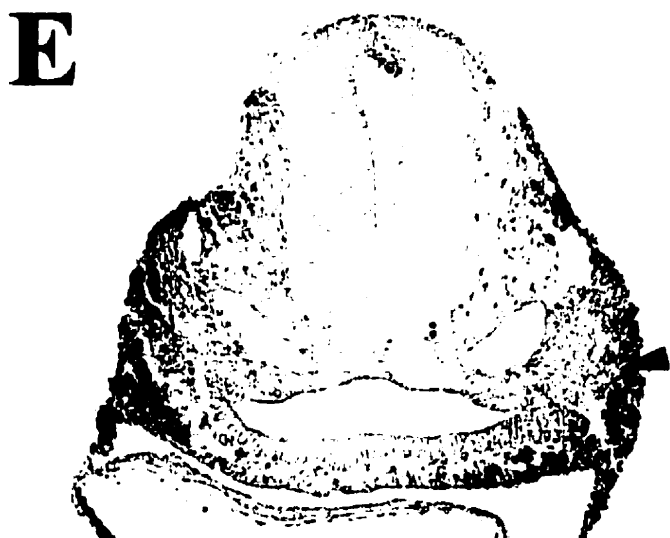


H



Figure 3.6 Expression pattern of the PEA3 mRNA in the 9.5 d.p.c. embryo.

(A) A side view of an embryo hybridized with an antisense PEA3 riboprobe. (B) A ventral view of the embryo in A. (C) A dorsal view of the embryo in A. (D-I) Serial transverse sections through the embryo in A. (red arrow = branchial arch mesenchyme; white arrow = pronephric tubules; blue arrow = endoderm lining the gut; orange arrow = somites, pink arrow = limb bud mesenchyme). Original magnification of A, B & C was 25X; original magnification of D-I was 200X, the bar in I = 100 μ m.



the optic and otic placodes at both of these stages (figure 3.7 A & B, dark green arrows). Between 10.0 and 10.5 d.p.c., the first branchial arch gives rise to both the maxillary and mandibular components of the jaw; by 10.5 d.p.c. PEA3 was detected in the sub-ectodermal mesenchyme of both components (figure 3.7 B, red arrows; data not shown). PEA3 was also expressed in the hyoid arch at 10.5 d.p.c. (figure 3.7 B; dark blue arrow).

There is also significant development of the olfactory placodes between 10.0 and 10.5 d.p.c.; they indent in their middle regions to form the medial and lateral ridges of the placodes. PEA3 was detected in the sub-ectodermal mesenchyme of the medial and lateral ridges of the olfactory placodes by 10.5 d.p.c. (figure 3.7 B, light blue arrow). PEA3 expression was detected in all of the somites along the rostrocaudal (RC) axis by 10.0 d.p.c. (figure 3.7 A, orange arrows); however, the signal in the rostral somites appeared much more intense than that in the more caudal somites (figure 3.7 A; compare signal intensity between the two orange arrows). This intensity difference was less pronounced by 10.5 d.p.c. (figure 3.7 B, orange arrows).

The PEA3 specific signal also lengthened along the dorsoventral (DV) axis of the rostral most somites beginning at 10.0 d.p.c. and continued through to the more caudal somites by 10.5 d.p.c. (figure 3.7 A & B, orange arrows). PEA3 was still detected in the tailbud through 10.5 d.p.c. (figure 3.7 B, yellow arrow). Both the forelimb and hindlimb buds had initiated outgrowth along their PD axes by 10.5 d.p.c. PEA3 was expressed in the distal regions of both pairs of limb buds at 10.0 and 10.5 d.p.c. (figure 3.7 A & B, pink arrows). Transverse sections through the limb buds revealed that the signal was

confined to the progress zone mesoderm (data not shown). PEA3 was still expressed in the mesonephric tubules at 10.0 d.p.c. (figure 3.7 A, white arrow) but was absent in this structure by 10.5 d.p.c. (figure 3.7 B).

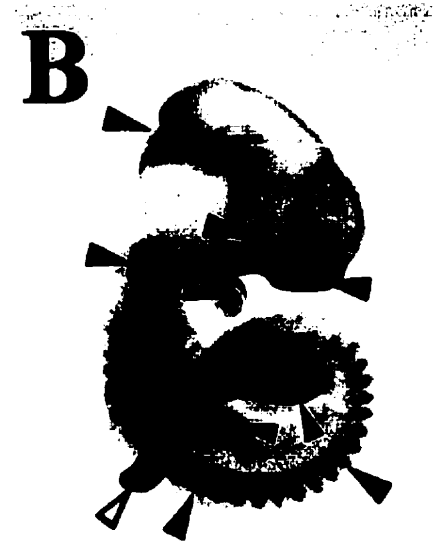
3.2.6 PEA3 expression pattern in the 11.0 and 11.5 d.p.c. embryo.

With a few exceptions, the PEA3 expression patterns at 11.0 and 11.5 d.p.c. were similar to that seen at 10.5 d.p.c. (compare figure 3.7 B with C & D). By 11.0 d.p.c., PEA3 expression in the midbrain-hindbrain junction became localized to the mesencephalon side of the boundary (figure 3.7 C, light green arrow). PEA3 was also detected in the head mesenchyme overlying this region (figure 3.7 C, black arrow). PEA3 was also expressed in the sub-ectodermal mesenchyme of the olfactory placodes and the maxillary, mandibular and hyoid arches by 11.5 d.p.c. (figure 3.7 D, light blue, red and dark blue arrows respectively; data not shown). This frontal view also illustrated PEA3 expression in the distal region of the forelimb bud (figure 3.7 D, pink arrow) and the dorsal aspects of the rostral somites (figure 3.7 D, orange arrow).

3.2.7 PEA3 expression pattern in the 12.0 through 12.75 d.p.c. embryo.

The PEA3 expression pattern at 12.0 and 12.5 d.p.c. was again very similar to that at 11.5 d.p.c. (compare figures 3.8 A & E with figure 3.8 D). However, a number of unique sites of expression were detected during these stages of development. Bilateral stripes appeared in the brachial region of the neural tube at 12.0 d.p.c. (figure 3.8 A, B & C, light green arrows). Transverse sections showed that this signal was located in the

Figure 3.7 Expression pattern of the PEA3 mRNA from 10.0 through 11.5 d.p.c. Embryos were hybridized with an antisense PEA3 riboprobe. **(A)** Side view of a 10.0 d.p.c. embryo. **(B)** Side view of a 10.5 d.p.c embryo. **(C)** Side view of an 11.0 d.p.c. embryo. **(D)** Frontal view of the facial region of an 11.5 d.p.c. embryo. (red arrows = maxillary and mandibular arches; dark blue arrow = hyoid arch; light green arrow = mesencephalon; dark green arrows = the optic and otic placodes; light blue arrow = olfactory placode; pink arrow = limb bud mesenchyme; orange arrow = somites; white arrow = pronephric tubules; yellow arrow = tailbud; black arrow = head mesenchyme). Original magnification of A & B was 25X; original magnification of C was 16X; original magnification of D was 40X.



ventral lateral regions of the neural tube, the location of the lateral motor column (LMC) neuron pools (data not shown; Lin et al., communication of unpublished data).

This signal was also present at 12.5 d.p.c. (figure 3.8 F & G, light green arrows) but was not detected in the brachial neural tube at 12.75 d.p.c. (figure 3.8 H). A similar pattern was detected in the lumbar region of the neural tube at 12.75 d.p.c. (figure 3.8 H, light green arrow). Again, transverse sections showed that this signal was present in the ventral lateral horns of the neural tube (data not shown).

PEA3 was expressed in the dorsal and ventral regions of the somites as they elongated ventrally to form the rib cage, intercostal muscles and body wall musculature from 12.0 to 12.5 d.p.c. (figure 3.8 A & E, orange arrows). However, by 12.5 d.p.c., the somites rostral to the forelimbs expressed PEA3 in their dorsal-most regions but not in their ventral regions (figure 3.8 E, compare the rostral pair of orange arrows with the caudal pair). By 12.75 d.p.c., the PEA3 signal was not detected in somites rostral to the forelimb, was faint but detectable in the somites between the fore and hindlimbs and was detected in the somites at and caudal to the hindlimb (figure 3.8 I, orange arrows). PEA3 was still expressed in the tailbud during these stages of development (figure 3.8 B, E & H, yellow arrows).

PEA3 was expressed in the distal progress zone mesoderm (PZM) of both the fore and hindlimbs at 12.0 and 12.5 d.p.c. (figure 3.8 A & F, pink arrows). However, by 12.75 d.p.c., PEA3 was detected in the interdigital mesenchyme of the forelimb paddle and in the distal PZM in the hindlimb paddle (figure 3.8 H, pink arrows). Furthermore, PEA3 expression was detected in the premuscle masses of the limbs at 12.0 and 12.5

d.p.c. (figure 3.8 B, C & G, orange arrows). But by 12.75 d.p.c., PEA3 was not detected in the limb musculature (figure 3.8 H & I). Interestingly, PEA3 was expressed in the mesenchyme of the genital eminence at 12.5 d.p.c. (figure 3.8 E, pale pink arrow).

Lastly, a region of PEA3 expression was detected in the body wall at the base of the forelimb in the 12.0 and 12.5 d.p.c. embryos (figure 3.8 A & F, black arrows). Although this signal was not detected in the transverse sections (data not shown), it was in the area of the developing mammary gland or mammary streak. PEA3 expression was still detected in this region at 12.75 d.p.c. but the signal was much less intense (figure 3.8 I, black arrow).

3.2.8 PEA3 expression pattern in the 13.0 d.p.c. embryo.

By 13.0 d.p.c., PEA3 expression was not detected in the derivatives of the somites rostral to the hindlimbs, however, it was detected in the somites caudal to the hindlimbs (figure 3.9 A, orange arrow). PEA3 was still expressed in the distal tip of the tail (figure 3.9 E, yellow arrow). Digit formation was occurring in both the fore and hindlimb paddles at 13.0 d.p.c., and PEA3 was expressed in the interdigital mesenchyme in all of the limb paddles (figure 3.9 G, pink arrows). PEA3 was also detected in the pericardial membrane at 13.0 d.p.c. (figure 3.9 E, white arrow). Transverse sections through this region showed that PEA3 was expressed in the cell layer that lined the pericardial cavity (data not shown).

Figure 3.8 Expression pattern of the PEA3 mRNA from 12.0 through 12.75 d.p.c.

(A) Side view of a ~ 12.0 d.p.c. embryo hybridized to an antisense PEA3 riboprobe. **(B)** Higher magnification of A. **(C)** Dorsal view of the brachial region of A. **(D)** Dorsal view of the lumbar region of A. **(E)** Side view of a ~ 12.5 d.p.c. embryo hybridized to an antisense PEA3 riboprobe. **(F)** Dorso-lateral view of E. **(G)** Dorsal view of the brachial region of E. **(H)** Side view of a ~ 12.75 d.p.c. embryo hybridized to an antisense PEA3 riboprobe. **(I)** Higher magnification of H. (orange arrow = somites or limb musculature; light green arrow = lateral motor column; pink arrow = limb mesenchyme; yellow arrow = tailbud; pale pink arrow = genital eminence; black arrow = mammary streak). Original magnification of A,C,D,E,G & H was 16X. Original magnification of B,F & I was 25X.

A



B



C



D



E



F



G



H



I



Interestingly, PEA3 expression was detected in three bud-like structures caudal to the forelimbs and one bud-like structure rostral to the hindlimbs (figure 3.9 D, black arrows). This pattern appeared on both sides of the embryo (figure 3.9 F, black arrow). These signals were never detected in PEA3 sense control hybridizations (figure 3.9 H & I). Unfortunately, these signals were too weak to be detected in transverse sections (data not shown); however, it is likely that these structures are the epithelial buds of the developing mammary glands. Lastly, PEA3 expression was still detectable in the lumbar region of the neural tube (figure 3.9 E, F & G, light green arrow).

3.2.9 Expression pattern of ERM and ER81 in the gastrulating embryo (~ 7.0 to 7.5 d.p.c.).

ERM was expressed in the posterior half of the 7.0 d.p.c. embryo (figure 3.10 A, yellow arrow). A posterior view revealed that this signal was bilateral and ran along the entire length of the PD axis on either side of the primitive streak (figure 3.10 B, yellow arrow). Hence, ERM was expressed in the primitive streak ectoderm during gastrulation. ER81 expression was not detected in the 7.0 d.p.c. embryo (figure 3.10 D to F).

ERM was also expressed in the posterior half of the 7.5/8.0 d.p.c. embryo (figure 3.11 A, yellow arrow). A posterior view of the caudal region again revealed that this signal was within the primitive streak ectoderm (figure 3.11 B, yellow arrow). At this stage, ERM was also expressed in the rostral half of the embryo (figure 3.11 A, red arrows). A ventral view of this region revealed that the signal was derived from the endoderm lining the opening to the foregut and possibly the mesenchyme of the

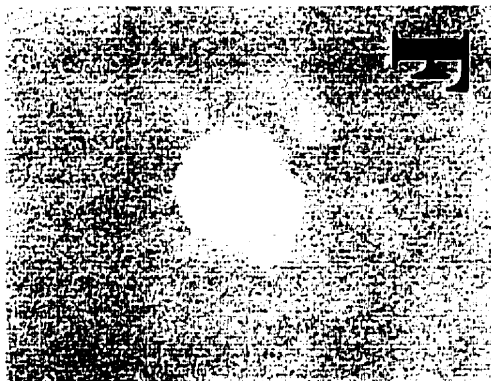
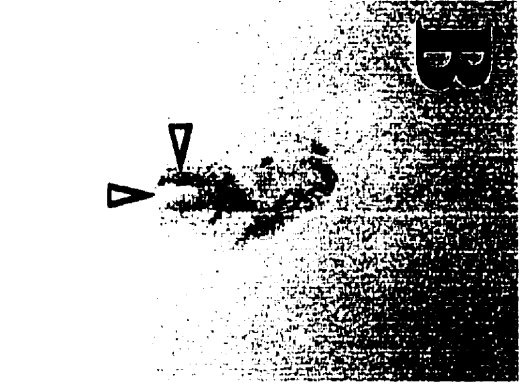
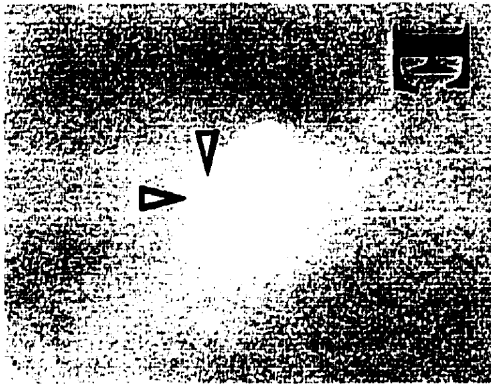
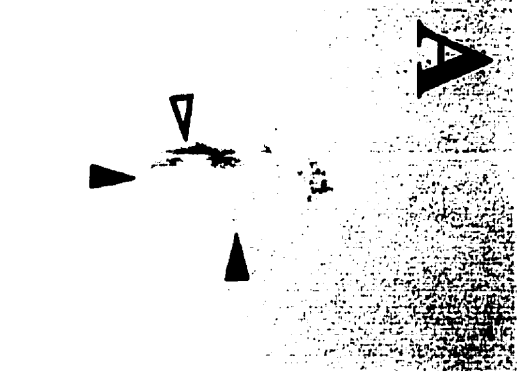
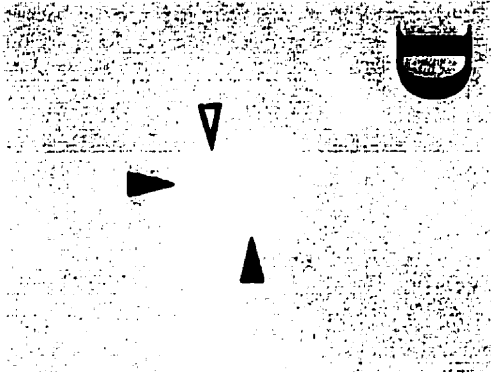
Figure 3.9 Expression pattern of the PEA3 mRNA in the 13.0 d.p.c. embryo.

(A) Side view of a ~13.0 d.p.c. embryo hybridized to an antisense PEA3 riboprobe. (B) Ventral view of A. (C) Dorsal view of brachial region of A. (D) Higher magnification of A highlighting the mammary buds. (E) Contra-lateral view of A. (F) Contra-lateral side view of A. (G) Higher magnification of A highlighting the limb paddles undergoing digit formation. (H) Side view of a ~13.0 d.p.c. embryo hybridized to a sense control PEA3 riboprobe. (I) Higher magnification of the side of the embryo in H. (orange arrow = somites; black arrow = mammary buds; yellow arrow = tailbud; light green arrow = lateral motor column; pink arrow = limb mesenchyme). Original magnification of A,B,C,E,F & H was 16X. Original magnification of D,G & I was 25X.



Figure 3.10 Expression pattern of ERM and ER81 mRNAs in the 7.0 d.p.c embryo.

(A) Side view of a whole mount embryo hybridized with antisense ERM. **(B)** Posterior view of embryo in A. **(C)** Anterior view of embryo in A. **(D)** Side view of a whole mount embryo hybridized with antisense ER81. **(E)** Posterior view of embryo in D. **(F)** Anterior view of embryo in D. The embryos in A and D are oriented with their rostral ends to the right side and their ventral surface facing down. (yellow arrow = primitive streak ectoderm; black arrow = the approximate position of the node; white arrow = primitive streak; blue arrow = headfold). Original magnification of A through F was 25X.



rudimentary first branchial arch (figure 3.11 C, red arrows). ER81 expression was not detected in the 7.5/8.0 d.p.c. embryo (figure 3.11 D to F).

3.2.10 Expression pattern of ERM and ER81 in the 8.5 d.p.c. embryo.

ERM was expressed in the posterior half of the 8.5 d.p.c. embryo caudal to the node (figure 3.12 A, yellow arrow). A dorsal view revealed that this signal was bilateral and much more diffuse in nature than in the previous stages (figure 3.12 B, yellow arrow). ERM was expressed in the rostral half of the 8.5 d.p.c. embryo (figure 3.12 A, red arrow). A ventral view revealed that this signal was also bilateral but was also more diffuse than the rostral pattern observed at 7.5/8.0 d.p.c. (compare 3.12 C, red arrow with figure 3.12 B, red arrow). This signal was derived from the foregut endoderm and likely the mesenchyme of the developing branchial arches. ERM was also expressed in a stripe that spanned the width of the anterior neural folds, a region destined to form the midbrain/hindbrain region of the future CNS (figure 3.12 B, green arrow). ER81 expression was not detected in the 8.5 d.p.c. embryo (figure 3.12 D to F).

3.2.11 Expression pattern of ERM and ER81 in the 9.0 d.p.c. embryo.

ERM was expressed in a number of regions in the 9.0 d.p.c. embryo. It was expressed in the region of the midbrain/hindbrain junction (figure 3.13 A & B, green arrows), the mesenchyme of the branchial arches (figure 3.13A & B, red arrows), the otic placodes (figure 3.13 B, black arrow), the forelimb bud mesenchyme (figure 3.13 A, pink arrow), the mesonephric tubules (figure 3.13 A, white arrow), the tailbud (figure

3.13 A, yellow arrow) and in the region of the developing nasal placodes (figure 3.13 C, green arrow). ER81 expression was not detected in any region of the 9.0 d.p.c. embryo (figure 3.13 D to F).

3.2.12 Expression pattern of ERM and ER81 in the 10.5 d.p.c. embryo.

The ERM expression patterns at 9.0 d.p.c. and 10.5 d.p.c. were similar but with a few additional sites of expression in the later. ERM was expressed in the region where the nasal placodes will develop and the otic placodes (figure 3.14 A & B, dark green arrows). ERM was also expressed in the midbrain/hindbrain junction (figure 3.14 A & B, light green arrow), the maxillary, mandibular and hyoid arches (figure 3.14 A, B & C, red arrows), the PZM of both the forelimb and hindlimb buds (figure 3.14 A, dark pink arrows) and in the mesonephric tubules (figure 3.14 C, white arrows). At this stage, a bilateral segmental expression pattern was detected on either side of the developing neural tube (figure 3.14 A, orange arrow) and represented the first appearance of the ERM mRNA in the developing somites.

ER81 expression was first detected in the ~ 11.0 d.p.c. embryo. It was expressed in the maxillary and mandibular arches (figure 3.14 D, red arrow), the medial and lateral ridges of the nasal placodes (figure 3.14 F, red arrows), the somites (figure 3.14 D, orange arrow) and in the dorsal root ganglia (DRG) running in a rostral to caudal direction along the length of the neural tube (figure 3.14 D, light blue arrows). ER81 expression was also detected in the optic placodes at 11.0 d.p.c. The signal intensity of the ER81

Figure 3.11 Expression pattern of the ERM and ER81 mRNAs in the 7.5/8.0 d.p.c. embryo.

(A) Side view of a whole mount embryo hybridized with antisense ERM. (B) Posterior view of the embryo in A. (C) Anterior view of the embryo in A. (D) Side view of a whole mount embryo hybridized with antisense ER81. (E) Posterior view of embryo in D. (F) Anterior view of embryo in D. The embryos in A and D are oriented with their rostral ends to the right side and their ventral surface facing down. (red arrow = branchial arch mesenchyme and foregut endoderm; yellow arrow = primitive streak ectoderm; white arrow = primitive streak; blue arrow = headfold; black arrow = the approximate position of the node). Original magnification of A through F was 25X.

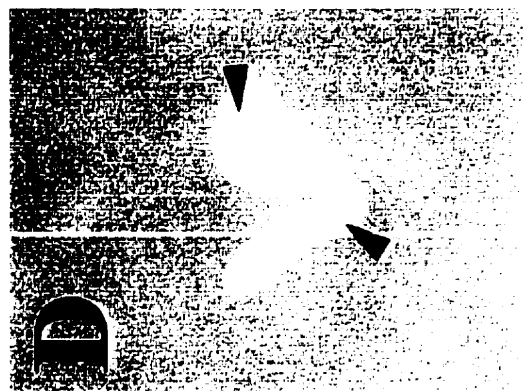
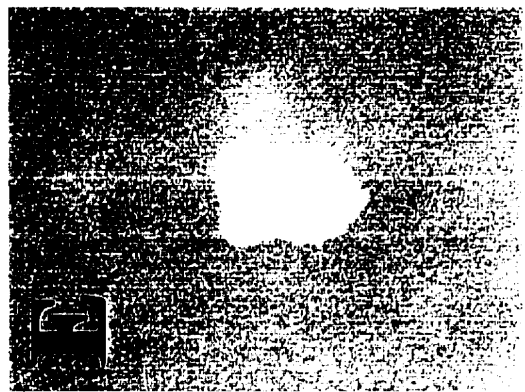
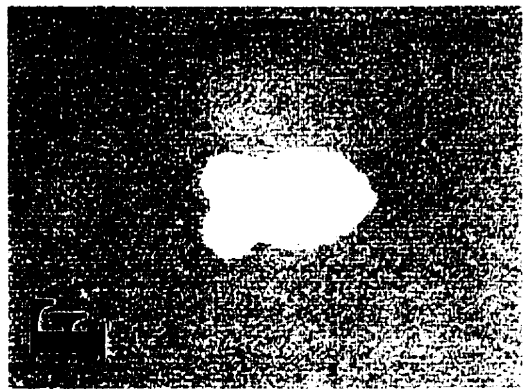
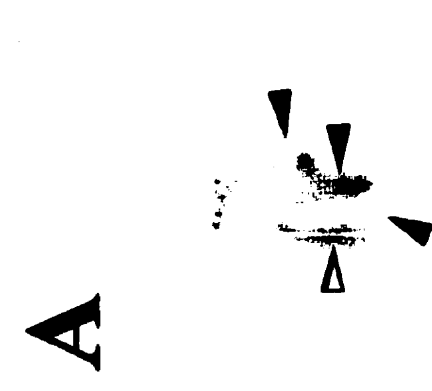
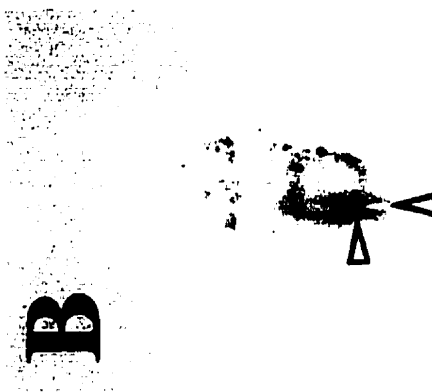


Figure 3.12 Expression pattern of the ERM and ER81 mRNAs in the 8.5 d.p.c. embryo.

(A) Side view of a whole mount embryo hybridized with antisense ERM. **(B)** Dorsal view of the embryo in A. **(C)** Ventral view of embryo in A. **(D)** Side view of a whole mount embryo hybridized with antisense ER81. **(E)** Dorsal view of embryo in D. **(F)** Ventral view of embryo in D. The embryos in A and D are oriented with their rostral ends to the right side and their ventral surfaces facing down. (red arrow = branchial arch mesenchyme and foregut endoderm; yellow arrow = primitive streak ectoderm; black arrow = the approximate position of the node; white arrow = heart; blue arrow = headfold). Original magnification of A through F was 25X.

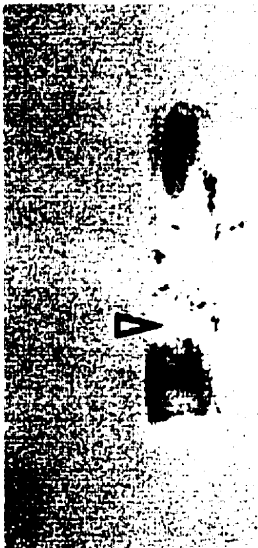
A



B



C



D



E

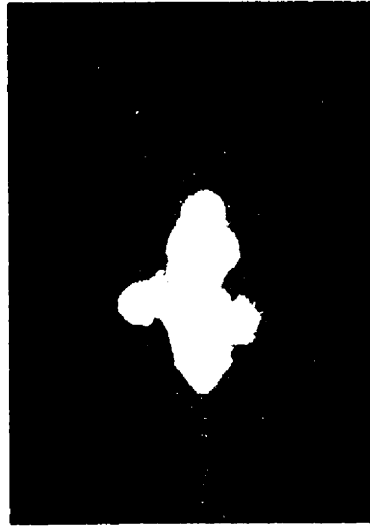
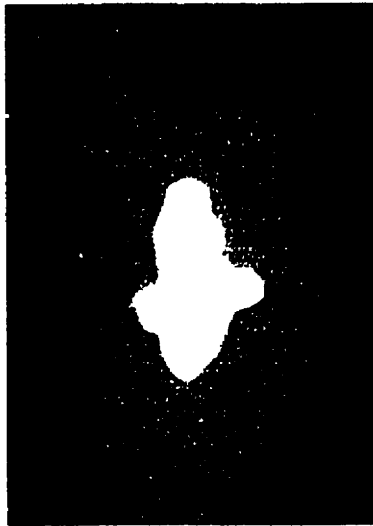
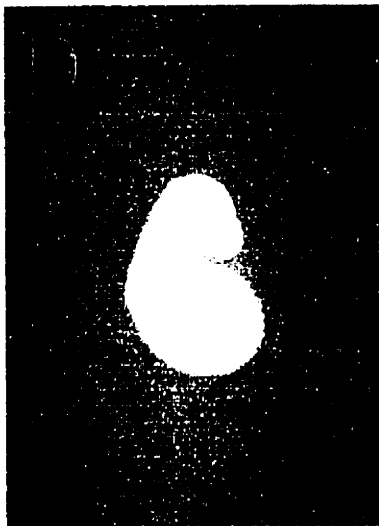
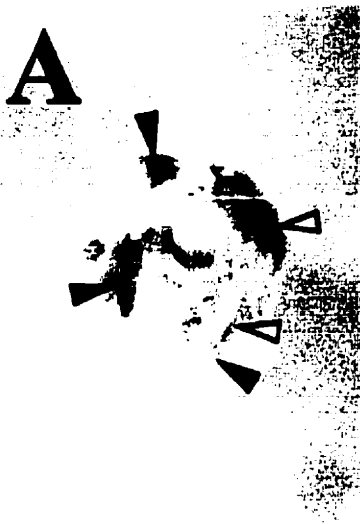


F



Figure 3.13 Expression pattern of the ERM and ER81 mRNAs in the 9.0 d.p.c. embryo.

(A) Side view of a whole mount embryo hybridized with antisense ERM. **(B)** Dorsal view of embryo in A. **(C)** Ventral view of the embryo in A. **(D)** Side view of whole mount embryo hybridized with antisense ER81. **(E)** Dorsal view of embryo in D. **(F)** Ventral view of embryo in D. (red arrow = branchial arch mesenchyme; dark green arrow = prosencephalon; yellow arrow = tailbud; white arrow = pronephric tubules; pink arrow = limb bud mesenchyme; black arrow = otic placode). Original magnification of A, B & C was 25X; original magnification of D, E & F was 16X.



riboprobe was consistently much reduced relative to that generated by the ERM riboprobe (compare figure 3.14 A with 3.14 D).

3.2.13 Expression pattern of ERM and ER81 in the 11.5 d.p.c. embryo.

ERM was detected at 11.5 d.p.c. in the midbrain/hindbrain junction (figure 3.15 A & B, light green arrows), the medial and lateral ridges of the nasal placodes (figure 3.15 A, light blue arrows), the optic placodes (figure 3.15 A, dark green arrow), the maxillary, mandibular and hyoid arches (figure 3.15 A, red arrows), the somites (figure 3.15 A, B & C, orange arrows), the PZM of the limb buds (figure 3.16 A & C, pale pink arrows), the pre-muscle mass of the forelimb buds (figure 3.15 A & C, black arrows), the otic placodes (figure 3.15 B, dark green arrow) and in the tailbud (figure 3.15 B, yellow arrow). ER81 was detected at 11.5 d.p.c. in the telencephalon (figure 3.15 D, dark green arrow), the optic placodes (figure 3.15 D, light green arrow), in the DRGs (figure 3.15 E & F) and in the maxillary and mandibular arches (figure 3.15 F). Again, the signal intensity of the ER81 riboprobe was consistently much reduced relative to that of the ERM riboprobe (compare figure 3.15 A with 3.15 D).

3.2.14 Expression pattern of ERM and ER81 in the 12.0 d.p.c. embryo.

At 12 d.p.c ERM expression was detected in the nasal region (figure 3.16 A, red arrow), the PZM of the forelimb and hindlimb buds (figure 3.16 A, dark pink arrows), in the dorsal and ventrolateral regions of the somites (figure 3.16 A, orange arrows), in the otic vesicles (figure 3.16 B) and in the mesodermal component of the genital folds

Figure 3.14 Expression pattern of the ERM and ER81 mRNAs in the ~10.5 d.p.c. embryo.

(A) Side view of a whole mount 10.5 d.p.c. embryo hybridized to an antisense ERM riboprobe. (B) Dorsal view of embryo in A. (C) Ventral view of embryo in A. (D) Side view of a whole mount 11 d.p.c. embryo hybridized to an antisense ER81 riboprobe. (E) Dorsal view of embryo in D. (F) Ventral view of embryo in D. Original magnification of A through C = 16X; D through F = 10X. (dark green arrow = forebrain and otic placodes; light green arrow = midbrain/hindbrain junction; red arrow = branchial arches; orange arrow = somites; pink arrow = limb buds; light blue arrow = dorsal root ganglia).

A



B



C



D



E



F



Figure 3.15 Expression pattern of the ERM and ER81 mRNAs in the 11.5 d.p.c. embryo.

(A) Side view of a whole mount 11.5 d.p.c. embryo hybridized to an antisense ERM riboprobe. (B) Dorsal view of embryo in A. (C) Ventral view of embryo in A. (D) Side view of a whole mount 11.5 d.p.c. embryo hybridized to an antisense ER81 riboprobe. (E) Dorsal view of embryo in D. (F) Ventral view of embryo in D. Original magnification of A through C = 16X; D through F = 10X. (A through C: dark green arrow = forebrain, optic & otic placodes; light green arrow = midbrain/hindbrain junction; red arrow = branchial arches; orange arrow = somites; pink arrow = limb buds; light blue arrow = nasal placodes; black arrow = limb bud pre-muscle mass; yellow arrow = tailbud; D through F: dark green arrow = telencephalon; light green arrow = optic placode).

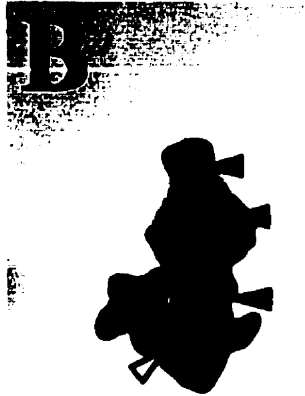


(figure 3.16 C, pale pink arrow). ER81 expression was detected only in the rostral most regions of the telencephalon at this stage of development (figure 3.16 D & E, green arrows).

3.2.15 Expression pattern of ERM and ER81 in the 13.0 d.p.c. embryo.

ERM expression was detected only in the forelimb and hindlimb paddles by 13 d.p.c. (figure 3.17 A, black arrows). Interestingly, ERM expression was confined to the distal most tips of the developing digits within the limb paddles (figure 3.17 B & C, black arrows). ER81 expression was still confined to the rostral most regions of the hemispheres of the telencephalon (figure 3.17 D & E, green arrows). This stage of embryonic development represented the last stage at which the technique of whole mount *in-situ* hybridization could be applied to mouse embryos. Hence, the stages of 14 d.p.c. through 21 d.p.c. of gestation were not analyzed in this study.

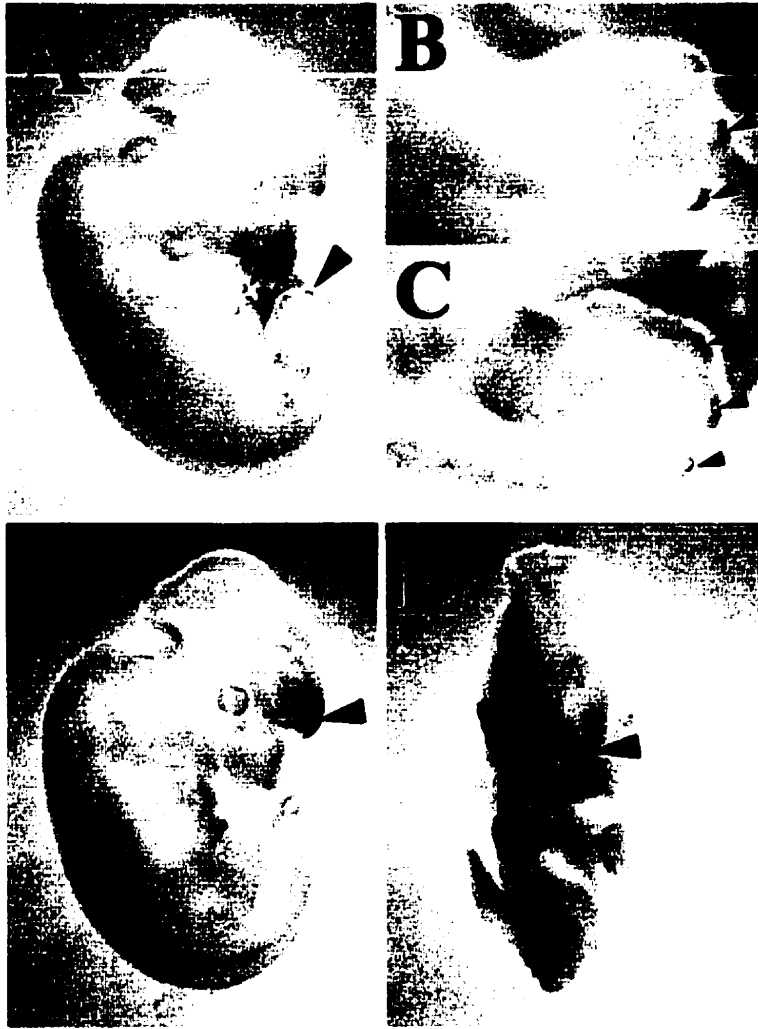
Figure 3.16 Expression pattern of the ERM and ER81 mRNAs in the 12.5 d.p.c. embryo.

(A) Side view of a whole mount embryo hybridized to an antisense ERM riboprobe. **(B)** Dorsal view of embryo in A. **(C)** Ventral view of the genital region of a 12.5 d.p.c. embryo hybridized with an antisense ERM riboprobe. **(D)** Side view of a whole mount embryo hybridized to an antisense ER81 riboprobe. **(E)** Ventral view of embryo in D. Original magnification of A,B,D & E = 10X, C = 25X. (red arrow = branchial arches; dark pink arrow = limb buds; orange arrow = somites; pale pink arrow = genital folds; green arrow = telencephalon).



Figure 3.17 Expression pattern of the ERM and ER81 mRNAs in the 13 d.p.c. embryo.

(A) Side view of a whole mount embryo hybridized to an antisense ERM riboprobe. **(B)** Close up of the forelimb paddle from the embryo in A. **(C)** Close up of the hindlimb paddle from the embryo in A. **(D)** Side view of a whole mount embryo hybridized with an antisense ER81 riboprobe. **(E)** Ventral view of the embryo in D. original magnification of A through E = 10X. (black arrow = limb paddle digits; green arrow = telencephalon).



3.3 DISCUSSION.

3.3.1 PEA3 expression during the pre-implantation stages of mouse development.

Although this study examined PEA3 expression in the post-implantation stages of mouse development, there is evidence suggesting that it may also be expressed in the mouse embryo prior to its implantation into the uterine wall. The zygote undergoes three rounds of cell division yielding an 8 cell morula (~ 2.5 d.p.c.) (figure 3.18 A). At the 8 to 16 cell stage, the morula undergoes a differentiation event referred to as compaction. The cells on the exterior of the morula form tight junctions with one another enclosing a population of cells on the inside.

The outer cell layer is composed of trophoblast cells; the interior cell layer is referred to as the inner cell mass (ICM) (figure 3.18 B & C). The trophoblast cells will give rise to components of the extraembryonic membranes and the placenta whereas the ICM will give rise to the embryo proper. As development proceeds, a central cavity develops and begins to expand as it fills with fluid. By ~4.5 d.p.c., the ICM is in contact with only one side of the trophoblast or polar trophoblast and separated from the mural trophoblast by the blastocoel. This embryo is referred to as a blastocyst (figure 3.18 C; reviewed in Hogan et al. 1986).

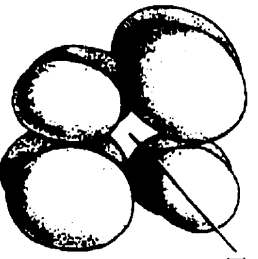
Hence, the cells of the ICM are totipotent or capable of differentiating into all of the cell types that constitute the embryo proper. Embryonic stem (ES) cells and embryonal carcinoma (EC) cells are derived from the ICM of the 4.5 d.p.c. blastocyst. These cell lines can be cultured under conditions that maintain their totipotency (section 2.16). The

Figure 3.18 Development of the murine inner cell mass (ICM) and blastocyst.

(A) Schematic diagram of an early 8 cell stage mouse embryo. **(B)** Schematic diagram of an 8 cell morula where the embryo in A has undergone the process of compaction. **(C)** Schematic diagram of the mouse blastocyst highlighting its major features (see text). (This diagram was modelled after Dulcibella, 1977). **(a)** Scanning electron micrograph of a non-compacted 8 cell embryo as depicted in A. **(b)** Scanning electron micrograph of a compacted 8 cell morula as depicted in B. (Photographs taken by C. Ziomek, from Gilbert, 1985).

A

Early 8 Cell



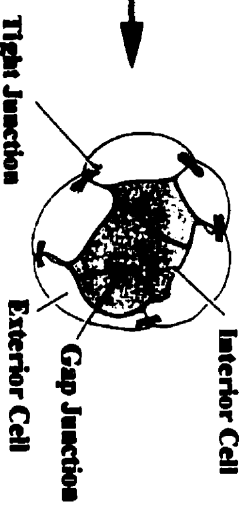
Large Intercellular Spaces

Compaction



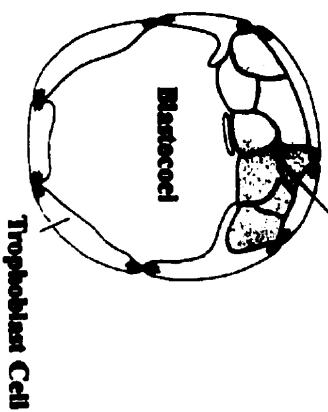
B

Morula

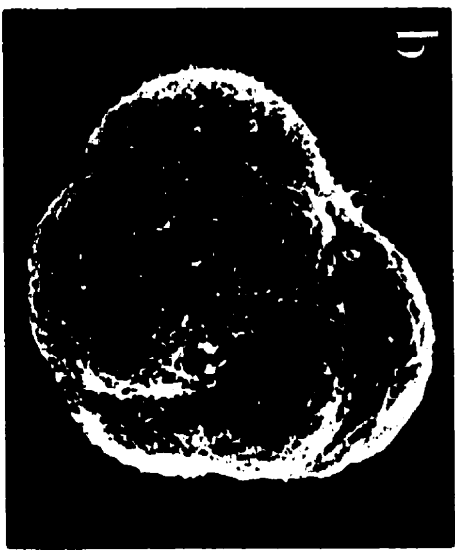


C

Blastocyst



a



b

PEA3 mRNA was shown to be expressed in two undifferentiated EC cell lines, P19 and F9 cells. When these cell lines were differentiated in the presence of retinoic acid, the steady state levels of the PEA3 mRNA were down regulated (Xin et al., 1992). Under the given conditions, P19 cells differentiated into neurons and astrocytes whereas the F9 cells differentiated into cells resembling primitive endoderm (Rudnicki and McBurney, 1987). Furthermore, the PEA3 mRNA was also expressed in undifferentiated D3 ES cells (data not shown). As all of the above cell lines represented the ICM at ~4.5 d.p.c., one can infer that PEA3 is expressed in the 4.5 d.p.c. blastocyst. Furthermore, its transcription may be up or down-regulated in a cell type specific manner as the three germ layers begin to differentiate.

Employing the whole mount *in-situ* technique on pre-implantation and early post-implantation embryos was technically challenging. Many attempts were carried out on ~6 to 6.5 d.p.c. egg cylinders; however, under the given conditions, background levels were too high in embryos hybridized with both sense and antisense PEA3 riboprobes (data not shown). Hence, data could not be generated for these early implantation stages of development. Recently, Silvia Arber generated a promoter trap *lacZ* mouse line targeted at the *Pea3* locus (Arber and Jessell, personal communication). This reagent should prove to be very useful in studying PEA3 expression in the very early stages of mouse development. It will be of considerable interest to determine which cell type(s) express PEA3 at 4.5 d.p.c. through 6.5 d.p.c.

3.3.2 PEA3 and ERM may play a role in effecting gastrulation.

This expression study of the PEA3 group genes began at ~7.0 d.p.c. of mouse development, a stage when the embryo was mid way through gastrulation. Gastrulation is the process where ectodermal (epiblast) cells in the posterior region of the embryo undergo cellular migration, rearrangement and differentiation giving rise to cells that will form the other two embryonic germ layers, the mesoderm and the definitive endoderm. This process is pivotal in that all of the tissues and organs of the adult body are derived from these three germ layers.

Gastrulation occurs when cells in the epiblast migrate towards a transient mid-line structure, the primitive streak, which runs the length of the PD axis of the early mouse embryo (Bellairs, 1986). Once the cells have reached the primitive streak, they undergo an epithelial to mesenchymal transition and then ingress into the space between the overlying epiblast and the underlying visceral endoderm. This process initiates in the proximal-most (posterior) region of the egg cylinder and proceeds in an anterior direction as the primitive streak lengthens distally (anteriorly). The cells that have gastrulated are referred to as mesendodermal cells. They will differentiate into either mesodermal cells or definitive endodermal cells that will replace the visceral endoderm (Hashimoto et al. 1989; reviewed by Tam and Behringer, 1997).

PEA3 was expressed in a bilateral pattern in posterior epiblast cells in regions both medial and lateral to the primitive streak from ~7.0 d.p.c. through ~8.5 d.p.c. Furthermore, its signal ran the length of the PD axis (figure 3.2, 3.3 & 3.4). This expression profile was consistent with PEA3 being expressed in epiblast cells that were

being recruited to migrate towards and then ingress through the primitive streak. Analysis of ERM expression during these stages of development revealed that it was also expressed in gastrulating epiblast cells (figure 3.10 A,B,C; figure 3.11 A,B,C; figure 3.12 A,B,C). ER81 expression was not detected in any of gastrulation staged embryos (figure 3.11 D,E,F; figure 3.12 D,E,F; figure 3.13 D,E,F). Furthermore, it appeared that PEA3 and ERM were not expressed in the cells that had ingressed through the primitive streak although this may have been due to the fact that they were expressed at much lower levels relative to the primitive streak ectoderm.

What function might PEA3 and ERM be affecting in gastrulating epiblast cells? In order to speculate on the answers to this question, we must first identify the obvious biological phenomena that are taking place within these cells. Firstly, epiblast cells are undergoing rapid proliferation and this accounts for the entire increase in tissue mass of the gastrulating embryo (MacAuley et al. 1993). Secondly, individual cells within the epiblast that are to be recruited to the primitive streak must become differentiated from their neighbours that will remain within the epiblast. Thirdly, these differentiated cells must migrate from lateral positions, through the epiblast to reach the primitive streak. Lastly, the ingressing epiblast cells undergo an epithelial to mesenchymal transition in their morphology (Takeichi, 1988; reviewed by Tam and Behringer, 1997).

It is unlikely that PEA3 and ERM are involved in affecting the proliferation of this cell population. The underlying mesendodermal cells also had a high mitotic index but either failed to express their transcripts or did so at much lower levels. Furthermore, it is unlikely that these genes affect the differentiation of the epiblast cells while they are pre-

migratory. PEA3 and ERM were expressed in both the medial and lateral regions of the posterior epiblast along the entire length of the proximal distal axis. As gastrulation initiated in the posterior or distal most region, we would have expected that both PEA3 and ERM would have been down regulated in this region by 7.5 d.p.c. if they were affecting differentiation alone.

However, their expression patterns were consistent with their involvement in affecting the migration of cells through the epiblast layer and/or changes in their cell adhesion properties leading to the epithelial/mesenchymal transition. Furthermore, these two processes are not mutually exclusive. The PEA3 group members are thought to confer an invasive or metastatic phenotype upon cancer cells by regulating the expression of secreted matrix metalloproteinases (MMPs) which in turn degrade the extracellular matrix (ECM) surrounding the cells (Higashino et al. 1995; Birkedal-Hansen, 1995). However, during gastrulation, a complex ECM has not yet been laid down and consists largely of fibronectin (Tam and Behringer, 1997). Furthermore, the MMPs are not expressed during gastrulation (Matrisian and Hogan, 1990; Adams and Watt, 1993). Hence, the mechanism by which the PEA3 group members are believed to contribute to the mobility of cancer cells cannot be the same as the mechanism at work during gastrulation.

Fgfr-1 was found to be expressed in migratory ectodermal cells during gastrulation (Yamaguchi et al. 1992). Furthermore, *Fgfr-1* null embryos failed to gastrulate and showed an accumulation of ectodermal cells within the primitive streak combined with a deficiency of mesodermal cells (Yamaguchi et al. 1994). A later study confirmed that *Fgfr-1* null cells failed to gastrulate whereas their wild type counter parts did in chimeric

embryos (Ciruna et al. 1997). This gastrulation defect was very similar to that described in the *Drosophila* mutation *heartless*, the *DFgfr-1* homolog (Beiman et al. 1996; Gisselbrecht et al. 1996).

This receptor tyrosine kinase was shown to signal via the Ras pathway (Whitman and Melton, 1992; MacNicol et al. 1993; Umbhauer et al. 1995). Furthermore, the transcriptional activities of PEA3 and ERM were activated by members of Ras/Raf/MapK cascades (O'Hagan et al. 1996; Janknecht et al. 1996). Hence, FGFR1 may affect gastrulation in part by regulating the activities of PEA3 and ERM through a Ras mediated signalling cascade. Interestingly, many FGFs are expressed in the posterior ectoderm during gastrulation including *Fgf3*, *Fgf4*, *Fgf5* and *Fgf8* (Faust and Magnuson, 1993; Yamaguchi and Rossant, 1995).

Hence there are many potential *Fgfr-1* ligands that are expressed in the gastrulating ectoderm. If PEA3 or ERM function downstream of *Fgfr-1* to affect cell migration, the target genes by which they accomplish this task remain unknown. One hypothesis might be that the PEA3 group members may regulate the remodelling of the cytoskeleton in migratory cells. A recent study showed that PEA3 was capable of transactivating the Vimentin promoter (Chen et al. 1996). Vimentin is an intermediate filament protein and its expression has been associated with cell migration. The other possibility is that PEA3 and ERM may be involved in regulating the expression of the *Fgfs* and/or their receptors in the gastrulating ectoderm.

Lastly, PEA3 and ERM may regulate the epithelial to mesenchymal transition of the ingressing epiblast cells. Cell adhesion is regulated by the expression of a number of

different cell adhesion molecules including the cadherins and the integrins (Takeichi, 1988). As the epiblast cells migrate towards the primitive streak they express E-cadherin. At the time of ingression, it is down-regulated and the cells then express N-cadherin (Takeichi, 1988; Tam and Trainor, 1993). E-cadherin has also been shown to promote cell adhesion in mouse L-cells and inhibit their invasive properties (Chen et al. 1997). Changes in cell adhesion may not only affect changes in cellular morphology, but they may also allow for cells in a continuous monolayer such as the epiblast, to become detached from their neighbours and allow them to become migratory.

The cadherin family is a large family of membrane spanning calcium dependant cell adhesion molecules. Their cytoplasmic domains interact with the members of the catenin family which in turn are linked to the actin cytoskeleton. A recent study revealed that *ETS* transcription factors were capable of transactivating the promoter of VE-cadherin (Gory et al. 1997). Although this cadherin is expressed only in vascular-endothelial cells, this study provides evidence that *ETS* genes are capable of regulating the expression of members of the cadherin family. Expression of the catenins could also be regulated by members of the *ETS* family. Hence, PEA3 and ERM may regulate the expression of target genes that govern both cell mobility and/or cell adhesion in the embryonic epiblast during gastrulation.

3.3.3 The PEA3 group members are expressed in branchial arch mesenchyme and may contribute to craniofacial development.

PEA3 and ERM were both expressed in a rostroventral region of the 8.0 d.p.c. embryo just behind the developing heart (figure 3.4 A; figure 3.12 A). The signal was located in the mesenchyme of the rudimentary first branchial arch. As development proceeded, PEA3 and ERM were expressed in the sub-ectodermal mesenchyme of all four branchial arches and the nasal placodes. Expression in the branchial arches was down-regulated by 12.75 d.p.c. although expression was still detected around the developing nostrils (figure 3.8 H; figure 3.16 A). Hence, down-regulation of their expression coincided with the differentiation of the mesenchyme into its adult tissue precursors. ER81 expression was detected in the branchial arches but only from ~ 11.0 d.p.c to 11.5 d.p.c. (figure 3.14 F; figure 3.15 F). Furthermore, it was confined to the nasal placodes and the upper and lower elements of the first branchial arch (see also Chotteau-Lelievre et al. 1997).

The first branchial arch forms the maxillary process (upper jaw) and the mandibular arch (lower jaw). Its associated mesenchyme will form the jaw bone, the malleus and incus of the inner ear and the muscles of mastication. The second branchial arch (hyoid arch) will give rise to the stapes of the inner ear, the hyoid bone in the throat as well as the facial musculature. The mesenchyme of the third and fourth branchial arches will give rise to the bones, cartilage and muscles of the larynx and lower pharynx (Carlson, 1996; Schilling, 1997).

PEA3 expression was also detected within the endodermal component of both the first and second pharyngeal membranes (figure 3.5 E; figure 3.6 D) (Chotteau-Lelievre et al. 1997). These membranes are located within the pharyngeal pouches in the upper pharynx between the first and second, and the second and third branchial arches respectively. These membranes will give rise to the tympanic membrane of the ear and the faucial tonsils of the lymphoid system respectively (Carlson, 1996).

Interestingly, branchial arch mesenchyme is not derived from the mesodermal derivatives formed by the ingression of the epiblast during gastrulation. It is derived from neural crest cells, an ectodermal cell population that originates in the apical neural tube. During development, these cells migrate ventrally and in the rostral regions, give rise to the branchial arch mesenchyme and the cranial ganglia. In the more caudal regions, they give rise to melanocytes and the neurons of the autonomic and sensory nervous systems (Anderson, 1989; Le Douarin and Smith, 1988; Murphy and Bartlett, 1993). The expression of all three PEA3 group members was previously reported in the cephalic and dorsal root ganglia (Chotteau-Lelievre, 1997; Lin, Arber & Jessell, personal communication); however, I was only able to detect ER81 in the DRGs (figure 3.15 D). Further discussions on the role of the PEA3 group members in the differentiation and function of neural crest derivatives can be found in chapter four (section 4.3.2).

Interestingly, both the *FGFR-1* and *FGFR-2* mRNAs are co-expressed in the bone and cartilage rudiments during craniofacial development. Furthermore, many human craniofacial abnormalities have now been attributed to mutations in these two receptors. Unfortunately, *Fgfr-1* and *Fgfr-2* knock-out mice die during early embryonic development

and do not provide suitable models for these human syndromes (reviewed by Muenke and Schell, 1995). However, these studies illustrate the possibility that the PEA3 group members may function downstream of FGFR mediated pathways to affect either the migration or differentiation of branchial arch mesenchyme.

The sequential appearance and order of the branchial arches during embryogenesis represents a form of segmentation along the embryo's RC axis. The *Hox* transcription factor family has been implicated in affecting the anteroposterior patterning of the CNS and mesoderm in vertebrate embryos (McGinnis and Krumlauf, 1992). Recently, members of this gene family were shown to regulate the development and differentiation of many derivatives of the branchial arches (Murphy and Bartlett, 1993; Schilling, 1997). The results from these *Hox* gene studies were very similar to those obtained from studies analyzing the effects of retinoic acid (RA) and the retinoic acid receptors (RARs) on rostro-caudal segmentation of the vertebrate embryo (Conlon, 1995).

These similarities resulted from the fact that RA and the RARs were found to be involved in regulating the sequential expression of the four *Hox* gene clusters (reviewed by Gruss and Kessel, 1991; Boncinelli et al. 1991). Results generated in our laboratory clearly showed that PEA3 mRNA expression was regulated by RA in F9 and P19 cells (Xin et al. 1992). How the members of the *RA* and *RAR*, *HOX*, and *ETS* gene families interact within the genetic regulatory hierarchy to affect the development of the branchial arches remains to be established.

3.3.4 PEA3 and ERM are expressed in the neural ectoderm of the mesencephalon-metencephalon (mes-met) boundary.

ERM was expressed in the presumptive midbrain (mesencephalon) hindbrain (rhombencephalon) neural ectoderm at 8.5 d.p.c. (figure 3.12 B, light green arrow). Its expression persisted on both sides of the mes-met boundary through 11.5/12.0 d.p.c. but was absent by 13.0 d.p.c. (figure 3.16 A; figure 3.17 A). PEA3 expression was also detected in this region but initiating slightly later at ~9.0 d.p.c. (figure 3.5 A, light green arrow). PEA3 was expressed on both sides of the mes-met border through ~11.5 d.p.c. At this stage, its signal appeared to be more intense on the mesencephalon side of the border.

PEA3 expression was difficult to discern in this region at 12.0 d.p.c. as the signal was obscured by its own expression in the cephalic mesenchyme overlying this border (Chotteau-Lelievre et al. 1997). ER81 expression was not detected in this region of the CNS; rather its expression was confined to the rostral aspects of the developing cerebral hemispheres beginning at 11.5 d.p.c. and continuing through 13.0 d.p.c. (figures 3.15, 3.16, 3.17; green arrows).

Segmentation of the developing brain initiates early during embryogenesis. It first segments into the rostral-most forebrain (prosencephalon), the midbrain (mesencephalon), and the caudal-most hindbrain (rhombencephalon). The prosencephalon later subdivides into the rostral telencephalon and caudal diencephalon. The rhombencephalon subdivides into the rostral metencephalon and the caudal myelencephalon. The telencephalon will form the cerebral hemispheres of the adult brain. The diencephalon will form the thalamus

and hypothalamus. The mesencephalon will form the cerebral aqueduct. The metencephalon will develop into the pons and cerebellum while the myelencephalon will give rise to the medulla (reviewed in Bally-Cuif and Wassef, 1995).

The expression of PEA3 and ERM in the mes-met boundary is of particular interest and was not reported in the previous study (Chotteau-Lelievre et al. 1997). The position of this boundary is established early in embryonic development by inductive signals emanating from the underlying mesoderm. Generally, it is thought that signals generated from members of the *Pax* transcription factor family induce the expression of the EN1 and EN2 transcription factors on both sides of the mes-met border.

This event then leads to the expression of the WNT1 signalling molecule in the middle of this boundary (reviewed by Joyner, 1996). EN1 and EN2 are co-expressed in this region as early 8.5 d.p.c. as is ERM. The function of the EN proteins are likely early signals that define the position of the mes-met border. Hence, the expression of ERM at 8.5 d.p.c. may also contribute to this positioning signal. PEA3 expression coincides with the expression of WNT1. WNT1 is thought to function in maintaining the integrity of the mes-met boundary (reviewed by Bally-Cuif, 1995; Joyner, 1996). Hence, both PEA3 and ERM may be involved in this aspect of CNS segmentation.

One important aspect in maintaining the mes-met boundary involves regulating the differential cell adhesion properties between and among the cell populations on each side of the boundary. WNT1 was shown to be essential for this function. Furthermore, studies showed that WNT1 could regulate cell adhesion by regulating the expression of E-cadherin and α N-catenin (reviewed by Bally-Cuif, 1995; Joyner, 1996). It is possible that WNT1

may regulate the expression of various cell adhesion molecules through members of the *Ets* family, specifically PEA3 and ERM. This hypothesis could be confirmed by showing that a subset of WNT1 target genes overlap with those of the PEA3 group proteins.

Expression of the PEA3 group members in other regions of the developing brain was reported for the later stages of embryonic development (Chotteau-Lelievre et al. 1997). Furthermore, all of the PEA3 group members were expressed in the adult brain (Xin et al. 1992; Brown and McKnight, 1992; Monte et al. 1994). RNase protection analysis of PEA3 expression in the adult mouse brain revealed that it was expressed in all of the morphological regions tested (Laing and Hassell, data not shown). However, we have yet to establish which specific cell types express PEA3 in the adult brain. These studies do indicate that the PEA3 group members have unique and overlapping functions in the development and maintenance of the brain. Further expression studies and reverse genetic approaches will be required to discern their roles in affecting CNS development.

3.3.5 PEA3 is expressed in somatic motor neurons that innervate the limb muscles.

PEA3 expression was detected in the developing spinal chord in two separate regions along its rostrocaudal length. The rostral-most signal was detected in the brachial region from ~ 12.0 through 12.5 d.p.c. It consisted of bilateral stripes (figure 3.8 C & F). The caudal-most signal was also bilateral but located in the lumbosacral region from ~ 12.75 through 13.0 d.p.c. (figure 3.8 H & I; figure 3.9 E, F & G). Furthermore, transverse sections through these regions revealed that the signals were located in the ventrolateral regions of the spinal chord (data not shown).

These observations were consistent with PEA3 being expressed in the somatic motor neurons of both the brachial and lumbosacral lateral motor column (LMC) (Tsuchida et al. 1994). ERM and ER81 were not detected in any region of the developing spinal chord in this study. These observations were first made in the laboratory of T.M. Jessell in the chick embryo (T.M. Jessell, personal communication). However, their results differed from those in this study in that they also detected ER81 expression in the LMC (Lin et al., communication of unpublished data).

In order to analyse the potential functions of PEA3 and ER81 in LMC neuron development, we must consider two phenomena. Firstly, neurons in the LMC are initially scattered throughout the ventral neural tube. Prior to axonal outgrowth, they must organize themselves into their specific LMC pools within the ventrolateral horns of the spinal column. Secondly, as the neurons initiate axonal outgrowth from within the LMC pools, they must be able to select specific pathways towards their target muscles in the limbs (reviewed in Tsuchida et al. 1994). The first phase was shown to be regulated by members of the *Lim* homeobox gene family, specifically *Islet-1*, *Islet-2*, *Lim-1* and *Lim-3* (Tsuchida et al. 1994). Furthermore, the organization of the LMC pools was completed prior to the expression of PEA3 and ER81 (Lin et al., communication of unpublished data).

The axons from LMC neurons respond to target signals that originate in the lateral plate mesenchyme at the base of the limbs. Initially, all axons from the LMC grow out along a common ventral root and stop when they reach the base of the limb. At this stage, the axons will decide between a dorsal or a ventral trajectory into the limb mesenchyme. Retrograde labelling studies revealed a subdivision within the LMC pools; dorsal target

muscles were innervated by neurons located within the lateral LMC (LMC_l) whereas ventral target muscles were innervated by neurons within the medial LMC (LMC_m). PEA3 expression was localized more precisely to the LMC_l. Hence, it was expressed in neurons that were destined to follow a dorsal trajectory (Lin et al., communication of unpublished data).

However, this subdivision of the LMC can already be determined by the co-expression of the *Lim* transcription factors *Islet-1*, *Islet-2* and *Lim-1*, prior to the expression of either PEA3 or ER81 (Tsuchida et al. 1994; Lin et al., unpublished data). Hence, although PEA3 is expressed in the LMC_l, these neurons have already been programmed to follow a dorsal trajectory prior to PEA3 expression. In each of the dorsal and ventral trajectories, the LMC neurons must make a decision between an anterior trajectory or a posterior trajectory and then finally target an individual muscle.

Achieving axonal targeting specificity is a complicated process. The PEA3 group proteins may regulate the expression of adhesion molecules that in turn regulate the specificity of axonal guidance. In support of this hypothesis, a recent study revealed that both ERM and PEA3 were able to transactivate the promoter of intercellular adhesion molecule-1 (ICAM-1) *in-vitro* (de Launoit et al. 1998). Many cell adhesion molecule gene families have been implicated in affecting axonal targeting including the cadherins, the selectins, members of the immunoglobulin superfamily and the integrins (reviewed in Hynes and Lander, 1992). Again, identifying the PEA3 group target genes in the LMC neurons will help to define their functions more precisely.

3.3.6 PEA3 and ERM are expressed in the somites and may play a role in affecting skeletal muscle development.

PEA3 was first detected in the rostral-most somites at 9.5 d.p.c. (figure 3.6 A). As somitogenesis proceeded in a rostral to caudal direction, PEA3 expression was detected in the more caudally located somites (figure 3.7). Furthermore, the boundaries of its expression signal in the somites lengthened along the dorsoventral axis in a rostral to caudal fashion as development progressed through to 12.5 d.p.c. (figure 3.8 A,B,E & F). However, by 12.75 d.p.c., PEA3 expression was not detected in the rostral most somites and was much reduced in the thoracic and abdominal somites (figure 3.8 I). Transverse sections through the somites revealed that the PEA3 signal resided in the sub-ectodermal or dorsal most aspect of the somites (figure 3.6 F & G; data not shown). This region is referred to as the dermamyotome. Hence, PEA3 expression was down-regulated in a rostral to caudal fashion initiating at ~12.5 d.p.c. By 13.0 d.p.c., PEA3 was detected only in somites caudal to the hindlimbs (figure 3.9 A).

ERM expression was also detected in the somites initiating between 9.5 and 10.0 d.p.c. (figure 3.14 A). Its expression pattern appeared to follow the same spatial and temporal kinetics as PEA3. However, ERM expression appeared to be down-regulated in a rostral to caudal fashion beginning at 12 d.p.c. and continuing through 12.5 d.p.c. (figure 3.16 A). ERM was not detected in any of the somites at 13.0 d.p.c. (figure 3.17 A). ER81 was detected only transiently in the somites between 11 and 11.5 d.p.c. (figure

3.14 D,E & F; figure 3.15 D,E & F); its signal was diffuse and appeared much less intense than that of either PEA3 or ERM.

Somitogenesis begins at ~8.0 d.p.c. when the paraxial mesoderm becomes organized into paired condensations along the RC axis. This process initiates at the rostral-most boundary of the paraxial mesoderm and progresses caudally. These metameric condensations segregate from one another forming pairs of epithelial somites that consist of an outer sphere of tightly associated epithelial cells surrounding a loosely packed mesenchymal core. Hence, somites establish the segmental nature of the vertebrate body plan along the RC axis of the embryo (Bumcrot and McMahon, 1995; Cossu et al. 1996). The *Hox* genes appear to be involved in establishing the positional identity of the somites along the RC axis (McGinnis and Krumlauf, 1992).

Somites also differentiate along their dorsoventral (DV) axis producing morphologically distinct compartments. The dorsal-most compartment, initially the dermamyotome, segregates into the dermatome, the dermamyotome and the myotome. The ventral medial region of the somite forms the sclerotome. The dermatome will give rise to the dermis and connective tissue. The myotome will give rise to the axial musculature. The dermamyotome will give rise to the muscles of the ribs, the lateral body wall and the limbs. The sclerotome will form the axial skeleton.

In recent years, genetic markers for these compartments have been identified. The transcription factors *Pax3*, *Pax7* and *Sim1* were expressed in the dermamyotome whereas *Pax1* and *Pax9* marked sclerotomal cells. A series of experiments implicated the dorsal neural tube and adjacent ectoderm as the source of dorsalizing signals for the somites. The

ectodermal signals have recently been attributed to two members of the TGF β family, BMP4 and BMP7. It has long been known that the notochord and the floorplate were the source of ventralizing signals for the somites and recent studies have since attributed this activity to *Shh* (Bumcrot and McMahon, 1995; Cossu et al. 1996). Hence, somite differentiation along the DV axis likely involves competing inductive signals, a dorsalizing signal(s) from the dorsal neural tube and the adjacent ectoderm, and ventralizing signals from the notochord and floorplate.

PEA3 and ERM were expressed in the dermamyotome at a time when embryonic myoblasts were proliferating and migrating to their proper positions within the embryo prior to differentiating. Their expression appeared to be down-regulated at a time when the myoblasts were differentiating into post-mitotic myocytes, the cells that will later align and fuse to form myotubes. Hence, these proteins may be involved in affecting myoblast proliferation and/or migration. However, PEA3 expression did not always correlate with cell proliferation. Although it was expressed in the proliferating epiblast during gastrulation, it was not expressed in the proliferating mesendodermal cells. Furthermore, PEA3 was also expressed in the post-mitotic neurons of the LMC.

It is possible that PEA3 and ERM are involved in affecting myoblast migration. Both the PAX3 transcription factor and the c-MET receptor tyrosine kinase were expressed in migratory myoblasts derived from the dermamyotome. Mutations in *Pax3* and *c-Met* both lead to an absence of muscles in the body wall and limbs. Furthermore, *c-Met* expression was not detected in *Pax3* mutant mice indicating that *c-Met* was downstream

of *Pax3*. These defects resulted from a failure of the myoblasts to migrate to their proper locals. *Pax3* may affect myoblast migration by up-regulating *c-Met* expression.

c-Met in turn may regulate the expression of the target genes that directly affect cell migration (Cossu et al. 1996; Rawls and Olson, 1997). *c-Met* may regulate target gene expression through both PEA3 and ERM. The PEA3 group members may in turn affect myoblast migration by regulating the processes of cell adhesion and/or migration as discussed (section 3.3.1). It will be important to demonstrate that PEA3 and ERM are co-expressed with PAX3 and c-MET in migrating myoblasts.

This hypothesis was supported by a recent study that showed that PEA3 expression was up-regulated in adult myoblasts (satellite cells) as a result of muscle injury (Taylor et al. 1997). Muscle injury leads to satellite cell activation where they proliferate and then migrate to the site of injury. Once they infiltrate the wounded region, they align themselves, differentiate into myocytes and then fuse into myotubes to affect skeletal muscle repair. PEA3 expression was found to be down regulated as the satellite cells began to differentiate (Taylor et al. 1997). Hence, PEA3's role in satellite cell activation may be closely related to its role in embryonic myoblasts in that it may affect the migratory properties of satellite cells or prevent their differentiation until they reach their target site.

It is also possible that the *Pax* genes up-regulate *c-Met* through the *ETS* genes. A recent study showed that ETS1 was capable of transactivating the *MET* promoter through an ETS responsive element located ~300 bp upstream of the transcription start site. Interestingly, they also showed that activated MET lead to the expression of the *ETS1*

mRNA. Therefore, this study showed that *ETS* genes could act both upstream and downstream of *MET* (Gambarotta et al. 1996). Hence, PEA3 and ERM may be involved in transactivating the *c-Met* promoter during myoblast development.

3.3.7 PEA3 and ERM may play a role in affecting the early morphogenesis of the urogenital system.

PEA3 and ERM were expressed in the earliest rudiments of the developing urogenital system. They were expressed at 9.0 d.p.c. in the mesoderm of the nephrogenic chords and the underlying pronephric ducts (figure 3.5 F,G & H). PEA3 was expressed in later derivatives of the kidney including the mesenchyme surrounding the mesonephric ducts from 9.5 through 10.0 d.p.c. (figure 3.6 A & B; figure 3.7 A). However, the PEA3 signal became 'patchy' in its appearance by 9.5 d.p.c. ERM expression followed the same spatial and temporal kinetics as PEA3 and was not detectable in this region after 10.5 d.p.c. (figure 3.15 C). ER81 expression was not detected in the early urogenital rudiments during this period of development (figure 3.13 D,E, & F; figure 3.14 D,E & F).

The development of the early embryonic kidney or urogenital system occurs in three stages. The first structures to develop are the pronephros which consist of a nephrogenic chord and an underlying pronephric duct that has not yet canalized. Both of these structures are derived from lateral plate mesoderm. The pronephros develop just caudad to the forelimb bud with the duct extending caudally into the tailbud. This structure is vestigial in mammalian development and later degenerates.

At this point, the mesonephros begin to form just caudad to the pronephric region. This structure consists of a series of tubules that interdigitate with the overlying mesoderm of the nephric chord. The mesonephric tubules join with the mesonephric duct, the caudal continuation of the pronephric duct, and together function as the embryonic kidney during mammalian development. Canalization of this duct occurs between 9.5 and 10.0 d.p.c. of mouse development (Kaufman, 1992; p 74). This system of tubules will soon degenerate and the mesonephric ducts will give rise to the ductus epididymis and the vas deferens of the adult male urogenital tract. Lastly, a small outgrowth of the caudal most region of the mesonephric duct, the uteric bud, begins to invade the overlying mesoderm to form the metanephros. This bud will form the metanephric duct and tubules which will give rise to the ductal tree of the adult kidney (reviewed in Carlson, 1996 pp 569-581; Kaufman, 1992 pp 74, 92, 110, 120).

This entire process is regulated by a series of inductive signals passing between the mesoderm of the nephrogenic chord and the epithelium of the underlying nephrogenic duct. The molecular mechanisms governing these early stages of development are ill defined as of yet. PEA3 and ERM were both expressed in the early pronephric ducts along their entire length. Their expression patterns became 'patchy' as the pronephric ducts began to canalize and give rise to the more caudally located mesonephric ducts. Hence, both PEA3 and ERM may play a role in ductal canalization.

PEA3 and ERM were also expressed in the mesoderm of the nephrogenic chords. Therefore, they may also play a role in transducing the signals that regulate the formation and arborization of the mesonephric duct and tubules. This region will give rise to the

ductus epididymis and vas deferens of the adult male urogenital system. Interestingly, PEA3, ERM and ER81 were all expressed in the proximal epididymis of the adult male mouse (data not shown), a convoluted tubule distal to the testis that is required for effecting sperm maturation (see discussion section 4.3). Hence, PEA3 and ERM play a role in the early development of the male urogenital tract.

PEA3 and ERM were expressed in the genital eminence at 12.5 d.p.c. Their expression patterns were identical and appeared as bilateral sheets with a centrally located chord-like structure (figure 3.8 E; figure 3.16 C). Transverse sections through this structure revealed that the signal was localized to the sub-ectodermal mesenchyme of the genital swellings and a central chord present in the caudal half of the eminence (data not shown; figure 3.16 C). By 13.0 d.p.c., their expression was down-regulated in this structure. ER81 expression was not detected in the genital eminence.

The genital eminence is a raised mass of cells that appears at ~12.0 d.p.c. just rostral to the proctodeal depression on the ventral midline at the base of the tail. This structure marks the initiation of the development of the external genitalia. The eminence differentiates to give two centrally located genital folds and laterally positioned genital swellings with a midline chord or central prominence. This structure will later give rise to the penis and scrotum in the adult male or the labia in the adult female (Carlson, 1996; pp603-606). The inductive signals that govern this morphogenetic process have yet to be identified.

Both PEA3 and ERM were expressed in the mesenchyme and may be contributing to its differentiation and/or remodelling. Regulating specific changes in the cell adhesion

properties of mesenchymal cells is essential to their being organized into tissues during organogenesis. It would be a difficult task to identify PEA3 group target genes within the mesenchyme of the genital eminence given such a small temporal window of expression. However, aside from a genetic approach, this would be the most appropriate avenue to explore in determining their specific functions in affecting genital development.

3.3.8 PEA3 and ERM are expressed in the developing limb.

PEA3 and ERM were both expressed in the early forelimb field mesenchyme prior to its outgrowth at 9.0 d.p.c. (figure 3.5 , A & C; figure 3.13 A). Transverse sections through this region revealed that the PEA3 signal was localized to the lateral plate mesoderm in the forelimb field but not within the overlying ectoderm (data not shown). PEA3 was expressed throughout the forelimb bud mesenchyme after outgrowth had commenced at 9.5 d.p.c. (figure 3.6 B). However, by 10 through 10.5 d.p.c., its expression became localized to the distal tips of the fore and hindlimb buds (figure 3.7 A & B). Transverse sections revealed that the signal was localized to the sub-ectodermal mesenchyme at the distal tips and was not within the distal ectoderm. ERM was also expressed in the fore and hindlimb bud mesenchyme at 10.5 d.p.c., but its signal was present throughout the mesenchyme (figure 3.14 A).

By 11.5 d.p.c., both PEA3 and ERM expression was localized to the distal sub-ectodermal mesenchyme of both the fore and hindlimb buds (data not shown, figure 3.7 C & D; figure 3.15 A). ERM was also expressed in a dorsal mesenchymal mass in the forelimb bud at 11.5 d.p.c.; PEA3 was never detected in this location (compare figure 3.7

D with figure 3.15 A). The origin of the ERM expressing mesenchyme has not been determined; hence it could be either the rudiment of the humerus or the premuscle mass. As ERM did not appear in any other skeletal rudiments later in limb morphogenesis, it was likely the later possibility.

PEA3 was expressed in the distal sub-ectodermal mesenchyme of the limb paddles at 12.0 and 12.5 d.p.c. It was also expressed in the anterior necrotic zone, a region demarcating the position of the future elbow (figure 3.8 B & E). PEA3 was also detected in the dorsal mesenchyme of the fore and hindlimbs at this stage. This signal was divided into an anterior and a posterior mass, each running along the PD axis of the limb (figure 3.8 B & E). Unfortunately this signal was never retained in transverse sections. However, this signal was consistent with the formation of either the radius and ulna/ tibia and fibula or the developing muscle masses within the limb. Since this signal was located in the dorsal aspects of the limbs, the later hypothesis is more likely. The ERM signal was consistently much less intense at 12.5 d.p.c. relative to the earlier stages; but it was clearly present within the distal mesenchyme of the fore and hindlimb paddles (figure 3.16 A).

PEA3 was expressed in the distal mesenchyme and the interdigital mesenchyme of the forelimb paddle at 12.75 d.p.c. but was still confined to the distal mesenchyme in the hindlimb paddle (figure 3.8 H & I). By 13.0 d.p.c., PEA3 was expressed in the interdigital mesenchyme of the fore and hindlimb paddles (figure 3.9 G). Interestingly, from 7.0 through 12.5 d.p.c., the ERM expression pattern appeared to overlap with that of PEA3's. However, at 13.0 d.p.c. ERM expression was localized to the tips of the

forming digits (figure 3.17 B & C). ER81 expression was never detected in the developing limbs from 9.0 through 13.0 d.p.c. (figure 3.13 through figure 3.17).

We must consider four general features of limb development in order to understand some of the potential functions that PEA3 and ERM may carry out to affect morphogenesis. Firstly, the positions of the limb fields must be specified on the lateral body wall. Secondly, the spatial axes within which a limb develops must be determined. Thirdly, the cells within the limb must proliferate and then differentiate into their appropriate derivatives during outgrowth. Lastly, specific cell populations within the limb must undergo programmed cell death or apoptosis in order to affect morphogenesis. The molecular signalling pathways that regulate these processes are gradually being defined (reviewed in Johnson and Tabin, 1997).

The region on the lateral body wall where a limb will develop is referred to as the presumptive limb field. It is composed of lateral plate and intermediate mesoderm and the overlying ectoderm. Studies revealed that signals derived from the flank mesoderm determined the position of the limb field and initiated limb bud outgrowth (reviewed in Tanaka and Gann, 1995). At this stage, the limb field mesoderm became highly proliferative and mesenchymal in character (reviewed by Tickle, 1995).

A recent study showed that *Fgf8* was capable of defining a limb field and initiating the outgrowth of a fully developed ectopic limb. Furthermore, *Fgf8* was expressed in the presumptive limb field mesenchyme prior to its outgrowth. Similar results were obtained using the *Fgf10* ligand (reviewed by Johnson and Tabin, 1997). Since *Fgf8* was expressed prior to *Fgf10* in the presumptive mesenchyme; it was thought that *Fgf8* initially

determined the position of the limb field mesenchyme and then induced its proliferation through *Fgf10*.

Hence, the evidence suggested that expression of *Fgf* ligands within the mesenchyme of the lateral body wall determined the position of the limb field and initiated the entire limb development program. Interestingly, the *FgfR* was expressed in a broad band along the length of the ventral body wall. Hence, localized expression of its ligands within this band may provide the mechanism by which limb field position is determined (Tanaka and Gann, 1995; Tickle, 1995; Johnson and Tabin, 1997). However, the molecules through which the *Fgfs* and their receptors initiate this process have yet to be identified.

It is noteworthy that PEA3 and ERM were expressed in the presumptive limb field mesenchyme prior to outgrowth. Hence, they are both candidate transcription factors that may be involved in transducing the signals through these *Fgf* mediated pathways. Previous studies demonstrated that both PEA3 and ERM were regulated by Ras mediated pathways downstream of receptor tyrosine kinases (O'Hagan et al. 1996; Janknecht et al. 1996). The limb field mesenchyme shares many similar properties with cells within the gastrulating epiblast. These cell populations are highly proliferative, undergo a dermal to mesenchymal transition and must remain pluripotent. Interestingly, *Fgf8*, *FgfR*, *Pea3* and *Erm* are expressed within both of these cell populations. Further studies will be required to determine which if any of these phenomena are affected by PEA3 and ERM (section 3.3.2).

Limb development occurs within the context of the three spatial axes, the anteroposterior (AP) axis, the dorsoventral (DV) axis and the proximodistal (PD) axis (Carlson, 1996). The expression patterns of PEA3 and ERM were symmetrical about both the AP and DV axes; hence, it was unlikely that they contributed to axes determination. PEA3 and ERM were expressed in the distal sub-ectodermal mesenchyme which implicated them in the PD outgrowth of the limb. The distal mesenchyme is referred to as the progress zone mesoderm (PZM). It lies just beneath the distal ectoderm at the tip of the limb bud. The distal most ectoderm is organized within a raised ridge referred to as the apical ectodermal ridge (AER) (reviewed by Johnson and Tabin, 1997).

Inductive signals that pass between the PZM and AER regulate the outgrowth of a limb along the PD axis. The formation of the AER is induced by the underlying limb field mesenchyme prior to outgrowth. Previous studies showed that removal of the AER resulted in the degeneration of the PZM and limb truncation along the PD axis. Similar studies revealed that removal of the PZM resulted in the degeneration of the AER and limb truncation along the PD axis (Tanaka and Gann, 1995). Hence, once these two inductive centers were determined, reciprocal interactions between them were required for their maintenance and the continued outgrowth of the limb along the PD axis.

The bone, cartilage, connective tissue, tendons and ligaments present within a limb are all derived from the PZM. Hence, as PD outgrowth continues, cells within the proximal portions of the PZM must differentiate into these derivatives (Carlson, 1996). PEA3 and ERM were expressed in the distal PZM, a region where the cells must remain highly proliferative and pluripotential. Hence, these proteins do not appear to affect the

differentiation of the PZM. Rather, PEA3 and ERM may be involved in maintaining the proliferative and/or pluripotential nature of the distal PZM.

Interestingly, the activity of the AER can be replaced by recombinant FGF2, FGF4 and FGF8 (Johnson and Tabin, 1997; Tanaka and Gann, 1995) and all three genes were expressed within the AER. *Fgf4* was expressed in the posterior two thirds of the AER whereas both *Fgf2* and *Fgf8* were expressed throughout the entire AER. Furthermore *Fgfr* was expressed within the PZM (Johnson and Tabin, 1997). Hence, it is possible that FGFs within the AER maintain the integrity of the distal PZM by regulating the activities of PEA3 and ERM through FGFR1. It is also possible that PEA3 and ERM may regulate the expression of the genes that maintain the integrity of the AER. Further studies will be required to answer these questions.

The functions of PEA3 and ERM appeared to diverge during the later stages of limb development. At 13.0 d.p.c., PEA3 was expressed in the interdigital mesenchyme of the limb paddles whereas ERM was expressed at the tips of the digits. The cells within the interdigital mesenchyme undergo apoptosis in order to affect digit formation. PEA3 was also expressed in the anterior necrotic zone, another cell population that undergoes apoptosis in the region of the elbow joint (Johnson and Tabin, 1997). This is the first evidence suggesting that PEA3 may be expressed in cells that are undergoing genetically programmed cell death. Its potential role in affecting this process remains to be determined.

CHAPTER 4

GENETIC ANALYSIS OF PEA3 FUNCTION

4.1 INTRODUCTION.

Defining the expression profile for a given gene is essential in attempting to define its functions within a living organism. When a gene is expressed in a given cell population, it implies that the gene product contributes to its development or stasis. For example, PEA3 was expressed in the neurons of the LMC which eventually innervate the limb musculature. Hence, it was concluded that PEA3 somehow contributed to their differentiation or development. However, we could only hypothesize as to which functions it may carry out to affect LMC neuron development (section 3.3.5). In order to assign a specific function to a given gene product, one must carry out a genetic analysis.

Bicoid is a specific genetic mutation that was identified in *Drosophila* embryos. The bicoid protein was normally expressed in a concentration gradient along the AP axis of the early embryo. Hence, one could hypothesize that this protein helps to establish the AP axis in the early embryo. Furthermore, due to its high level of expression in the anterior region of the embryo, one could speculate that it may affect the morphogenesis of anterior structures. However, it was the absence of anterior structures within *bicoid* mutant embryos that confirmed the above hypotheses (section 1.1). Hence, the expression

data and the genetic data complimented each other to define an essential function of the bicoid gene during embryonic development.

PEA3 was expressed throughout embryonic development and was detected in tissues derived from all three germ layers (Chotteau-Lelievre et al. 1997; Brown et al. 1998; chapter 3). In the adult mouse, its expression was restricted to the brain and epididymis (Xin et al. 1992). PEA3 was also overexpressed in human metastatic mammary adenocarcinomas and correlated with the overexpression of *HER2* (*ErbB2*, *c-neu*), a member of the EGF receptor family of tyrosine kinases (Benz et al. 1997; Hynes and Stern, 1994). This observation was also made in two transgenic mouse models for this disease (Trimble et al. 1993). Hence, PEA3 functions to affect normal embryonic development and likely contributes to the stasis of specific cell populations within the adult brain and epididymis.

Furthermore it may contribute to the genesis or progression of human breast cancer. A subset of the target genes for the PEA3 group proteins, and specifically PEA3, are members of the matrix metalloproteinase (MMP) family and their inhibitors. *PEA3* (*E1A-F*) was also capable of conferring an invasive phenotype upon MCF-7 cells (Kaya et al. 1996; section 1.4.3; section 1.5.2). Hence, PEA3 has a potential role in affecting tumor cell invasion and metastasis.

However, PEA3's role in tumorigenesis may not be limited solely to invasion and metastasis; it may also involve tumor induction and growth. Recent studies showed that both *E1A-F* (*PEA3*) and *ETV-1* (*ER81*) were translocated to the *EWS* locus in primitive neuroectodermal tumors and Ewing's sarcomas (Jeon et al. 1994; Kaneko et al. 1996;

Urano et al. 1996). These translocations likely produced chimeric EWS-ETS proteins that functioned as highly active transcription factors with ETS target gene specificity (Bailly et al. 1994; Braun et al. 1995; section 1.5.1).

It was necessary to employ a genetic approach in order to define the functions of PEA3 either during embryogenesis or in the maturation and maintenance of adult tissues. Using the technique of homologous recombination in embryonic stem (ES) cells, we attempted to generate a mouse line harbouring a null allele at the *Pea3* locus (figure 4.1 A; figure 4.2). If *Pea3* null mice were viable, they would provide a means of carrying out a genetic analysis of PEA3 function in the induction and progression of mammary adenocarcinomas.

Furthermore, various cell lines derived from this mouse line would provide a valuable means of assessing PEA3's role in affecting their cellular proliferation, differentiation and transformation *in-vitro*. Tissues and cell lines from a *Pea3* null mouse line will also provide reagents with which we can attempt to identify *bona fide* PEA3 target genes. Identifying the target genes that are regulated by PEA3 will help to further define its functions.

Lastly, the *ETS* family is very large and the proteins retain a high degree of sequence conservation within their ETS domains (section 1.4; 1.4.1). Furthermore, PEA3 is the founding member of an *ETS* subfamily, the PEA3 group (section 1.4.4). Hence, there is likely a significant amount of functional redundancy within this gene family. In support of this hypothesis, I was able to show that both PEA3 and ERM had very similar embryonic expression patterns from 7.0 d.p.c. through 12.5 d.p.c (chapter 3). ER81

expression shared limited sites of overlap with PEA3 and ERM. These findings suggested that PEA3 and ERM might serve redundant functions for a significant part of embryogenesis. This hypothesis will be tested in the future by intercrossing *Pea3* null mice with *Erm* null mice and assessing the phenotypes within the double mutants.

4.2 RESULTS.

4.2.1 Generation and isolation of heterozygous embryonic stem (ES) cell clones harbouring a deletion at the *Pea3* Locus.

pBSneo9331 was linearized and electroporated into J1 ES cells in two separate experiments. In the first experiment, 5×10^7 ES cells were electroporated in the presence of 25 μg of the linearized targeting vector. A total of 384 G418 resistant clones were picked and 350 clones survived. In the second experiment, 1.62×10^7 ES cells were electroporated in the presence of 25 μg of the linearized vector. A total of 574 G418 clones were picked of which 500 survived.

The predicted recombination event at the *Pea3* locus should generate two bands in a Southern blot when genomic DNA is digested with *Cl*I and *Eco*RI, an 8.21 kbp wild-type band and a 7.46 kbp recombinant band. These bands would be detected by an 840 bp *Cl*I/*Kpn*I probe that lies just outside of the 5' border of the targeting construct (figure 4.1 A). A total of 12 targeted ES cell clones were identified using this screen (figure 4.1 B, lanes 3, 5, 7, 9, 11, 13, 15, 17, 19 & 21).

The *Pea3* gene harbours an *Eag*I site in exon 2. A second *Eag*I site (present in the PGKneoPA cassette) would be introduced into the locus by the targeting construct (figure 4.1 A). The 840 bp probe should detect a 10 kbp *Eag*I fragment from targeted ES clones. The *Eag*I digest confirmed that recombination occurred in the predicted manner at the *Pea3* locus only where the *Cl*I/*Eco*RI doublet was detected (figure 4.1 B; lanes 4, 6, 8, 10, 12, 14, 16, 18, 20 & 22). The clone designated A.D10 (figure 4.1 B; lanes 1 & 2)

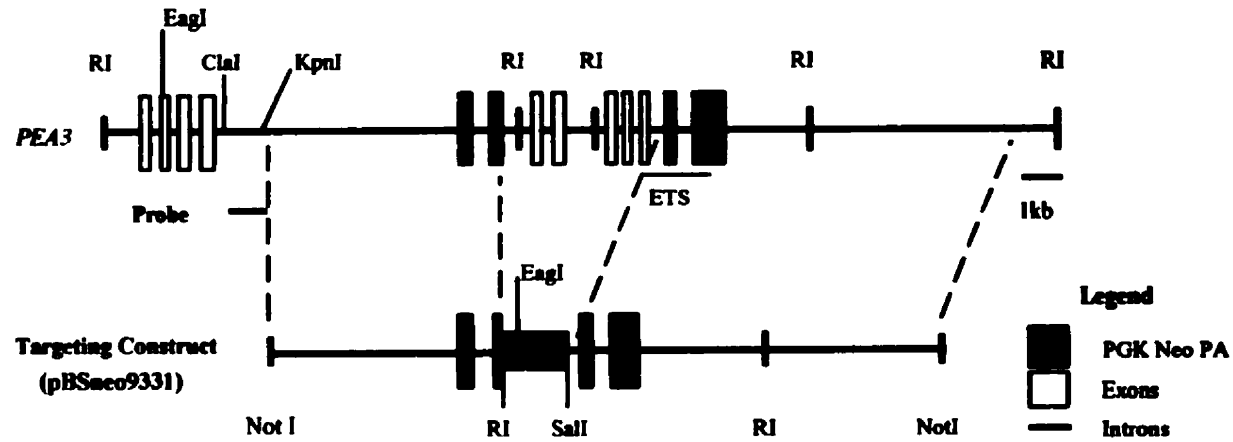
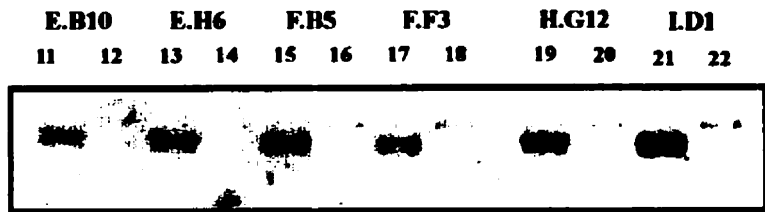
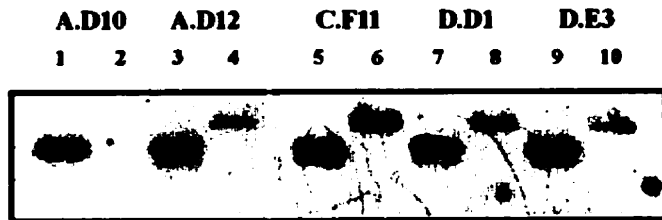
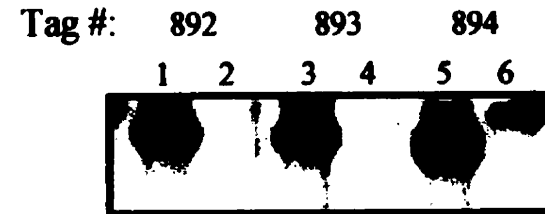
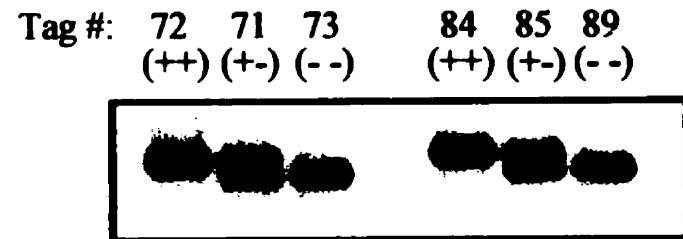
served as a negative control. Two other targeted clones, B.G8 and I.D2, were left out of this composite analysis. pBSneo9331 contained a total of 17.2 kbp of homologous sequence to the *Pea3* locus; the targeting frequency was 1/70 with positive selection alone.

4.2.2 Establishing a *Pea3* knock-out mouse line.

Three targeted ES cell clones were injected into Balb/c blastocysts, C.F11, D.D1 and D.E3 (figure 4.1 B). Only those injections with the D.D1 clone produced chimeric mice. One male chimera was back-crossed to balb/c females. Although its coat colour indicated ~ 50% chimerism, only 20% of his offspring were ES cell derived. However, the PEA3 knock-out mutation was transmitted to the F₁ generation (figure 4.1 C, lanes 5 & 6). This Balb/C/129/sv outbred mouse line was named after the ES cell clone that it was derived from; it was referred to as the D.D1 mouse line. All of the analyses in this study were carried out on this mouse line. Heterozygous F₁ mice were intercrossed to produce the F₂ generation. PEA3 +/+ mice had only the 8.21 kbp band, PEA3 +/- mice had both the 8.21 kbp and the 7.46 kbp bands while the PEA3 -/- mice had only the 7.46 kbp band (figure 4.1 D). The D.D1 chimeric male was also back-crossed with female 129/sv mice in order to establish an inbred knock out mouse line; it was referred to as the D.D1/sv line.

Figure 4.1 Generation of ES cell lines and a mouse line targeted at the *Pea3* genomic locus.

(A) Schematic diagram of the *Pea3* gene and the targeting construct, pBSneo9331, designed to generate a null allele. Genotype analysis was carried out via Southern blot analysis using the 840 bp *Clal/KpnI* probe 5' to the left flank of pBSneo9331. (B) Southern blot analysis of the ES cell clones isolated containing the targeted deletion at the *Pea3* locus. DNA samples in the odd numbered lanes were digested with *Clal* and *EcoRI*. DNA samples in the even numbered lanes were digested with *EagI*. Clone A.D10 served as a negative control. Two other positive clones, B.G8 and I.D2, were left out of this composite analysis. (C) Southern blot of tail DNA from the F₁ generation produced from a single male chimera derived from the D.D1 ES clone; DNA digested with *Clal* and *EcoRI* (lanes 1,3,5) or *EagI* (lanes 2,4,6). (D) Southern blot of tail DNA from the F₂ generation showing the banding pattern used to distinguish between the three genotypes using a *Clal/EcoRI* digest (section 2.19).

A**B****C****D**

4.2.3 PEA3 +/- and -/- mice harboured the predicted deletion mutation at both the RNA and protein levels.

It was important to confirm that the knock-out construct generated the predicted null allele prior to any analysis. A 323 bp 5' KpnI fragment derived from the PEA3.9 cDNA (Xin et al., 1992) was ligated into the KpnI site of pGEM7Zf(+). This plasmid was cut with XbaI and transcribed with SP6 RNA polymerase producing an antisense riboprobe that spanned exons 5 through 7, the region where the PGKneoPA cassette was introduced into the targeting vector (figure 4.2 A). When used in an RNase protection, this probe should protect a 323 bp fragment representing the full length PEA3 mRNA. However, there were actually four protected species present in the +/+ brain RNA sample (~ 323 bp, ~ 176 bp, ~ 170 bp & ~ 147 bp) (figure 4.2 B). The three later species likely resulted from alternative splicing of the PEA3 message.

The targeting construct should delete exon 6 (3' of NcoI(EcoRI)) and exon 7 from the genome. Hence, a knock-out specific protected species of 153 bp should be detected from the targeted locus (figure 4.2 A). A protected fragment of this size was detected in the +/- and -/- samples derived from total brain RNA (figure 4.2 B). Furthermore, this signal was present in an ~ 1:2 ratio from +/- to -/- when normalized to the PGK-1 internal control and quantitated using a phosphoimager (Molecular Diagnostics) (figure 4.2 B; data not shown). Finally, the 323 bp species representing the full length message, was not present in the -/- sample (figure 4.2 B). Therefore, these results were consistent with the presence of the predicted knock-out mutation at the *Pea3* locus and showed that a null allele was generated.

Furthermore, embryonic fibroblast cell lines were derived from 13.5 d.p.c embryos for both the $+/+$ and $-/-$ genotypes. Nuclear extracts from two independently derived cell lines for both the $+/+$ and $-/-$ genotypes were subjected to western blot analysis using PEA3 specific monoclonal antibodies. The two $+/+$ lines expressed the three wild type isoforms of PEA3 whereas the two $-/-$ lines did not express any of the PEA3 isoforms (figure 4.2 C, compare lanes 1 & 2 with lanes 3 & 4). This result confirmed that the targeting construct generated a null allele at the *Pea3* locus.

4.2.4 *Pea3* is not essential for embryonic development.

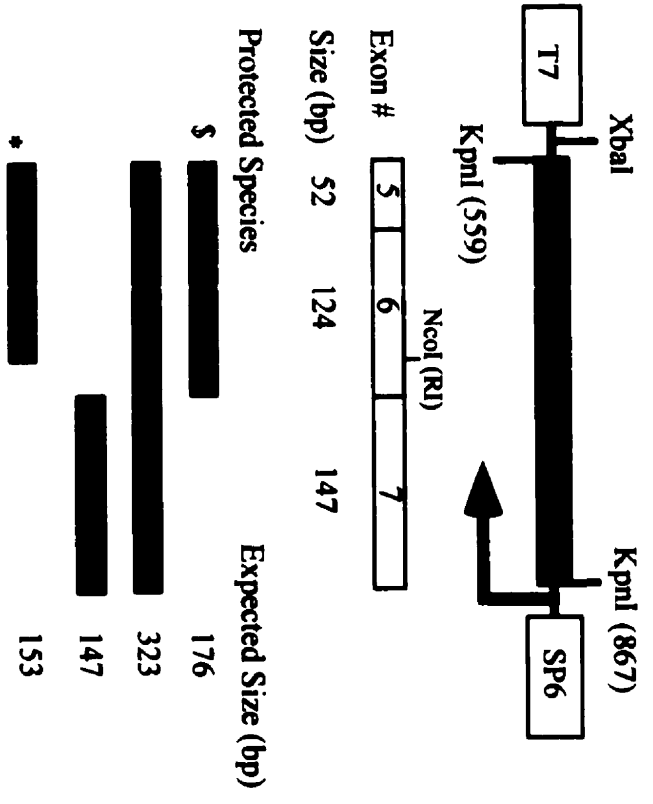
The PEA3 mRNA was expressed from the very early stages of embryonic development (~ day 7.0 d.p.c.) through organogenesis (chapter 3). It was expressed in tissues of ectodermal, mesodermal and endodermal origin (Chotteau-Lelievre et al. 1997; Brown et al. 1998). However, in the adult mouse (≥ 12 wks), its expression became restricted to the brain and epididymis (Xin et al., 1992). Despite its embryonic and adult expression patterns, *Pea3* null mice were viable.

Chi-square analysis of the genotype frequencies for the F2 generation revealed that the $-/-$ genotype occurred at the expected frequency at three weeks of age (table 4.1). Furthermore, there did not appear to be any overt differences in their overall state of health or behaviour when compared to their $+/+$ litter mates. The average masses for the $+/+$ and $-/-$ genotypes were 28.9 and 27.1 grams respectively at eight weeks of age. These values were close to the reported value of 27.8 gms (Rugh, 1968) indicating that the growth of the $-/-$ mice was not affected (table 4.2).

Figure 4.2 Molecular characterization of the *Pea3* null allele.

(A) Schematic diagram of the PEA3 5' KpnI riboprobe spanning exons 5 through 7 of the full length cDNA. The NcoI site in exon 6 marks the 5' border of the deleted region within the null allele. This riboprobe protects three wild type species (323 bp, 176 bp and 147 bp; see text). This riboprobe should protect a 153 bp species that would be transcribed from the null allele. **(B)** RNase protection analysis of 30 μ g of total brain RNA from +/+, +/- and -/- mice. Note that the -/- sample reveals only a \sim 153 bp protected species as expected. **(C)** Western blot of 25 μ g of nuclear extract from mouse embryonic fibroblasts established from individual d 13.5 p.c. embryos. Lane 1, MEF-4 +/+; Lane 2, MEF-D +/+; Lane 3, MEF-1 -/- and Lane 4, MEF-H -/-. This western was carried out using a mixture of the PEA3 specific monoclonal antibodies MP-13 and MP-16. The full length PEA3 protein and its splice variant species migrate with molecular weights of 69,000; 64,000 and 63,000 daltons respectively.

A

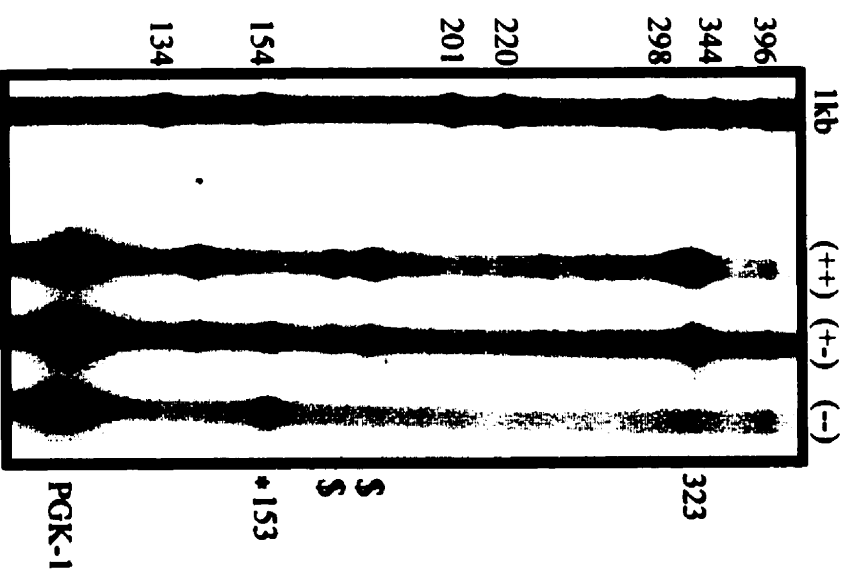


Exon # 5 6 7

Size (bp) 52 124 147

Protected Species	Expected Size (bp)
\$	176
\$	323
\$	147
*	153

B



C

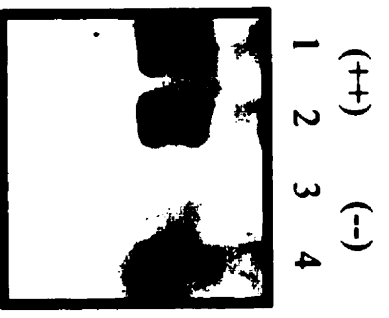


Table 4.1. Analysis of Genotype Frequencies.

n = 116	Genotype		
	+/+	+/-	-/-
Expected	29	58	29
Observed	33	57	26

$$\chi^2 = d^2/exp = 0.485 + 0.018 + 0.364 = 0.894$$

This χ^2 value will occur randomly ~65% of the time when n = 116.

Table 4.2. Comparison of Average Mass of +/+ vs -/- Mice By Difference of Means.

Hypothesis (H): $\mu_1 - \mu_2 = 0$

	+/+	-/-
sample size	17	32
average mass	28.9	27.1
variance	16.37	15.5
standard deviation	+/- 4.05	+/- 3.94

$z = 1.50$; this value does not fall into the critical region for $p < 0.01$ ($z \leq -2.576$ or $z \geq 2.576$).

4.2.5 Male *Pea3* null mice are infertile.

When establishing both the D.D1 and D.D1/sv mouse lines, mating pairs of all genotype and sex combinations were set up. After a few months it became apparent that only mating pairs that included a male *-/-* failed to produce litters. Furthermore, after 12 months, nine individual male *Pea3* null mice had failed to produce a single litter. The female null mice were fertile and their average litter sizes were similar to those of the *+/+* and *+/-* mice (table 4.3). This observation was also made for the D.D1/sv mouse line (table 4.4).

Furthermore, in collaboration with the laboratory of Dr. Thomas Jessell (Columbia University, NY, NY), Silvia Arber has since generated two different promoter-trap *Pea3* knock-out mouse lines, both of which exhibited male infertility (Silvia Arber, personal communication). Hence, this male infertility phenotype has now been reproduced in three different mouse lines targeted by homologous recombination at the *Pea3* locus. It had been previously established that the PEA3 mRNA was expressed in the adult epididymis (Xin et al., 1992). This organ is responsible for affecting sperm maturation; hence, male infertility was a candidate phenotype in the male knock-out mouse.

4.2.6 PEA3 mRNA is expressed in both the testes and epididymides prior to sexual maturity.

PEA3 was not expressed in the adult testes (Xin et al., 1992), but its expression had not been examined in this organ prior to sexual maturity. RNase protection analysis of total RNA from the testes and epididymides of mice at three and four weeks

Table 4.3. Fertility of the Outbred D.D1 PEA3 mice.

Genotype	Sample size	No. of Litters	No. of Pups	Avg. Litter Size
female +/-	16	39	260	6.67
male +/-	15	37	239	6.46
female -/-	10	32	192	6.00
* male -/-	9	0	0	0

* observations followed for one year.

Table 4.4. Fertility of the Inbred D.D1/sv PEA3 mice.

Genotype	Sample size	No. of Litters	No. of Pups	Avg. Litter Size
female +/-	13	63	329	5.2
male +/-	11	49	255	5.2
female -/-	5	12	43	3.6
* male -/-	5	0	0	0

* observations followed for one year.

of age revealed that the PEA3 mRNA was expressed in both organs at comparable levels (figure 4.3 A & B, lanes 14 & 15). This result implied that PEA3 function was not restricted to sperm maturation alone, but that PEA3 may also be involved in the development of the epididymis, germ cell development, spermatogenesis and/or spermiogenesis. It has yet to be established which cell type(s) within the developing testes express PEA3.

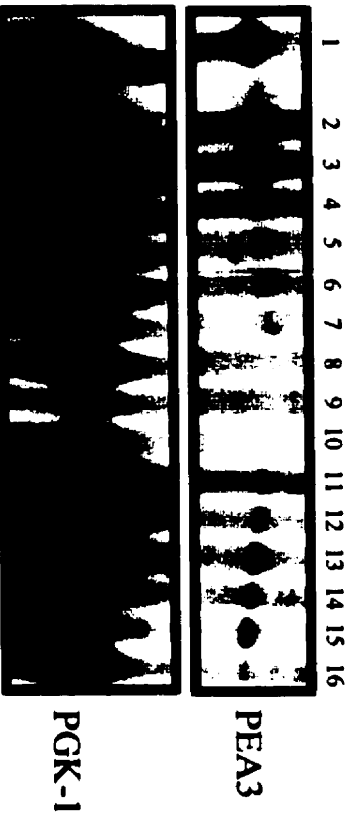
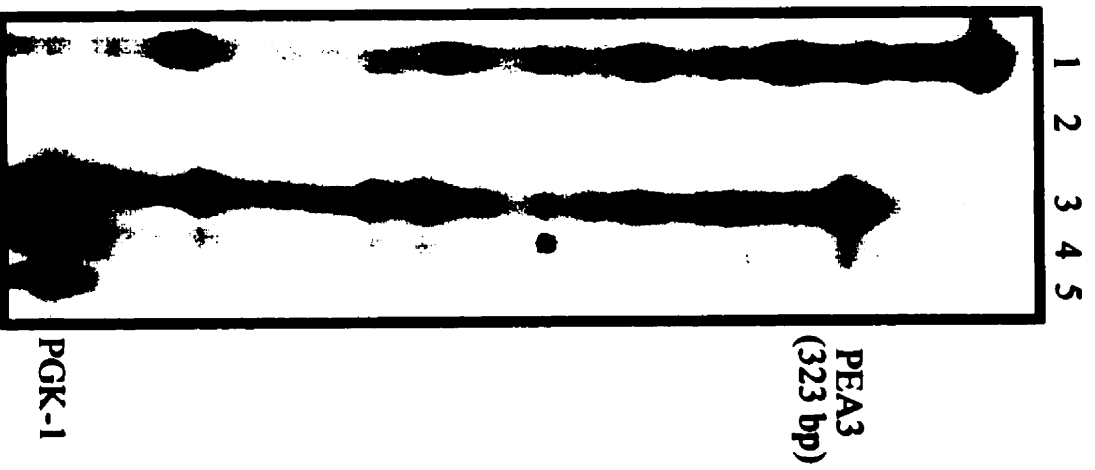
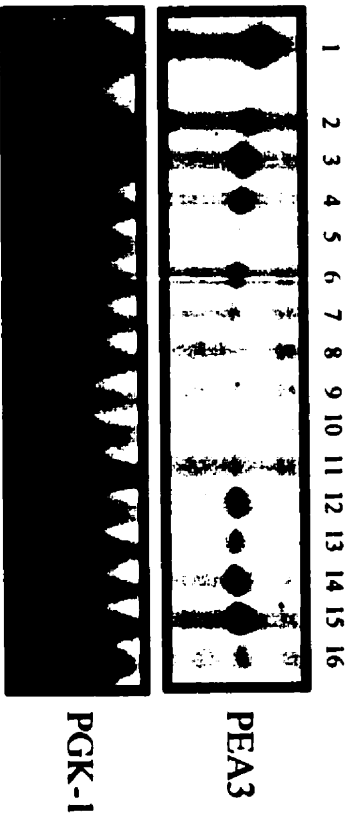
The epididymis is a long convoluted tube that spermatozoa enter via the efferent ducts of the testes. It has been divided into three morphologically distinct regions; the proximal region including the initial segment and caput epididymis, the middle region or corpus epididymis and the most distal region, the cauda epididymis, where mature sperm are stored prior to ejaculation (Amann et al. 1993). PEA3 mRNA expression was restricted to the proximal region of the epididymis (figure 4.3 C, lane 3). *In-situ* hybridization analysis carried out on rat epididymides has further localized PEA3 expression to the epithelium of the initial segment (Lan et al. 1997).

4.2.7 Histology of the testes and epididymides from *Pea3* null mice appears normal.

Based upon the above expression data, histological analyses of the testes and epididymides were carried out. The gross structure of the *-/-* testes appeared normal in comparison to the *+/+* testes (figure 4.4, compare A with C). The architecture of the seminiferous epithelium appeared normal in the three genotypes; Sertoli cells, spermatogonia, primary spermatocytes, spermatids and spermatozoa were all present (figure 4.4, B & D; data not shown). The sections also revealed the presence of Leydig

Figure 4.3 RNase protection analysis of various organs from juvenile mice and the major regions of the adult epididymis.

(A) Organ recital from mice at 3 wks of age. **(B)** Organ recital from mice at 4 wks of age. (lane 1, FM3A; lane 2, cerebrum; lane 3, cerebellum; lane 4, spinal chord; lane 5, heart; lane 6, thymus; lane 7, lung; lane 8, liver; lane 9, pancreas; lane 10, spleen; lane 11, kidney; lane 12, small intestine; lane 13, skeletal muscle; lane 14, testes; lane 15, epididymis; lane 16, salivary gland). PEA3 marks the 323 bp protected species; the ~ 124 bp PGK-1 protected species serves as an internal control for RNA loading. **(C)** RNase protection of the three major regions of the adult epididymis; lane 1, PEA3 and PGK-1 riboprobes alone; lane 2; riboprobes + RNase T2; lane 3; initial segment and caput epididymis; lane 4, corpus epididymis; lane 5, cauda epididymis. Each sample lane contained 30 μ g total RNA for (A), (B) and (C).

A**C****B**

cells and stromal cells outside of the basal laminae surrounding the seminiferous tubules (figure 4.4 B & D).

Interestingly, it was the epithelium of the initial segment that failed to differentiate in *Ros* knock-out mice. This was revealed by both standard histological analysis and β -galactosidase staining of the epididymis (Sonnenberg-Riethmacher et al. 1996). There is an endogenous β -galactosidase activity present in the epithelium of the initial segment and it can serve as a marker of its differentiation (Nanba and Suzuki, 1990). The initial segment of the *Ros* null epididymis failed to stain blue showing this epithelium had failed to differentiate properly. The epididymides from wild-type and *Pea3* null mice contained this enzymatic activity in the initial segment (figure 4.5). Hence, this result indicated that the epithelium of the initial segment differentiated properly in the *Pea3* null genetic background.

There were no visible histological abnormalities detected within any region of the *-/-* epididymis (figure 4.6), including the epithelium of the initial segment. Both basal cells and principal cells containing stereocilia were present forming the high columnar epithelium characteristic of the initial segment (figure 4.6 A & B) (Sun and Flickinger, 1979). Furthermore, significant amounts of spermatozoa were stored in the cauda region of the null epididymis when compared to the wild-type epididymis (figure 4.6, compare G with H).

Figure 4.4 Histology of the testes from +/+ and -/- mice.

(A) Seminiferous tubules of a +/+ testis; b marks the individual tubule magnified in B.

(B) Seminiferous epithelium of a +/+ seminiferous tubule. **(C)** Seminiferous tubules of

a -/- testis; d marks the individual tubule magnified in D. **(D)** Seminiferous epithelium of

a -/- tubule. Original magnification of A & C is 100 X; the bar in C is 250 μm . Original

magnification of B & D is 400 X; the bar in D is 50 μm . Lu = lumen; sp =

spermatogonia; ps = primary spermatocyte; sd = spermatid; sz = spermatozoa; st =

Sertoli cell; l = Leydig cell.

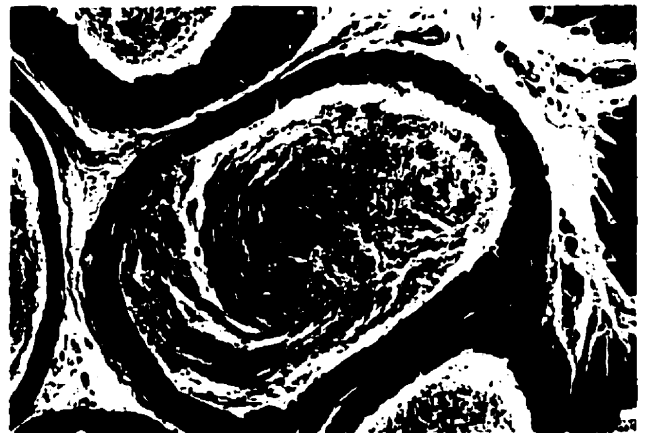
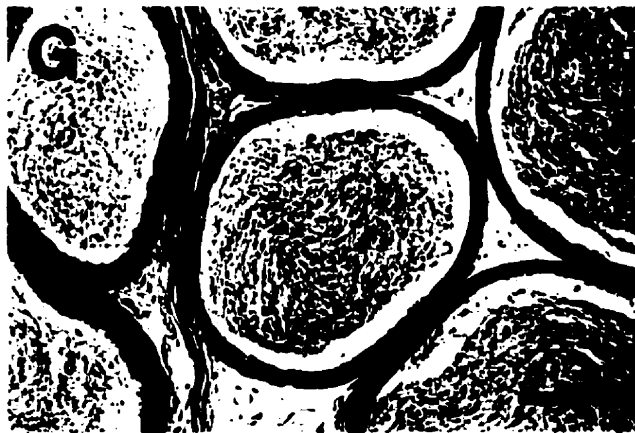
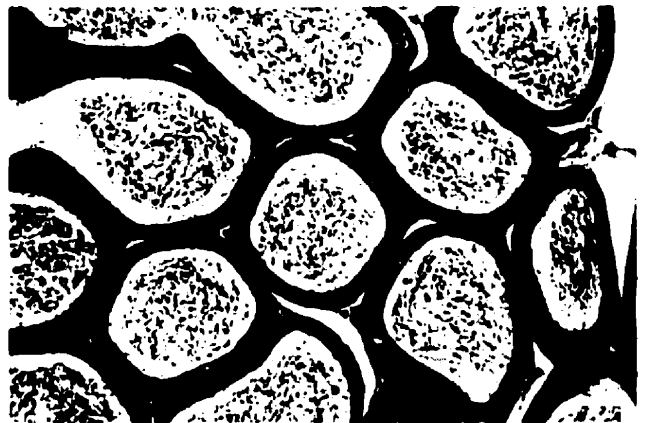
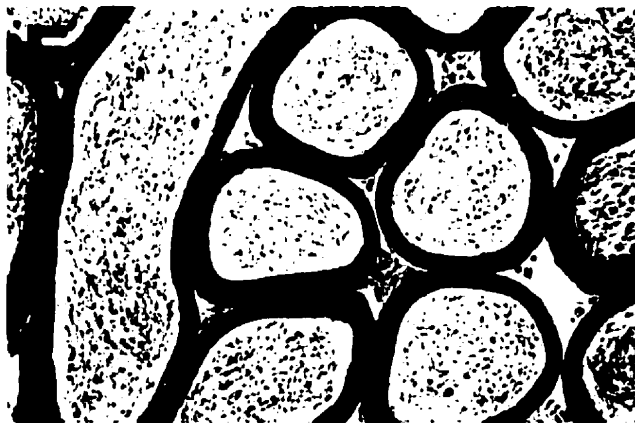
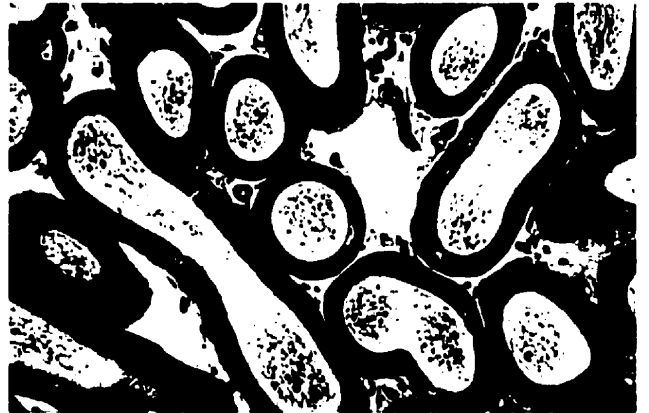
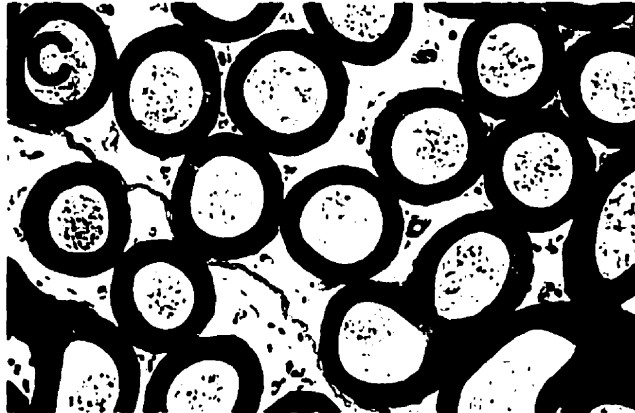
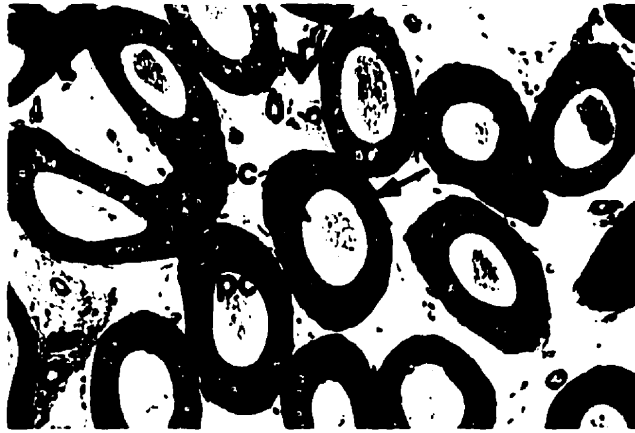
Figure 4.5 Whole mount β -galactosidase staining of +/+ and -/- epididymides.

(A) Whole mount of the proximal half of a +/+ epididymis; is = initial segment; cap = caput epididymis. **(B)** Whole mount of the proximal half of a -/- epididymis; arrows point at the is and cap respectively. The original magnifications for A and B was 16X.



Figure 4.6 Histology of the epididymides from +/+ and -/- mice.

(A) & (B) Sections through the initial segment of +/+ and -/- epididymides respectively. pc = principal cell; bc = basal cell; sc = stereocilia. **(C) & (D)** Sections through the caput region of +/+ and -/- epididymides respectively. **(E) & (F)** Sections through the corpus region of +/+ and -/- epididymides respectively. **(G) & (H)** Sections through the cauda region of +/+ and -/- epididymides respectively. Original magnifications of A through H are 200 X; bars in G & H are 100 μ m.



4.2.8 Sperm derived from *Pea3* null males is functional *In Vitro*.

The fact that the epithelium of the -/- initial segment differentiated properly and that ample sperm appeared to be stored in the cauda region of the -/- epididymis did not reveal whether or not the sperm were actually functional. *In-vitro* fertilization analysis was employed to test if -/- derived spermatozoa were capable of fertilizing oocytes. A series of seven experiments were carried out comparing spermatozoa samples from an outbred wild type mouse strain (ICR) with those of +/+ and -/- mice from the D.D1 line. This analysis revealed that spermatozoa derived from *Pea3* null mice fertilized as efficiently *in-vitro* as the sperm samples derived from both of the control mice (table 4.5). Statistical analysis revealed that the mean fertilization rates were not significantly different between any of the genotypes. Hence, the *Pea3* null males did not appear to harbour an overt defect in spermatogenesis, spermiogenesis or sperm maturation.

4.2.9 *In-Vivo* fertilization analysis.

Spermatozoa taken directly from the lumen of the seminiferous tubules are not capable of fertilizing oocytes *in vitro*. Spermatozoa must travel through the epididymis where they are exposed to different luminal microenvironments generated by secretions from the specialized epithelia within each of the different regions of this organ (Amann et al. 1993). During this process, specialized proteins and carbohydrate moieties are attached to or modified on the sperm's surface. These surface antigens are necessary for sperm-egg interactions (Snell and White 1996). Sperm also acquire motility during passage through the epididymis. All of these modifications would be required for sperm to survive,

Table 4.5 Mean represents the percentage of the total # of eggs fertilized for each genotype in the seven experiments. The mean fertilization rates were analyzed by one way analysis of variance followed by Tukey's multiple range test. Tukey's was used rather than Duncan's because of the unequal N value for each group. None of the three means were significantly different. N = number of individual mice tested; S.D. = standard deviation; S.E.M. = standard error of the mean.

Table 4.5. *In Vitro* Fertilization Analysis.

Experiment #	Control (ICR)		+/+		-/-	
	# eggs	%fert	# eggs	%fert	# eggs	%fert
1	33	51.0	29	24.0	30	50.0
2	28	71.0	N.D.	N.D.	26	80.0
3	N.D.	N.D.	N.D.	N.D.	29	68.9
4	19	68.0	18	61.0	20	80.0
5	30	43.3	29	44.8	27	44.0
6	26	62.0	27	56.0	30	60.0
7	48	65.0	38	55.2	37	67.5
Total # eggs	184		141		199	
N	6		5		7	
Mean	60.05		48.20		64.34	
S.D.	10.713		14.755		13.901	
S.E.M.	4.37		6.60		5.25	

travel, bind to and fertilize cumulus cell-enclosed oocytes present in the oviducts of the female reproductive tract.

Interestingly, although *Ros* null males were infertile, their sperm was capable of fertilizing oocytes *in-vitro*. However, even though these mice set copulatory plugs, their sperm failed to fertilize *in-vivo* (Sonnenberg-Riethmacher et al. 1996). This may have been due to incomplete sperm maturation caused by subtle defects within the *Ros* null epididymides. Therefore sperm derived from *Pea3* null mice had to be analyzed for its ability to function *in-vivo*.

Female Balb/C mice were superovulated and paired overnight with males of all three genotypes from the D.D1 line. The next morning, the females were examined for the presence of a copulatory plug. Approximately 70 % of the matings set up with either $+/+$ or $+/-$ males were successful as judged by this criterion (table 4.6). Interestingly, no plugs were set in any of the 113 matings set up with *Pea3* null males ($n=36$) (table 4.6).

Furthermore, female reproductive tracts were routinely flushed and examined for the presence of spermatozoa; no traces were ever observed within the females mated with *Pea3* null males (data not shown). Pronucleation rates were ~80% from matings set with $+/+$ and $+/-$ males whereas it was less than 2% in the $-/-$ group (table 4.6). Of the two eggs from the $-/-$ group that did undergo cleavage, their first divisions were unequal and both eggs failed to develop further in culture (data not shown). Hence these two celled embryos were not likely the result of a fertilization event (Bliel, 1991).

Interestingly, *Pea3* null males exhibited normal grooming and mating behaviour and frequently attempted to mount the females while they were paired. Furthermore, the

Table 4.6. *In Vivo* Fertilization Analysis.

Exp.	Genotype					
	+/+		+/-		-/-	
	# plugged	#matings	# plugged	#matings	# plugged	#matings
1	3	/ 6	3	/ 4	0	/ 10
2	2	/ 6	2	/ 4	0	/ 10
3	1	/ 5	3	/ 5	0	/ 7
4	4	/ 5	3	/ 5	0	/ 7
5	4	/ 5	4	/ 5	0	/ 7
6	3	/ 5	3	/ 5	0	/ 7
7	7	/ 8	11	/ 13	0	/ 16
8	8	/ 8	14	/ 14	0	/ 16
9	6	/ 6	18	/ 22	0	/ 21
10	4	/ 7	1	/ 7	0	/ 7
11	4	/ 7	3	/ 7	0	/ 5
<hr/>						
% plugs set	46/70 (65.7%)		65/90 (72.2%)		0/113 (0%)	
% pronuc eggs	304/392 (78%)		334/411 (81%)		* 2/105 (<2%)	
n (number of male mice tested)	24		30		36	

concentrations of the sex hormones, follicle stimulating hormone (FSH), luteinizing hormone (LH) and testosterone, were determined by radio-immunoassay. Their levels were all within the normal limits in the null mice and did not differ significantly from those of the $+/+$ and ICR control mice (table 4.7). This observation suggested that male infertility was not a consequence of a neuroendocrine disorder. Therefore, *Pea3* null male mice were infertile because they failed to set copulatory plugs when mated with females in oestrus.

4.2.10 *Pea3* null mice exhibit a defect in the branching morphogenesis of their developing mammary glands.

A second phenotype was recently observed in the *Pea3* null mice by Lesley MacNeil, a graduate student in our laboratory. She prepared whole mount mammary gland preparations (section 2.26) in order to view the branching pattern of the epithelial ducts within the mammary gland fat pad. A whole mount preparation from a six month old virgin female mouse revealed a significant reduction in the branching pattern when compared to an age matched sample from a wild-type litter mate (figure 4.7, compare A with B). Specifically, the null gland contained many primary ducts but had a vastly reduced number of secondary, tertiary and quaternary ducts. This result has been repeated numerous times at different stages in the development of the virgin mammary gland (MacNeil and Hassell, unpublished observations).

Table 4.7 The mean concentrations of testosterone, FSH and LH were determined by RIA for the male mice sacrificed for the *in vitro* fertilization analysis. The data were analyzed by one way analysis of variance followed by Tukey's multiple range test. None of the mean hormone concentrations differed significantly between the three groups.

Table 4.7. Mean Hormone Concentrations for IVF's.

Hormone	Control (ICR) Mice (ng/ml)	+/+ (ng/ml)	-/- (ng/ml)
Testosterone	12.69	16.38	18.97
Follicle- Stimulating Hormone (FSH)	12.43	10.00	10.48
Luteinizing Hormone (LH)	2.52	1.18	2.60

Figure 4.7 Whole mount mammary gland preparations from 6 month old virgin females from the D.D1 mouse line.

(A) Whole mount mammary gland preparation from a $+/+$ 6 month old virgin female. (B) Whole mount mammary gland preparation from a $-/-$ 6 month old virgin female. LN = lymph node. Original magnification of A & B was 25X. The whole mount preparations were prepared by Lesley MacNeil, a graduate student under the supervision of Dr. J.A. Hassell.



4.2.11 ERM expression during the development of *Pea3* null embryos.

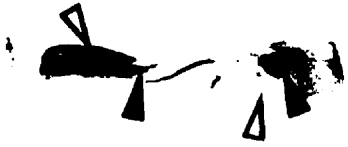
The preceding embryonic expression analysis revealed that both PEA3 and ERM shared many sites of expression from gastrulation (~7.0 d.p.c.) through to early organogenesis (~12.5 d.p.c.) (Chapter 3). Hence, it seems probable that ERM may provide redundant functions during these stages of embryonic development in *Pea3* null embryos. In order to support this contention, it was necessary to show that the ERM expression pattern was comparable between wild-type and *Pea3* null embryos.

Whole mount *in-situ* hybridizations were carried out on 8.5, 9.0, 11.0 and 12.5 d.p.c. *Pea3* null embryos using an antisense ERM riboprobe. ERM expression was detected in the expected regions during all of these stages of development (figure 4.8). Interestingly, ERM was detected in the somites of the 9.0 d.p.c. *Pea3* null embryo (figure 4.8 D) whereas it was not expressed until ~10 d.p.c. in the wild-type background (figure 3.15 A). Further studies will be required to determine if the early appearance of ERM in the *Pea3* null somites is a compensatory regulatory mechanism or simply due to differences in the genetic backgrounds of the wild-type and *Pea3* null embryos.

Figure 4.8 Expression pattern of the ERM mRNA in *Pea3* null embryos.

(A) Whole mount *in-situ* hybridization of an antisense ERM riboprobe to an 8.5 d.p.c. PEA3 *-/-* embryo. (B) Dorsal view of A. (C) Ventral view of A. (D) Whole mount *in-situ* hybridization of an antisense ERM riboprobe to a 9 d.p.c. PEA3 *-/-* embryo. (E) Dorsal view of D. (F) Ventral view of D. (G) Whole mount *in-situ* hybridization of an antisense ERM riboprobe to a ~10.5/11 d.p.c. PEA3 *-/-* embryo. (H) Ventral view of G. (I) Whole mount *in-situ* hybridization of an antisense ERM riboprobe to a 12.5 d.p.c. PEA3 *-/-* embryo. Original magnification of A through F = 25X; original magnification of G & H = 16X; I = 10X. (yellow arrow = primitive streak ectoderm or tailbud; white arrow = heart; red arrow = branchial arches; dark green arrow = forebrain; light green arrow = midbrain/hindbrain junction; black arrow = position of node in A, otic placode in E; orange arrow = somites; pink arrow = limb buds; light blue arrow = nasal placodes).

A



B



C



D



E



F



G



H



I



4.3 DISCUSSION.

4.3.1 PEA3 is not required for embryonic development.

Despite the widespread expression of *Pea3* during embryonic development, homozygous null mice were viable and appeared healthy (table 4.1 & table 4.2). Hence, *Pea3* was dispensable for embryogenesis. This result may reflect the fact that PEA3 is either not required or that its functions are redundant with those of ERM, ER81 or other *ETS* genes during embryogenesis (Chotteau-Lelievre et al. 1997; chapter 3). The latter explanation seemed likely as there were many sites of overlapping expression between PEA3 and ERM throughout embryogenesis (chapter 3, section 3.2). This hypothesis was strengthened by the fact that the ERM expression pattern appeared to be normal in *Pea3* null embryos (figure 4.8).

Previous studies revealed that all three PEA3 group genes were expressed in the adult brain (Xin et al. 1992; Brown and McKnight 1992; Monte et al. 1993). This fact may explain why the adult null mice failed to exhibit any overt phenotypes associated with a defect in the central nervous system (CNS). The above observations do not limit the candidate redundant *ETS* members to the PEA3 group alone. The embryonic expression patterns for many of the 23 known *ETS* genes have yet to be determined for the early stages of embryonic development. Furthermore, many of these proteins including cETS1, cETS2 and PU.1 are capable of activating the transcription of target genes by binding to PEA3 cis elements 5'-AGGAAG-3' present in their promoter regions. However, this study

did uncover two essential functions for *Pea3* in the adult mouse and they will be addressed in the following discussion.

4.3.2 PEA3 is required for male fertility.

Homozygous null male mice were infertile. To date, not one homozygous null male mouse has produced a single litter. This observation was made in both the outbred balb/C-129/sv (DD.1) and inbred 129/sv (DD.1/sv) genetic backgrounds. Infertility was restricted to the null male mice; null females were fully fertile (table 4.3 and table 4.4). Male infertility was one of the expected phenotypes based upon the expression of PEA3 in the adult epididymides (Xin et al. 1992). In attempting to define at which time in development *Pea3* expression became restricted to the adult pattern, we found that it was also expressed in the testes and epididymides prior to sexual maturity (figure 4.3 A & B, lanes 14 & 15 respectively).

Furthermore, PEA3 and ERM were expressed in the embryonic precursors of both the epididymis and penis (section 3.3.7). However, upon dissection of adult male mice, no visible abnormalities were detected in the gross morphology of the epididymis or penis. Hence, male infertility is not likely the result of a congenital abnormality present within the urogenital tract of male null mice. Therefore, based upon the above observations, aberrant spermatogenesis, spermiogenesis and sperm maturation were considered the more likely candidate causes of this phenotype.

Spermatogenesis and spermiogenesis occur within the testes. The histology of the seminiferous epithelium from *Pea3* null testes was identical to that of wild-type testes. The null epithelium contained Sertoli cells, spermatogonia, primary spermatocytes, spermatids and spermatozoa. The stroma also appeared normal and contained both Leydig cells, the cells responsible for producing testosterone (T), and stromal cells (figure 4.4). These observations suggested that both spermatogenesis and spermiogenesis were taking place. Furthermore, sperm production did not appear to be insufficient as the lumen of the cauda epididymides from the null mice were full of spermatozoa (figure 4.6 G & H). The cauda epididymis is the region where mature sperm are stored prior to ejaculation (Amann et al. 1993).

Spermatozoa taken directly from the lumen of the seminiferous tubules are incapable of fertilizing oocytes *in vitro*. They must travel through the epididymis, a long convoluted tubule distal to the testes, in order to acquire full fertilizing potential. The epididymis is divided into four major regions, each characterized by a distinct epithelial lining. The proximal-most region includes the initial segment and caput epididymis, the middle and distal-most regions are referred to as the corpus and cauda epididymis respectively (Amann et al. 1993). The epithelium produces and secretes many different proteins and enzymes into the luminal fluid that bathes the spermatozoa. These proteins and enzymes modify the antigens present on the sperm's surface such that they acquire the ability to bind to and fuse with receptors on the oocyte (Snell and White, 1996). Sperm must also pass through the epididymis in order to acquire motility (Amann et al. 1993).

The epididymis also secretes enzymes into the luminal fluid that are responsible for protecting spermatozoa from oxidative damage. The enzyme gamma-glutamyl transpeptidase (GGT) plays an important role in this process within the epididymis (Hinton et al. 1995). A recent study identified PEA3 as a potential transcriptional regulator of GGT mRNA-IV, a splice variant of GGT specifically expressed in the initial segment of the rat epididymis. This study showed that PEA3 mRNA expression was restricted to the epithelium of the initial segment and that it was positively regulated by testicular factors (Lan et al. 1997). We confirmed that PEA3 expression was localized within the proximal epididymis of the mouse by RNase protection (figure 4.3 C).

The epithelium of the initial segment is characterized as high columnar. It is composed of two cell types, basal cells and principal cells. Their luminal surfaces have stereocilia that flush sperm through to the caput epididymis (Sun and Flickinger, 1979). Interestingly, this epithelium failed to differentiate in *Ros* null mice. The *Ros* gene encoded a receptor tyrosine kinase that was expressed in the initial segment of the epididymis (Riethmacher et al. 1994). This defect was illustrated by a lack of endogenous β -galactosidase activity in the initial segment of *Ros* null epididymides as well as by standard histological analysis (Sonnenberg-Riethmacher et al. 1996).

We employed the above methods to analyze the differentiation of the epithelium within the initial segment of *Pea3* null epididymides. In contrast to the results from the *Ros* knock-out, the *Pea3* null epithelium appeared to differentiate properly (figures 4.5 & 4.6). Surprisingly, both *Ros* and *Pea3* null derived spermatozoa were capable of fertilizing oocytes *in vitro* at an efficiency equal to the control samples (Sonnenberg-Riethmacher et

al. 1996; table 4.5). Hence, these analyses indicated that sperm maturation appeared to be occurring normally in both the *Ros* and *Pea3* null mice in that their sperm was capable of binding to and fusing with oocytes *in vitro*.

Furthermore, *Ros* null males set copulatory plugs when mated with females. This finding suggested that their sperm were not capable of fertilizing oocytes *in vivo*. Hence, *Ros* null spermatozoa either failed to survive long enough to reach the oviducts or was incapable of travelling to the oviducts. These findings suggested that the *Ros* null epididymis was defective in some essential capacity (Sonnenberg-Riethmacher et al. 1996). In contrast, *Pea3* null males failed to set copulatory plugs in 113 mating trials set up with superovulated females (table 4.6). Hence, our observations suggested that the *Pea3* null males suffered from an erectile and/or ejaculatory dysfunction.

Pea3 null males exhibited normal mating behaviour. They engaged in grooming behaviour and repeatedly mounted the female mice during the mating trials. These observations lead us to rule out any gross behavioral abnormalities as an underlying cause of this phenotype. In order to test if there was a neuroendocrine defect in the *Pea3* null males, we determined the serum concentrations of luteinizing hormone (LH), follicle stimulating hormone (FSH) and testosterone (T). Their concentrations were all within the normal range (table 4.7). Hence, communication between the hypothalamus and the anterior pituitary gland appeared to be occurring normally.

Many studies have shown that T levels affect erectile function (Mills et al. 1992; Carani et al. 1992). However, the normal T concentrations in *Pea3* null males suggested

that a reduced T level was not the likely cause of an erectile dysfunction. These findings were not unexpected as fertility defects resulting from neuroendocrine dysfunction are often manifested in the form of defects in the maturation of the secondary sexual characteristics such as hypogonadism (Zonszein, 1995). These types of defects were not observed in the *Pea3* null male mice.

Both the erectile and ejaculatory reflexes are controlled by the autonomic nervous system which is in turn controlled, at least in part, by the limbic system in the brain. The limbic system is thought to regulate homeostasis of the organism as well as its emotional states and desires, including those of a sexual nature. The PEA3 mRNA was expressed in all regions of the adult brain (Laing and Hassell, unpublished data). Despite this finding, no abnormalities were observed in the null mice with respect to their feeding behaviour or sexual activity. Therefore it seemed unlikely that male infertility resulted from a defect within the CNS components that regulate sexual behaviour. However, we cannot yet rule out a CNS specific defect in the pathways that regulate erectile and ejaculatory function.

The erectile response is affected by the parasympathetic nervous system. Preganglionic parasympathetic neurons emanate from the spinal chord via the sacral parasympathetic ganglion at the levels of S2, S3 and S4. These neurons travel via the pelvic nerve to the pelvic plexus where the postganglionic parasympathetic axons travel via the cavernous nerve to the erectile tissue of the penis, the corpus cavernosum. These neurons are believed to synapse with the smooth muscle cells that control blood flow into the cavernous spaces. There are three candidate neurotransmitters that affect smooth muscle relaxation within the corpus cavernosum via the cavernous nerve; they are

acetylcholine, vasoactive intestinal polypeptide (VIP) and nitric oxide (NO). Hence, when the corpus cavernosum receives parasympathetic stimulation, the smooth muscles cells relax and allow blood to flow into the cavernous spaces. This results in an increased intracavernosal pressure and causes an erection (reviewed in Benson 1981; Giuliano et al. 1995).

The anti-erectile response, or detumescence, is affected by the sympathetic nervous system. Sympathetic neurons emanating from the spinal chord at the levels of T11 through L2 innervate the corpus cavernosum via neurons travelling through the superior hypogastric plexus and the pelvic plexus (Giuliano et al. 1995). These neurons affect the contraction of the cavernous smooth muscle and cause detumescence of the penis. Evidence suggests that the neurotransmitter responsible for this contraction is Noradrenaline.

Recent studies have suggested that penile flaccidity may be an actively maintained state and only when the noradrenergic neurons are inhibited, can an erectile response be elicited by the parasympathetic nervous system (Junemann et al. 1989; Giuliano et al. 1993; Giuliano et al. 1995). The mechanism by which the sympathetic nervous system acts to maintain flaccidity is still being debated. The sympathetic neurons may synapse directly with the cavernous smooth muscle and actively lead to their contraction. They may also synapse on the nerve terminals of the parasympathetic neurons and illicit inhibitory presynaptic potentials (IPSPs) to prevent smooth muscle relaxation. Hence, an erectile dysfunction could result from a localized defect in either the parasympathetic or

sympathetic innervation of cavernous smooth muscle. Furthermore, these two possibilities are not mutually exclusive.

A defect in the parasympathetic nervous system could involve any of the three neurotransmitters that affect penile erection including NO, VIP and acetylcholine. NO was shown to relax the vascular smooth muscle of the corpus cavernosum. It is synthesized in nerve terminals by the enzyme neuronal nitric oxide synthase (nNOS). This enzyme has two other isoforms, an endothelial specific isoform (eNOS) and a macrophage specific isoform (iNOS) (Giuliano et al. 1995). nNOS is the primary isoform that produces NO in parasympathetic neurons. Some investigators believe that eNOS, expressed in the endothelial lining of the cavernosal vasculature, may also contribute to NO production and in turn affect erection. However, the NO pathway is not likely defective in *Pea3* null males. *nNos* null male mice are fertile and display hyperaggressive sexual behaviour. They repeatedly mount females that are not in oestrus (Huang et al. 1993; Nelson et al. 1995). Furthermore, male infertility was not reported in the *eNos* null male mice (Wilson et al. 1997).

Hence, both the VIPergic and the cholinergic pathways are possible targets for the PEA3 mutation. The current literature suggests that it may be the cholinergic pathway that is defective in *Pea3* null males. Recent studies established that acetylcholine receptor (*AchR*) expression was up-regulated at the neuromuscular synapse by neuregulin and heregulin dependant mechanisms (Jo et al. 1995; Zhu et al. 1995; Altiok et al. 1997). These molecules act as ligands for the receptor tyrosine kinases *erbB2* and *erbB3* respectively (Carraway and Cantley 1994). Recent evidence demonstrated that PEA3 was

a downstream target of *erbB2* (HER2/c-neu) (Benz et al. 1997). Furthermore, there appeared to be a positive feedback loop where PEA3 transactivated its own promoter and the *erbB2* promoter (O'Hagan et al. 1997).

Interestingly, PEA3 was expressed in adolescent skeletal muscle and adult skeletal muscle myoblasts (figure 4.3 A & B, lane 13; Taylor et al. 1997). Hence, PEA3 may affect expression of *AchR* either directly or indirectly at the synapse between somatic motor neurons and skeletal muscle myofibers. A recent study showed that a novel ETS transcription factor, PET-1, bound to and transactivated the promoter of *nAChR* (Fyodorov et al. 1998). Hence, this study established that *Ets* family members could directly regulate *AchR* expression *in vivo*. This scenario provides a working model for synapse formation between autonomic neurons and the smooth muscle cells of the corpus cavernosum and cauda epididymis. This mechanism requires that PEA3 be expressed in the vascular smooth muscle of these target organs, a fact that remains to be established.

The erectile or ejaculatory defect may also reside within the sympathetic nervous system. As flaccidity is currently viewed as an actively maintained state, an over-active sympathetic nervous system could also lead to erectile dysfunction (Giuliano et al. 1995). Hence, this may also be a potential consequence of the *Pea3* null mutation.

It should be noted that defects in either the parasympathetic or sympathetic nervous system are not mutually exclusive. These neurons as well as their associated glial cells have a common developmental origin; they are derived from neural crest cells (Le Douarin & Smith 1988; Anderson 1989). PEA3 is expressed in many neural crest derivatives during embryogenesis including the mesoderm of the branchial arches and distinct cell

types within the cephalic ganglia (chapter 3; Chotteau-Lelievre et al. 1997). PEA3 expression has also been detected in the dorsal root ganglia (Lin et al., communication of unpublished data).

Although we do not yet know if this is the case for parasympathetic and/or sympathetic ganglia, we cannot rule out a subtle localized congenital defect in the autonomic innervation of the male genitalia. There is evidence that suggests that migrating neural crest cells are triggered to differentiate into autonomic neurons by exogenous signals released from localized regions along the rostral-caudal axis (Anderson et al. 1989). Hence, this supports the notion that a localized defect could occur. It is also possible that PEA3 may affect the expression of these secreted factors that signal neural crest cells in the sacral region to become autonomic neurons. Defining whether or not PEA3 is expressed in the appropriate autonomic ganglia will aid in supporting or refuting this hypothesis.

This study has not ruled out the existence of a spermatozoa autonomous defect within *Pea3* null males. The *Ros* null males set copulatory plugs. Furthermore, sperm derived from the *Ros* null mice was functional *in vitro*; hence, they failed to function *in vivo* (Sonnenberg-Riethmacher et al. 1996). This result likely reflects incomplete sperm maturation within the epididymis. In contrast, *Pea3* null males failed to set copulatory plugs despite the fact that they exhibited normal mating behaviour. Although sperm derived from *Pea3* null males was functional *in vitro*, its function *in vivo* remains to be tested.

The apparent absence of any gross histological defects in the epithelium of the initial segment of *Pea3* null epididymides may be a consequence of functional redundancy from within the PEA3 group. Northern blot analysis revealed that both ERM and ER81 were expressed in the proximal region of the epididymis in both the wild-type and mutant mice (data not shown).

In conclusion, *Pea3* null male mice are infertile because they fail to set copulatory plugs. This phenotype is likely the result of an erectile and/or ejaculatory dysfunction which may reflect a congenital neural crest cell defect. However, the current body of evidence suggests that the underlying defect may reside in the autonomic innervation of the smooth muscle within the male genitalia. The *Pea3* null mouse model may be useful in pharmacological studies that are directed towards understanding and treating these dysfunctions in the human population.

4.3.3 PEA3 affects ductal morphogenesis within the developing mammary gland.

Recently, a defect in the branching pattern of the epithelial ducts in the mammary gland was observed in *Pea3* null mice (MacNeil and Hassell, unpublished observations). The mammary gland is a specialized reproductive organ that evolved in the class *Mammalia* such that these placental bearing animals could feed their young. The development of this gland can be organized into four stages, (i) the embryonic stage, (ii) the adolescent stage, (iii) the lactating stage, and finally (iv) the involuting stage (reviewed in Hennighausen and Robinson, 1998).

Whole mount mammary gland preparations from six month old virgin *Pea3* null females revealed a significant reduction in the ductal arborization in comparison to age matched control samples (figure 4.7). Although *Pea3* null glands had a significant number of well developed primary ducts, there was a reduction in the number of secondary, tertiary and quaternary branches (MacNeil and Hassell, unpublished observations, figure 4.7 A & B). Hence, *Pea3* null virgin females exhibit a defect in the branching morphogenesis of their quiescent mammary glands.

Despite this phenotype, *Pea3* null females appeared to lactate normally. They were capable of feeding their pups through to the time they were weaned. This fact was evident in that the litter sizes of the null females were comparable in size to those of their wild-type counterparts (table 4.3 and table 4.4). Furthermore, milk was observed in the intestines of pups from female *Pea3* null litters (Laing and Hassell, unpublished observation). Hence, there did not appear to be a functional defect in the development of the *Pea3* null mammary glands to the lactation and secretion stages. It remains to be determined whether or not this phenotype is present in the lactating mammary gland. However, in order to understand how the absence of PEA3 may affect this phenotype, we need only consider the gland's development from the embryonic stages through to sexual maturation.

The rudiments of the mammary glands first appear at 11.0 d.p.c. of embryogenesis. A raised ridge of ectodermal cells, the mammary streak, runs along the mid-ventral body wall of the embryo from the caudal base of the forelimb to the rostral base of the hindlimb. By 12.0 d.p.c., these epidermal cells migrate to different positions

forming five pairs of lens shaped mammary buds. At 13.0 d.p.c., sexual differentiation initiates in the mouse embryos. In male embryos, testosterone induces the regression of the mammary buds.

in the absence of androgen, the epithelial cells within the bud will enter into a slow proliferative state at ~14.0 d.p.c. By 16.0 d.p.c., they enter into a rapid phase of proliferation which leads to the formation of mammary sprouts. At 17.0 d.p.c., the sprouts begin elongating into the underlying fatty stroma giving rise to the primary ducts. Initially, the primary ducts undergo minimal branching. Hence, by the end of gestation there are 15 to 20 primary ducts per mammary gland. This entire process is initiated and maintained by inductive signals that pass between the epithelial cells that form the ducts and the surrounding stroma that later forms the mammary fat pad (reviewed by Sakakura, 1991).

From the time of birth through to adolescence, the branching pattern of the mammary gland remains largely unchanged. However, during the stages of sexual maturation, between four and six weeks of age, the distal ends of the primary ducts differentiate into specialized structures called terminal end buds (TEBs) (Sakakura, 1991). TEBs are sac-like structures composed of a layer of luminal epithelial cells along the sides of the ducts, and continuous with this layer, a layer of cap cells lining the distal tip of the TEB. The ducts and the proximal region of the TEB are surrounded by a third type of epithelial cell, the myoepithelial cells. The cap cells are believed to be stem cells that give rise to both the luminal and myoepithelial cells (Humphreys et al. 1996).

The distal ends of the TEBs are surrounded by a basal lamina. In the proximal half of the TEB, the myoepithelial cells are in contact with the basal lamina; in the distal region

of the TEB, it is the cap cells that are in direct contact with the basal lamina (reviewed by Rudland et al. 1998). The TEBs are responsible for initiating both ductal elongation and ramification. Hence, as sexual maturity is reached, the mammary ducts further elongate into the fat pad and undergo significant branching resulting in secondary, tertiary and quaternary ducts (Daniel and Silberstein, 1987). At this stage, the mammary gland is considered to be in a quiescent but mature state ready to respond to the hormonal cues of the estrus cycle and/or a pregnancy. It is in this state that the branching morphogenesis phenotype was first observed (figure 4.7; MacNeil and Hassell, unpublished observations).

Although PEA3 may be expressed in both the mammary streak at 12 d.p.c. and the mammary buds at 13.0 d.p.c. (figure 3.8 F; figure 3.9 D, black arrows), its absence does not appear to have an adverse effect on the embryonic stages of mammary gland development. Despite a reduction in the arborization of the virgin *Pea3* null glands, they are otherwise well developed, consisting of a significant number of primary ducts with a minimal amount of side branching (figure 4.7). Furthermore, this phenotype does not appear to have a negative impact on lactation or milk secretion as *Pea3* null females sired healthy litters. Hence, PEA3 is required for efficient ramification at the TEBs leading to the formation of secondary, tertiary and quaternary ducts but is not required for alveolar differentiation and milk secretion.

What are the requirements for branching at the TEBs? Firstly, the epithelial cells must be able to respond to the proliferative signals of the estrogen/estrogen receptor transcription factor complex. This complex is responsible for driving ductal elongation into the fat pad (Hennighausen and Robinson, 1998). Secondly, the basal lamina surrounding

the TEB must be degraded to allow for ductal elongation and branching (Rudland et al. 1998). I believe that it is this second requirement that may be adversely affected in the *Pea3* null mammary glands.

The basal lamina is a membrane that is mainly composed of type IV collagen, laminin and heparan sulphate proteoglycans (HSGPs). This membrane forms a physical barrier between the epithelial cells of the TEBs and its surrounding stroma (Rudland, 1993). During the quiescent stages, the basal lamina is protected from degradation by the expression and secretion of transforming growth factor β 1 (TGF β 1) from the stroma. However, when the TEBs receive a proliferative signal, TGF β 1 is down-regulated in the stroma which in turn leads to the breakdown of the basal lamina (Silberstein et al. 1992; reviewed by Roskelley et al. 1995). The precise molecular mechanism by which this degradation occurs is not yet understood. It is possible that the basal lamina, if not fully degraded at the time the TEB initiates elongation and branching, may inhibit its ramification.

PEA3 appeared to be expressed in the epithelial cells of the TEBs (MacNeil and Hassell, unpublished observations). When the TEBs receive proliferative signals via estrogen and glucocorticoids, these hormones may directly or indirectly lead to the expression of PEA3 in the epithelial cells. It has also been established that many of the matrix metalloproteinases (MMPs) are target genes for PEA3 and the PEA3 group members (Higashino et al. 1995; sections 1.4.2; 1.5.2) Hence, up-regulation of PEA3 could lead to the expression and secretion of specific MMPs which would then be able to

initiate degradation of the basal lamina. The components of the basal lamina are viable substrates for the putative MMP PEA3 target genes (reviewed by Coussens and Werb, 1996).

Degradation of the basal lamina may initiate branching of the TEB. The myoepithelial cells of the TEB express and secrete FGF2 (bFGF). Furthermore, these cells express its high affinity receptor, FGFR-1. FGF2 was not associated with the myoepithelial cells in quiescent TEBs, rather it was associated with the basal lamina (Rudland et al. 1998). This was due to the fact that most of the FGFs bind to HSGPs which are considered to be the low affinity receptors for many of the FGFs. FGF2 has many biological activities; it can induce cell proliferation as well as the formation and branching of blood vessels (reviewed in Basilico and Moscatelli, 1992). Hence, degradation of the basal lamina would release FGF2-HSGP monomers and allow them to bind with the epithelial cells expressing FGFR1. It was shown that the FGF2 pool became associated with the myoepithelial cells of the TEBs after the degradation of the basal lamina (Rudland et al. 1998).

PEA3 is expressed in the epithelial cells of the TEB; furthermore, the core promoter of PEA3 contains transcription factor binding sites for both the estrogen receptor and the glucocorticoid receptor (MacNeil, Barrett, Kahn and Hassell, unpublished observations). Hence, PEA3 may be directly up-regulated via these two hormones and affect the above mechanism. Therefore, the absence of PEA3 in the TEB may lead to the retention of FGF2 in the intact basal lamina and inhibit branching by inhibiting the

formation of FGF2-HSGP/FGFR1 complexes. It will be important to establish the integrity of the basal laminae surrounding the TEBs in *Pea3* null mammary glands. Furthermore, it will be important to establish the location of the FGF2 pool during these stages of development.

CHAPTER 5
REFERENCES

Adams, J.C., and F.M. Watt. (1993). Regulation of development and differentiation by the extracellular matrix. *Development* **117**: 1183-1198.

Altiook, N., S. Altiook, and J. Changeux. (1997). Heregulin-stimulated acetylcholine receptor gene expression in muscle: requirement for MAP kinase and evidence for a parallel inhibitory pathway independent of electrical activity. *EMBO J.* **16(4)**: 717-725.

Amann, R.P., R.H. Hammerstedt, and D.N.R. Veeramachaneni. (1993). The Epididymis and Sperm Maturation: a Perspective. *Reprod. Fert. Dev.* **5**: 361-381.

Andermarcher, E., M.A. Surani, and E. Gherardi. (1996). Co-expression of the *HGF/SF* and *c-met* genes during early mouse embryogenesis precedes reciprocal expression in adjacent tissues during organogenesis. *Developmental Genetics* **18**: 254-266.

Anderson, D.J. (1989). The Neural Crest Cell Lineage Problem: Neurogenesis? *Neuron* **3**: 1-12.

Baeuerle, P.A., and D. Baltimore. (1988). Activation of DNA binding activity in an apparently cytoplasmic precursor of the NF- κ B transcription factor. *Cell* **63**: 211-217.

Bailly, R., R. Bosselut, J. Zucman, F. Cormier, O. Delattre, M. Roussel, G. Thomas, and J. Ghysdael. (1994). DNA-Binding and Transcriptional Activation Properties of the EWS-FLI-1 Fusion Protein Resulting from the t(11;22) Translocation in Ewing's Sarcoma. *Mol. Cell. Biol.* **14**: 3230-3241.

Bally-Cuif, L., and M. Wassef. (1995). Determination events in the nervous system of the vertebrate embryo. *Curr. Opin. in Gen. & Dev.* **5**: 450-458.

Basilico, C., and D. Moscatelli. (1992). The *fgf* family of growth factors and oncogenes. *Adv. in Can. Res.* **59**: 115-165.

Beg, A.A., S.M. Ruben, R.L. Scheinman, S. Haskill, C.A. Rosen, and A.S. Baldwin Jr. (1992). κ B interacts with the nuclear localization sequences of the subunits of NF- κ B: a mechanism for cytoplasmic retention. *Genes & Dev.* **6**: 1899-1913.

Beiman, M., B. Shilo, and T. Volk. (1996). Heartless, a *Drosophila* FGF receptor homolog, is essential for cell migration and establishment of several mesodermal lineages.

Genes & Dev. **10**: 2993-3002.

Ben-David, Y., Giddens, E., Lewtin, K., and Bernstein, A. (1991). Erythroleukemia induction by Friend murine leukemia virus: insertional activation of a new member of the *ets* gene family, *Fli-1*, closely linked to *c-ets-1*. *Genes & Dev.*, **5**, 908-918.

Benson, G.S. (1981). Mechanisms of Penile Erection. *Invest. Urol.* **19(2)**: 65-69.

Benz, C.C., R.C. O'Hagan, B. Richter, G.K. Scott, C. Chang, X. Xiong, K. Chew, B. Ljung, S. Edgerton, A. Thor, and J.A. Hassell. (1997). HER-2/neu and the Ets transcription activator PEA3 are coordinately upregulated in human breast cancer.

Oncogene **15(13)**: 1513-1525.

Berleth, T., M. Burri, G. Thoma, D. Bopp, S. Richstein, G. Frigerio, M. Noll, and C. Nusslein-Volhard. (1988). The role of localization of *bicoid* RNA in organizing the anterior pattern of the *Drosophila* embryo. *EMBO J.* **7**: 1749-1756.

Bhat, N.K., K.L. Komschlies, S. Fujiwara, R.J. Fisher, B.J. Mathieson, T.A. Gregorio, H.A. Young, J.W. Kasik, K. Ozato, and T.S. Papas. (1989). Expression of *ets* Genes in Mouse Thymocyte Subsets and T Cells. *J. of Imm.* **142**: 672-678

Bhat, N.K., R.J. Fisher, S. Fujiwara, R. Ascione, and T.S. Papas. (1987). Temporal and tissue-specific expression of mouse *ets* genes. *Proc. Natl. Acad. Sci. USA.* **84**: 3161-3165.

Birnboim, H.C., and J. Doly. (1979). A rapid alkaline extraction procedure for screening recombinant plasmid DNA. *Nucleic Acids Res.* **7**: 1513.

Birkedal-Hansen, H. (1995). Proteolytic remodelling of extracellular matrix. *Cur. Opin. in Cell Biol.* **7**: 728-735.

Bleil, J.D. (1993). *In Vitro* Fertilization. *Methods in Enzymology* **225**: 253-263.

Boguski, M.S., and F. McCormick. (1993). Proteins regulating *ras* and its relatives. *Nature* **366**: 643-654.

Boncinelli, E., A. Simeone, D. Acampora, and F. Mavillio. (1991). *HOX* gene activation by retinoic acid. *Trends In Genetics* **7(10)**: 329-334.

Bories, J., D.M. Willerford, D. Grevin, L. Davidson, A. Camus, P. Martin, D. Stehelin, and F.W. Alt. (1995). Increased T-cell apoptosis and terminal B-cell differentiation induced by inactivation of the Ets-1 proto-oncogene. *Nature* **377**: 635-638.

Boulukos, K., P. Pognonec, A. Begue, F. Galibert, J. Gesquiere, D. Stehelin, and J. Ghysdael. (1988). Identification in chickens of an evolutionarily conserved cellular ets-2 gene (*c-ets-2*) encoding nuclear proteins related to the products of the *c-ets* proto-oncogene. *EMBO J.* **7**: 697-705.

Boulukos, K.E., P. Pognonec, B. Rabault, A. Begue, and J. Ghysdael. (1989). Definition of an Ets-1 Protein Domain Required for Nuclear Localization in Cells and DNA Binding Activity In Vitro. *Mol. Cell. Biol.* **9**: 5718-5721.

Bradley, A. (1987). Production and analysis of chimeric mice. In *Teratomas and Embryonic Stem Cells: A Practical Approach*, E.J. Robertson, ed. (Oxford: IRL Press), pp. 113-152.

Braun, B.S., R. Frieden, S.L. Lessnick, W.A. May, and C.T. Denny. (1995). Identification of Target Genes for the Ewing's Sarcoma EWS/FLI Fusion Protein by Representational Difference Analysis. *Mol. Cell. Biol.* **15(8)**: 4623-4630.

Brown, L.A., A. Amores, T.F. Schilling, T. Jowett, J Baert, Y. de Launoit, and A.D. Sharrocks. (1998). Molecular characterization of the zebrafish PEA3 ETS-domain transcription factor. *Oncogene* **17**: 93-104.

Brown, T., and S. McKnight. (1992). Specifications of protein-protein and protein-DNA interaction of GABP α and two newly defined *ets*-related proteins. *Genes & Dev.* **6**: 2502-2512.

Bumcrot, D.A., and A.P. McMahon. (1995). Sonic signals somites. *Curr. Biol.* **5(6)**: 612-614.

Burgess, W.H., C.A. Dionne, J. Kaplow, R. Mudd, R. Friesel, A. Zilberstein, J. Schlessinger, and M. Jaye. (1990). Characterization and cDNA cloning of phospholipase C-g, a major substrate for heparin-binding growth factor 1 (acidic fibroblast growth factor) activated tyrosine kinase. *Mol & Cell. Biol.* **10(9)**: 4770-4777.

Cantley, L.C.; K.R. Auger, C. Carpenter, B. Duckworth, A. Graziani, R. Kapeller, and S.Soltoff. (1991). Oncogenes and signal transduction. *Cell* **64**: 281-302.

Carlson, B.M. (1996). *Patten's Foundations of Embryology* (6th ed.), pp 537-545; pp 569-581; pp393-425; pp 603-606., McGraw-Hill Inc., New York, NY.

Carraway III, K.L., and L.C. Cantley. (1994). A New Acquaintance for ErbB3 and ErbB4: A Role for Receptor Heterodimerization in Growth Signaling. *Cell* **78**: 5-8.

Chang, C.H., G.K. Scott, W.L. Kuo, X. Xiong, Y. Suzdaltseva, J.W. Park, P. Sayre, K. Erny, C. Collins, J.W. Gray, and C.C. Benz. (1997). *ESX*: a structurally unique *Ets* overexpressed early during human breast tumorigenesis. *Oncogene* **14**: 1617-1622.

Chen, H., N.E. Paradies, M. Fedor-Chaiken, and R. Brackenbury. (1997). E-cadherin mediates adhesion and suppresses cell motility via distinct mechanisms. *J. of Cell Sci.* **110**: 345-356.

Chen, J. (1985). The Proto-Oncogene *c-ets* Is Preferentially Expressed in Lymphoid Cells. *Mol. Cell. Biol.* **5**: 2993-3000.

Chen, J.H., C. Vercamer, Z. Li, D. Paulin, B. Vandembunder, and D. Stehelin. (1996). PEA3 transactivates vimentin promoter in mammary epithelial and tumor cells. *Oncogene* **13**: 1667-1675.

Chirwigin, J., A. Przybla, R. MacDonald, and W. Rutter. (1979). Isolation of biologically active ribonucleic acid from sources enriched in ribonuclease. *Biochem.* **18**: 5294-5299.

Chotteau-Lelievre, A., X. Desbains, H. Pelezar, P. Defossez, and Y. de Launoit. (1997). Differential expression patterns of the PEA3 group transcription factors through murine embryonic development. *Oncogene* **15**: 937-952.

Ciruna, B.G., L. Schwartz, K. Harpal, T.P. Yamaguchi, and J. Rossant. (1997). Chimeric analysis of fibroblast growth factor receptor-1 (*Fgfr-1*) function: a role for FGFR1 in morphogenetic movement through the primitive streak. *Development* **124**: 2829-2841.

Crinac, D. (1997). The construction and characterization of a chimeric transcription factor: EWS-PEA3. M.Sc Thesis. Dept. of Biochemistry, McMaster University. Copyright Diana Crinac, 1997.

Conlon, R. A. (1995). Retinoic acid and pattern formation in vertebrates. *Trends in Genetics* **11(8)**: 314-319.

Copeland, N., Jenkins, N., Gilbert, D., Eppig, J., Maltais, L., Miller, J., Dietrich, W., Weaver, A., Lincoln, S., Steen, R., Stein, L., Nadeau, J., and Lander, E. (1993). A genetic linkage map of the mouse: current applications and future prospects. *Science*, **262**: 57-66.

Cossu, G., S. Tajbakshi, and M. Buckingham. (1996). How is myogenesis initiated in the embryo? *Trends in Genetics* **12**: 218-223.

Coussens, L., Yang-Feng, T., Liao, Y., Chen, E., Gray, A., McGrath, J., Seeburg, P., Libermann, T., Schlessinger, J., Francke, U., Levinson, A., and Ullrich, A. (1985). Tyrosine kinase receptor with extensive homology to EGF receptor shares chromosomal location with *neu* oncogene. *Science* **230**: 1132-1138.

Coussens, L.M., and Z. Werb. (1996). Matrix metalloproteinases and the development of cancer. *Chem. & Biol.* **3**: 895-904.

Crowley, T.E., T. Hoey, J. Liu, Y.N. Jan, L.Y. Jan, and R. Tijan. (1993). A new factor related to TATA-binding protein has highly restricted expression patterns in *Drosophila*. *Nature* **361**: 557-561.

Dalton, S., and Treisman, R. (1992). Characterization of SAP-1, a protein recruited by Serum Response Factor to the *c-fos* Serum Response Element. *Cell* **68**: 597-612.

Daniel, C.W., and G.B. Silberstein. (1987). Postnatal development of the rodent mammary gland. In *The Mammary Gland: Development, Regulation, and Function*. (ed. M.C. Neville and C.W. Daniel), pp 3-36. Plenum Press, New York, NY.

Daum, G., I. Eisenmann-Tappe, H. Fries, J. Troppmair, and U.R. Rapp. (1994). The ins and outs of raf kinases. *TIBS* **19**: 474-480.

de Castro, C.M., S.M. Rabe, S.D. Langdon, D.E. Fleenor, K. Slentz-Kesler, M.N. Ahmed, M.B. Qumsiyeh, and R.E. Kaufman. (1997). Genomic Structure and Chromosomal Localization of the Novel ETS Factor, PE-2 (ERF). *Genomics* **42**: 227-235.

Degnan, B.M., S.M. Degnan, T. Naganuma, and D.E. Morse. (1993). The *ets* multigene family is conserved throughout the Metazoa. *Nucleic Acids Res.* **21**: 3479-3484.

de Launoit, Y., J.L. Baert, A. Chotteau, D. Monte, P.A. Defossez, L. Coutte, H. Pelczar, and F. Leenders. (1997). Structure-function relationships of the PEA3 group of *ets*-related transcription factors. *Biochem. & Mol. Med.* **61**: 127-135.

de Launoit, Y., M. Audette, H. Pelczar, S. Plaza, and J.L. Baert. (1998). The transcription of the intercellular adhesion molecule-1 is regulated by Ets transcription factors. *Oncogene* **16**: 2065-2073.

Dellatre, O., J. Zucman, B. Plougastel, C. Desmaze, T. Melot, M. Peter, H. Kovar, I. Joubert, P. de Jong, G. Rouleau, A. Aurias, and G. Thomas. (1992). Gene fusion with

an ETS DNA-binding domain caused by chromosome translocation in human tumors.

Nature **359**: 162-165.

Donaldson, L.W., J.M. Petersen, B.J. Graves, and L.P. McIntosh. (1996). Solution structure of the ETS domain from murine Ets-1: a winged helix-turn-helix DNA binding motif. *EMBO J.* **15**: 125-134.

Driever, W. and C. Nusslein-Volhard. (1988). A gradient of *bicoid* protein in *Drosophila* embryos. *Cell* **54**: 83-93.

Driever, W., and C. Nusslein-Volhard. (1989). The *bicoid* protein is a positive regulator of *hunchback* transcription in the early *Drosophila* embryo. *Nature* **337**: 138-143.

Dulcibella, T. (1977). Surface changes of the developing trophoblast cell. In M.H. Johnson (ed.), *Development in Mammals 1*. Elsevier North-Holland, New York, pp. 5-30.

Edwards, D.R., H. Rocheleau, R.R. Sharma, A.J. Wills, A. Cowie, J.A. Hassell, and J.K. Heath. (1992). Involvement of AP1 and PEA3 binding sites in the regulation of murine tissue inhibitor of metalloproteinase-1 (TIMP-1) transcription. *Biochim. et Biophys. Acta.* **1171**: 41-55.

Emili, A., J. Greenblatt, and C.J. Ingles. (1994). Species-specific interaction of the glutamine rich activation domains of Sp1 with the TATA box-binding protein. *Mol. Cell. Biol.* **14**: 1582-1592.

Fantl, W.J., J.A. Escobedo, G.A. Martin, C.W. Tuck, M. del Rosario, F. McCormick, and L.T. Williams. Distinct phosphotyrosines on a growth factor receptor bind to specific molecules that mediate different signalling pathways. *Cell* **69**: 413-423.

Faust, C., and T. Magnuson. (1993). Genetic control of gastrulation in the mouse. *Curr. Opin. in Gen. and Dev.* **3**: 491-493.

Feinberg, A., and B. Vogelstein. (1983). A technique for radiolabelling DNA restriction endonuclease fragments to high specific activity. *Anal. Biochem.*, **132**: 6.

Frohnhofer, H. , and C. Nusslein-Volhard. (1986). Organization of anterior pattern in the *Drosophila* embryo by the maternal gene *bicoid*. *Nature* **324**: 120-125.

Fujiwara, S., R.J. Fisher, A. Seth, N.K. Bhat, S.D. Showalter, M. Zweig, and T.S. Papas. (1988). Characterization and localization of the products of the human homologs of the *v-ets* oncogene. *Oncogene* **2**: 99-103.

Futreal, P., Liu, Q., Shattuck-Eidens, D., Cochran, C., Harshman, K., Tavtigian, S., Bennett, L., Haugen-Strano, A., Swensen, J., Miki, Y., Eddington, K., McClure, M., Frye, C., Weaver-Feldhaus, J., Ding, W., Gholami, Z., Soderkvist, P., Terry, L., Jhanwar, S., Berchuck, A., Iglehart, J., Marks, J., Ballinger, D., Barrett, J., Skolnick, M., Kamb, A., and Wiseman, R. (1994). *BRCA1* mutations in primary breast and ovarian carcinomas. *Science* **266**: 120-122.

Fyodorov, D., T. Nelson, and E. Deneris. (1998). Pet-1, a novel ETS domain transcription factor that can activate neuronal nAChR gene transcription. *J. Neurobiol.* **34(2)**: 151-163.

Gambarotta, G., C. Boccaccio, S. Giordano, M. Ando, M.C. Stella, and P.M. Comoglio. (1996). *Ets* up-regulates *MET* transcription. *Oncogene* **13**: 1911-1917.

Garoff, H. (1985). Using recombinant DNA techniques to study protein targeting in the eukaryotic cell. *Ann. Rev. Cell Biol.* **1**: 403-445.

Gaul, U., and H. Jackle. (1990). Role of gap genes in early *Drosophila* development. Academic Press Inc. *Advances in Genetics* **27**: 239-272.

Gegonne, A., D. Leprince, M. Duterque-Coquillaud, B. Vandebunder, A. Flourens, J. Ghysdael, B. Debuire, and D. Stehelin. (1987). Multiple Domains for the Chicken Cellular Sequences Homologous to the *v-ets* Oncogene of the E26 Retrovirus. *Mol. Cell. Biol.* **7**: 806-812.

Ghysdael, J., A. Gegonne, P. Pognonec, D. Dernis, D. Leprince, and D. Stehelin. (1986). Identification and preferential expression in thymic and bursal lymphocytes of a *c-ets* oncogene-encoded Mr 54,00 cytoplasmic protein. *Proc. Natl. Acad. Sci. USA.* **83**: 1714-1718.

Gilbert, S.F. (1988). *Developmental biology* (2nd Edition). Sinauer Associates, Inc. Sunderland MA. pp 92; pp 62-65; pp 283-288; pp 288-293; pp 724-728.

Giovane, A., A. Pintzas, S. Maira, P. Sobieszczuk and B. Wasyluk. (1994). Net, a new *ets* transcription factor that is activated by Ras. *Genes & Dev.* **8**: 1502-1513.

Gisselbrecht, S., J.B. Skeath, C.Q. Doe, and A.M. Michelson. (1996). *heartless* encodes a fibroblast growth factor receptor (DFR1/DFGF-R2) involved in the directional migration of early mesodermal cells in the *Drosophila* embryo. *Genes & Dev.* **10**: 3003-3017.

Giuliano, F., J. Bernabe, A. Jardin, and J.P. Rousseau. (1993). Antierectile Role of the Sympathetic Nervous System in Rats. *J. of Urol.* **150**: 519-524.

Giuliano, F., O. Rampin, G. Benoit, and A. Jardin. (1995). Neural Control of Penile Erection. *Urol. Clin. of Nor. Am.* **22(4)**: 747-766.

Golay, J., M. Introna, and T. Graf. (1988). A Single Point Mutation in the *v-ets* Oncogene Affects both Erytroid and Myelomonocytic Cell Differentiation. *Cell* **55**: 1147-1158.

Golub, T.R., G.F. Barker, M. Lovett, and D.G. Gilliland. (1994). Fusion of PDGF Receptor β to a Novel *ets*-like Gene, *tel*, in Chronic Myelomonocytic Leukemia with *t(5;12)* Chromosomal Translocation. *Cell* **77**: 307-316.

Gory, S., J. Dalmon, M. Prandini, T. Kortulewski, Y. de Launoit, and P. Huber. (1998). Requirement of a GT box (Sp1 site) and two ETS binding sites for vascular endothelial cadherin gene transcription. *J. Biol. Chem.* **273(12)**: 6750-6755.

Graf, T., K. McNagny, G. Brady, and J. Frampton. (1992). Chicken "Erythroid" Cells Transformed by the Gag-Myb-Ets-Encoding E26 Leukemia Virus are Multipotent. *Cell* **70**: 201-213.

Graham, A., N. Papalopulu, and R. Krumlauf. (1989). The murine and *Drosophila* homeobox complexes have common features of organization and expression. *Cell* **57**: 367-378.

Green, M. (1986). PRE-mRNA splicing. *Ann. Rev. Genet.* **20**: 671-708.

Greenblatt, J. (1991). Roles of TFIID in transcriptional initiation by RNA polymerase II. *Cell* **66**: 1067-1070.

Gruss, P., and M. Kessel. (1991). Axial specification in higher vertebrates. *Cur. Opin. in Gen. & Dev.* **1**: 204-210.

Gurdon, J.B. (1992). The generation of diversity and pattern in animal development. *Cell* **68**: 185-199.

Guy, C., Cardiff, R., and Muller, W. (1992a). Induction of mammary tumors by expression of polyomavirus middle T oncogene: A transgenic mouse model for metastatic disease. *Mol. Cell. Biol.* **12**: 954-961.

Guy, C., Webster, M., Schaller, M., Parsons, T., Cardiff, R., and Muller, W. (1992b). Expression of the *neu* proto-oncogene in the mammary epithelium of transgenic mice induces metastatic disease. *Proc. Natl. Acad. Sci. USA*, **89**: 10578-10582.

Han, K., M.S. Levine, and J.L. Manley. (1989). Synergistic activation and repression of transcription by *Drosophila* homeobox proteins. *Cell* **56**: 573-583.

Hassell, J.A., W.J. Muller, and C.R. Mueller. (1986). The dual role of the polyomavirus enhancer in transcription and DNA replication. *Cancer Cells* **4**: 561-569.

Hennighausen, L., and G.W. Robinson. (1998). Think globally, act locally: the making of a mouse mammary gland. *Genes & Dev.* **12**: 449-455.

Herskowitz, I. (1995). MAP kinase pathways in yeast: for mating and more. *Cell* **80**: 187-197.

Hida, K., M. Shindoh, M. Yasuda, M. Hanzawa, K. Funaoka, T. Kohgo, A. Amemiya, Y. Totsuka, K. Yoshida, and K. Fujinaga. (1997). Antisense E1AF transfection restrains oral cancer invasion by reducing matrix metalloproteinase activities. *Am. J. of Pathol.* **150(6)**: 2125-2132.

Higashino, F., K. Yoshida, T. Noumi, M. Seiki, and K. Fujinaga. (1995). Ets-related protein E1A-F can activate three different matrix metalloproteinase gene promoters. *Oncogene* **10**: 1461-1463.

Higashino, F., K. Yoshida, Y. Fujinaga, K. Kamio, and K. Fujinaga. (1993). Isolation of a cDNA encoding the adenovirus E1A enhancer binding protein: a new human member of the *ets* oncogene family. *Nucleic Acids Res.* **21**: 547-553.

Hinton, B.T., M.A. Pallidino, D. Rudolph, and J.C. Labus. (1995). The Epididymis as Protector of Maturing Spermatozoa. *Reprod. Fertil. Dev.* **7**: 731-745.

Hoey, T., and M.S. Levine. (1988). Divergent homeobox proteins recognize similar DNA sequences in *Drosophila*. *Nature* **332**: 858-861.

Hogan, B., F. Costantini, and E. Lacy. (1986). *Manipulating the Mouse Embryo*, pp 250-257. Cold Spring Harbor Laboratory, Cold Spring Harbor, New York.

Horstadius, S. (1939). The mechanics of sea urchin development studied by operative methods. *Biol. Rev.* **14**: 132-179.

Huang, P.L., T.M. Dawson, D.S. Brecht, S.H. Snyder, and M.C. Fishman. (1993). Targeted Disruption of the Neuronal Nitric Oxide Synthase Gene. *Cell* **75**: 1273-1286.

Humphreys, R.C., M. Krajewska, S. Krnacik, R. Jaeger, H. Weiler, S. Krajewska, J.C. Reed, and J.M. Rosen. (1996). Apoptosis in the terminal endbud of the murine mammary gland: a mechanism of ductal morphogenesis. *Development* **122**: 4013-4022.

Hunter, T. (1997). Oncoprotein networks. *Cell* **88**: 333-346.

Hunter, T., and M. Karin. (1992). The regulation of transcription by phosphorylation. *Cell* **70**: 375-387.

Hynes, N.E., and Stern, D. (1994). The biology of *erbB-2/neu/HER-2* and its role in cancer. *Biochim. et Biophys. Acta*, **1198**: 165-184.

Hynes, R.O., and A.D. Lander. (1992). Contact and adhesive specificities in the associations, migrations and targeting of cells and axons. *Cell* **68**: 303-322.

Ichkawa, H., K. Shimizu, Y. Hayashi, and M. Ohki. (1994). An RNA-binding Protein Gene, *TLS/FUS*, Is Fused to *ERG* in Human Myeloid Leukemia with t(16;21) Chromosomal Translocation. *Cancer Res.* **54**: 2865-2868.

Isobe, M., F. Yamagishi, K. Yoshida, F. Higashino, and K. Fujinaga. (1995). Assignment of the ets related transcription factor E1A-F gene (*ETV4*) to human chromosome region 17q21. *Genomics* **28**: 357-359.

Iwasaka, C., K. Tanaka, M. Abe, and Y. Sato. (1996). Ets-1 regulates angiogenesis by inducing the expression of urokinase-type plasminogen activator and matrix metalloproteinase-1 and the migration of vascular endothelial cells. *J. of Cell. Physiol.* **169**: 522-531.

Janknecht, R. (1996). Analysis of the ERK-Stimulated ETS Transcription Factor ER81. *Mol. Cell. Biol.* **16**(4): 1550-1556.

Janknecht, R., and A. Nordheim. (1993). Gene regulation by Ets proteins. *Biochim. et Biophys. Acta* **1155**: 346-356.

Janknecht, R., D. Monte, J. Baert, and Y. de Launoit. (1996). The ETS-related transcription factor ERM is a nuclear target of signaling cascades involving MAPK and PKA. *Oncogene* **13**: 1745-1754.

Janknecht, R., W.H. Ernst, and A. Nordheim. (1995). SAP1a is a nuclear target of signaling cascades involving ERKs. *Oncogene* **10**: 1209-1216.

Jeon, I., J.N. Davis, B.S. Braun, J.E. Sublett, M.F. Roussel, C.T. Denny, and D.N. Shapiro. (1995). A variant Ewing's sarcoma translocation (7;22) fuses the *EWS* gene to the ETS gene *ETV1*. *Oncogene* **10**: 1229-1234.

Jo, S.A., X. Zhu, M.A. Marchionni, and S.J. Burden. (1995). Neuregulins are concentrated at nerve-muscle synapses and activate ACh-receptor gene expression. *Nature* **373**: 158-161.

Johnson, R.L., and C.J. Tabin. (1997). Molecular models for vertebrate limb development. *Cell* **90**: 979-990.

Joyner, A. (1996). *Engrailed*, *Wnt* and *Pax* genes regulate midbrain-hindbrain development. *Trends in Genetics* **12**(1): 15-20.

Junemann, K.P., C. Persson-Junemann, T.F. Lue, A. Tanagho, and P. Alken. (1989). Neurophysiological Aspects of Penile Erection: the Role of the Sympathetic Nervous System. *Brit. J. of Urol.* **64**: 84-92.

Kalderon, D., B.L. Roberts, W.D. Richardson, and A.E. Smith. (1984). A short amino acid sequence able to specify nuclear location. *Cell* **32**: 499-509.

Kaneko, Y., K. Yoshida, M. Handa, Y. Toyoda, H. Nishihira, Y. Tanaka, Y. Sasaki, S. Ishida, F. Higashino, and K. Fujinaga. (1996). Fusion of an *ETS*-family Gene, *E1AF*, to *EWS* by t(17;22)(q12;q12) Chromosome Translocation in an Undifferentiated Sarcoma of Infancy. *Genes, Chrom. & Can.* **15**: 115-121.

Kaufman, M.H. (1992). *The atlas of mouse development*, pp 74, 92, 110, 120. Academic Press Ltd., London, U.K.

Kaya, M., K. Yoshida, F. Higashino, T. Mitaka, S. Ishii, and K. Fujinaga. (1996). A single *ets*-related transcription factor, E1AF, confers invasive phenotype on human cancer cells. *Oncogene* **12**: 221-227.

Keegan, L., G. Gill, and M. Ptashne. (1986). Separation of DNA binding from the transcription-activating function of a eukaryotic regulatory protein. *Science* **231**: 699-703.

Kessel, M., and P. Gruss. (1990). Murine developmental control genes. *Science* **249**: 374-379.

Kessel, M., and P. Gruss. (1991). Homeotic transformations of murine vertebrae and concomitant alteration of hox codes induced by retinoic acid. *Cell* **67**: 89-104.

Klemsz, M.J., S.R. McKercher, A. Celada, C. Van Beveren, and R.A. Maki. (1990). The Macrophage and B Cell-Specific Transcription Factor PU.1 Is Related to the *ets* Oncogene. *Cell* **61**: 113-124.

Kola, I., S. Brookes, A.R. Green, R. Garber, M. Tymms, T.S. Papas, and A. Seth. (1993). The Ets1 transcription factor is widely expressed during murine embryo development and is associated with mesodermal cells involved in morphogenetic processes such as organ formation. *Proc. Natl. Acad. Sci. USA*. **90**: 7588-7592.

Kraut, N., J. Frampton, K. McNagny, and T. Graf. (1994). A functional Ets DNA-binding domain is required to maintain multipotency of hematopoietic progenitors transformed by Myb-Ets. *Genes & Dev*. **8**:33-44.

Laird, P.W., A. Zijderveld, K. Linders, M.A. Rudnicki, R. Jaenisch, and A. Berns. (1991). Simplified mammalian DNA isolation procedure. *Nuc. Acids Res*. **19(15)**: 4293.

LaMarco, K., Thompson, C., Byers, B., Walton, E., and McKnight, S. (1991). Identification of *Ets*- and *Notch* related subunits in GA binding protein. *Science* **253**: 789-792.

Lan, Z., M.A. Palladino, D.B. Rudolph, J.C. Labus and B.T. Hinton. (1997). Identification, Expression and Regulation of the Transcriptional Factor Polyomavirus Enhancer Activator 3, and Its Putative Role in Regulating the Expression of Gamma-Glutamyl Transpeptidase mRNA-IV in the Rat Epididymis. *Biol. of Reprod.* **57**: 186-193.

Lautenberger, J.A., L.A. Burdett, M.A. Gunnell, S. Qi, D.K. Watson, S.J. O'Brein, and T.S. Papas. (1992). Genomic dispersal of the *ets* gene family during metazoan evolution. *Oncogene* **7**: 1713-1720.

Le Douarin, N.M., and J. Smith. (1988). Development of the peripheral nervous system from the neural crest. *Ann. Rev. Cell Biol.* **4**: 375-404.

Lee, K.A.W., A. Bindereif, and M.R. Green. (1988). A small-scale procedure for preparation of nuclear extracts that support efficient transcription and pre-mRNA splicing. *Gene Anal. Techn.* **5**: 22-31.

Leprince, D., A. Gégonne, J. Coll, C. de Taisne, A. Schneeberger, C. Lagrou, and D. Stehelin. (1983). A putative second cell-derived oncogene of the avian leukemia retrovirus E26. *Nature* **306**: 395-397.

Lesnick, S., Braun, S., Denny, C., and May, W. (1994). Multiple domains mediate transformation by Ewing's sarcoma *EWS/FLI-1* fusion gene. *Oncogene*, **10**: 423-431.

Levine, M.S., and J.L. Manley. (1989). Transcriptional repression of eukaryotic promoters. *Cell* **59**: 405-408.

Lewin, B. (1990). Commitment and activation at pol II promoters: a tail of protein-protein interactions. *Cell* **61**: 1161-1164.

Liang, H., E.T. Olejniczak, X. Mao, D.G. Nettesheim, L. Yu, C.B. Thompson, and S.W. Fesik. (1994). The secondary structure of the ets domain of human Fli-1 resembles that of the helix-turn-helix DNA-binding motif of the *Escherichia coli* catabolite gene activator protein. *Proc. Natl. Acad. Sci. USA*. **91**: 11655-11659.

Lichter, P., Tang, C., Call, K., Hermanson, G., Evans, G., Housman, D., and Ward, D. (1990). High resolution mapping of human chromosome 11 by in situ hybridization with cosmid clones. *Science* **247**: 64-69.

Lin, J.H., T. Saito, D.J. Anderson, C. Lance-Jones, T.M. Jessell, and S. Arber. (personal communication of manuscript in preparation). Coordinate expression of ETS domain proteins defines matching motor neuron pool and muscle sensory afferent subtypes.

Liu, D., E. Pavlopoulos, W. Modi, N. Moschonas, and G. Mavrothalassitis. (1997). ERF: Genomic organization, chromosomal localization and promoter analysis of the human and mouse genes. *Oncogene* **14**: 1445-1451.

Luton, D., O. Sibony, J.F. Oury, P. Blot, F. Dieterlen-Lievre, and L. Pardanaud. (1997). The c-ets-1 protooncogene is expressed in human trophoblast during the first trimester of pregnancy. *Early Human Development* **47**: 147-156.

MacAuley, A., Z. Werb, and P. Mirkes. (1993). Characteristics of the unusually rapid cell cycles during rat gastrulation. *Development* **117**: 873-883.

MacNicol, A.M., A.J. Muslin, and L.T. Williams. (1993). Raf-1 kinase is essential for early *xenopus* development and mediates the induction of mesoderm by fgf. *Cell* **73**: 571-583.

Marais, R., J. Wynne, and R. Treisman. (1993). The SRF Accessory Protein Elk-1 Contains a Growth Factor-Regulated Transcriptional Activation Domain. *Cell* **73**: 381-393.

Margolis, B. (1992). Proteins with SH2 domains: transducers in the tyrosine kinase signalling pathway. *Cell Growth & Diff.* **3**: 73-80.

Maroulakas, I., T.S. Papas, and J.E. Green. (1994). Differential expression of *ets-1* and *ets-2* proto-oncogenes during murine embryogenesis. *Oncogene* **9**: 1551-1565.

Martin, M.E., J. Piette, M. Yaniv, W-J. Tang, and W.R. Folk. (1988). Activation of the polyomavirus enhancer by a murine activator protein 1 (AP-1) homolog and two contiguous proteins. *Proc. Natl. Acad. Sci.* **85**: 5839-5843.

Martin, M.E., X.Y. Yang, and W.R. Folk. (1992). Expression of a 91-Kilodalton PEA3-Binding Protein Is Down-Regulated during Differentiation of F9 Embryonal Carcinoma Cells. *Mol. & Cell. Biol.* **12(5)**: 2213-2221.

Matrisian, L.M., and B.L.M. Hogan. (1990). Growth factor regulated proteases and extracellular matrix remodelling during mammalian development. *Curr. Topics in Dev. Biol.* **24**: 219-259.

McBurney, M.W., L.C. Sutherland, C.N. Adra, B. Leclair, M.A. Rudnicki, and K. Jardine. (1991). The mouse PGK-1 gene promoter contains an upstream activator sequence. *Nuc. Acids Res.* **19(20)**: 5755-5761.

McGinnis, W., and R. Krumlauf. (1992). Homeobox genes and axial patterning. *Cell* **68**: 283-302.

Melet, F., B. Motro, D.J. Rossi, L. Zhang, and A. Bernstein. (1996). Generation of a Novel Fli-1 Protein by Gene Targeting Leads to a Defect in Thymus Development and a Delay in Friend Virus-Induced Erythroleukemia. *Mol. & Cell. Biol.* **16(6)**: 2708-2718.

Miki, Y., Swensen, J., Shattuck-Eidens, D., Futreal, P., Harshman, K., Tavtigian, S., Liu, Q., Cochran, C., Bennett, L., Ding, W., Bell, R., Rosenthal, J., Hussey, C., Tran, T., McClure, M., Frye, C., Hattier, T., Phelps, R., Haugen-Strano, A., Katcher, H., Yakumo, K., Gholami, Z., Shaffer, D., Stone, S., Bayer, S., Wray, C., Bogden, R., Dayananth, P., Ward, J., Tonin, P., Narod, S., Bristow, P., Norris, F., Helvering, L., Morrison, P., Rosteck, P., Lai, M., Barrett, J., Lewis, C., Neuhausen, S., Cannon-Albright, L., Goldgar, D., Wiseman, R., Kamb, A., and Skolnick, M. (1994). A strong candidate for the breast and ovarian cancer susceptibility gene *BRAC1*. *Science* **266**: 66-71.

Mitchell, P., and Tjian, R. (1989). Transcriptional regulation in mammalian cells by sequence specific DNA binding proteins. *Science*, **245**: 371-378.

Miyazaki, Y., X. Sun, H. Uchida, J. Zhang, and S. Nimer. (1996). MEF, a novel transcription factor with an Elf-1 like DNA binding domain but distinct transcriptional activating properties. *Oncogene* **13**: 1721-1729.

Monte, D., J. Baert, P. Defossez, Y. de Launoit, and D. Stehelin. (1994). Molecular cloning and characterization of human ERM, a new member of the Ets family closely related to mouse PEA3 and ER81 transcription factors. *Oncogene* **9**: 1397-1406.

Monte, D, L. Coutte, J. Baert, I. Angeli, D. Stehelin, and Y. de Launoit. (1995). Molecular characterization of the ets- related human transcription factor ER81. *Oncogene* **11**: 771-779.

Moreau-Gachelin, F., A. Tavitian, and P. Tambourin. (1988). *Spi-1* is a putative oncogene in virally induced murine erythroleukemias. *Nature* **331**: 277-280.

Muenke, M., and U. Schell. (1995). Fibroblast growth factor receptor mutations in human skeletal disorder. *Trends in Genetics* **11(8)**: 308-313.

Murphy, M., and P.F. Bartlett. (1993). Molecular regulation of neural crest development. *Mol. Neurobiol.* **7(2)**: 111-135.

Mustelin, T., and P. Burn. (1993). Regulation of *src* family tyrosine kinases in lymphocytes. *TIBS* **18**: 215-220.

Muthuswamy, N., K. Barton, and J.M. Lieden. (1995). Defective activation and survival of T cells lacking the Ets-1 transcription factor. *Nature* **377**: 639-642.

Nanba, E., and K. Suzuki. (1990). Molecular Cloning of Mouse Acid β -Galactosidase cDNA: Sequence, Expression of Catalytic Activity and Comparison with the Human Enzyme. *Biochem. & Biophys. Res. Comm.* **173(1)**: 141-148.

Nelson, R.J., G.E. Demas, P.L. Huang, M.C. Fishman, V.L. Dawson, T.M. Dawson, and S.H. Snyder. (1995). Behavioural abnormalities in male mice lacking neuronal nitric oxide synthase. *Nature* **378**: 383-386.

Nerlov, C., Rorth, P., Blasi, F., and Johnsen, M. (1991). Essential AP-1 and PEA3 binding elements in the human urokinase enhancer display cell type specific activity. *Oncogene*, **6**, 1583-1592.

Nunn, M.F., P.H. Seeburg, C. Moscovici, and P.H. Duesberg. (1983). Tripartite structure of the avian erythroblastosis virus E26 transforming gene. *Nature* **306**: 391-395.

Nunn, M., H. Weiher, P. Bullock, and P. Duesberg. (1984). Avian Erythroblastosis Virus E26: Nucleotide Sequence of the Tripartite *onc* Gene of the LTR and Analysis of the Cellular Prototype of the Viral *ets* Sequence. *Virology* **139**: 330-339.

Nye, J.A., J.M. Petersen, C.V. Gunther, M.D. Jonsen, and B.J. Graves. (1992). Interaction of murine Ets-1 with GGa-binding sites establishes the ETS domain as a new DNA-binding motif. *Genes & Dev.* **6**: 975-990.

O'Hagan, R.C., and J.A. Hassell. (1998). The PEA3 Ets Transcription Factor is a Downstream Target of the HER2/Neu Receptor Tyrosine Kinase. *Oncogene* **16**: 301-310.

O'Hagan, R.C., R.G. Tozer, M. Symons, F. McCormick, and J.A. Hassell. (1996). The activity of the Ets transcription factor PEA3 is regulated by two distinct MAPK cascades. *Oncogene* **13**: 1323-1333.

Olson, E.N., and W.H. Klein. (1994). bHLH factors in muscle development: dead lines and commitments, what to leave in and what to leave out. *Genes & Dev.* **8**: 1-8.

Oettgen, P., Y. Akbarli, J. Boltax, J. Best, C. Kunsch, and T.A. Libermann. (1996). Characterization of NERF, a Novel Transcription Factor Related to the Ets Factor ELF-1. *Mol. Cell. Biol.* **16(9)**: 5091-5106.

Pabo, C.O., and R.T. Sauer. (1992). Transcription factors: structural families and principles of DNA recognition. *Ann. Rev. Biochem.* **61**: 1053-1095.

Paul, R., S. Schuetze, S.L. Kozak, C.A. Kozak, and D. Kabat. (1991). The *Sfpi-1* Proviral Integration Site of Friend Erythroleukemia Encodes the *ets*-Related Transcription Factor Pu.1. *J. Virol.* **65**: 464-467.

Pawson, T., and G.D. Gish. (1992). SH2 and SH3 domains: from structure to function. *Cell* **71**: 359-362.

Ptashne, M. (1988). How eukaryotic transcriptional activators work. *Nature* **331**: 683-689.

Ptashne, M., and A.A.F. Gann. (1990). Activators and targets. *Nature* **346**: 329-331.

Queva, C., D. Leprince, D. Stehelin, and B. Vandebunder. (1993). p54^{c-ets-1} and p68^{c-ets-1}, the two transcription factors encoded by the c-ets-1 locus, are differentially expressed during the development of the chick embryo. *Oncogene* **8(3)**: 2511-2520.

Rao, V.N., T.S. Papas, E. Shyam, and P. Reddy. (1987). *erg*, a Human *ets*-Related Gene on Chromosome 21: Alternative Splicing, Polyadenylation, and Translation. *Science* **237**: 635-639.

Rao, V.N., K. Huebner, M. Isobe, A. AR-Rushdi, C.M. Croce, E. Shyam, and P. Reddy. (1988). *elk*, Tissue-Specific *ets*-Related Genes on Chromosome X and 14 near Translocation Breakpoints. *Science* **244**: 66-70.

Rave, N., R. Crkvenjakov, and H. Boedtker. (1979). Identification of procollagen mRNAs transferred to diazobenzyloxymethyl paper from formaldehyde agarose gels. *Nucleic Acids Res.* **6**: 3359.

Rawls, A., and E.N. Olson. (1997). MyoD meets its maker. *Cell* **89**: 5-8.

Ray, D., R. Bosselut, J. Ghysdael, M. Mattei, A. Tavitian, and F. Moreau-Gachelin. (1992). Characterization of Spi-B, a Transcription Factor Related to the Putative Oncoprotein Spi-1/PU.1. *Mol. Cell. Biol.* **12**: 4297-4304.

Richardson, W.D., B.L. Roberts, and A.E. Smith. (1986). Nuclear location signals in polyoma virus large-T. *Cell* **44**: 77-85.

Riethmacher, D., O. Langholz, S. Godecke, M. Sachs, and C. Birchmeier. (1994). Biochemical and functional characterization of the murine *ros* protooncogene. *Oncogene* **9**: 3617-3626.

Robertson, E.J. (1987). Embryo-derived stem cell lines. In *terato-carcinomas and embryonic stem cells: A Practical Approach*, E.J. Robertson, ed. (Oxford: IRL Press), pp 71-112.

Roskelley, C.D., A. Srebrow, and M.J. Bissell. (1995). A hierarchy of ECM-mediated signalling regulates tissue-specific gene expression. *Cur. Opin. in Cell Biol.* **7**: 736-747.

Rudland, P.S. (1993). Epithelial stem cells and their possible role in the development of the normal and diseased human breast. *Histol. Histopathol.* **8**: 385-404.

Rudland, P.S., R. Barraclough, D.G. Fernig and J.A. Smith. (1998). Growth and differentiation of the normal mammary gland and its tumours. *Biochem. Soc. Symp.* **63**: 1-20.

Rudnicki, M.A. and M.W. McBurney. (1987). Cell culture method and induction of differentiation of embryonal carcinoma cell lines. In *Teratocarcinomas and embryonic stem cells: A practical approach* (ed. E.J. Robertson), pp. 19-49. IRL Press, Oxford, UK.

Ruppert, S., E.H. Wang, and R. Tijan. (1993). Cloning and expression of human TAFii250: a TBP associated factor implicated in cell-cycle regulation. *Nature* **362**: 175-181.

Sakakura, T. (1991). New aspects of stroma-parenchyma relations in mammary gland differentiation. *Int. Rev. of Cytol.* **125**: 165-201.

Sambrook, J., Fritsch, E., and Maniatis, T. (1989). *Molecular Cloning: A Laboratory Manual*. 2nd Ed. Cold Spring Harbor University Press, Cold Spring Harbor.

Schilling, T.F. (1997). Genetic analysis of craniofacial development in the vertebrate embryo. *BioEssays* **19(6)**: 459-468.

Schuetze, S., P.E. Stenberg, and D. Kabat. (1993). The Ets-Related Transcription Factor PU.1 Immortalizes Erythroblasts. *Mol. & Cell. Biol.* **13(9)**: 5670-5678.

Scott, E.W., M.C. Simon, J. Anastasi, and H Singh. (1994). Requirement of Transcription Factor PU.1 in the Development of Multiple Hematopoietic Lineages. *Science* **265**: 1573-1577.

Scott, G., Daniel, J., Xiong, X., Maki, R., Kabat, D., and Benz, C. (1994). Binding of an ETS related protein within the DNaseI hypersensitive site of the *HER2/neu* promoter in human breast cancer cells. *J. Biol. Chem.* **269**: 19848-19858.

Scott, M.P., and A.J. Weiner. (1984). Structural relationships among genes that control development: sequence homology between Antennapedia, Ultrabithorax and fushi tarazu loci of *Drosophila*. *Proc. Natl. Acad. of Sci.* **81**: 4115-4119.

Seth, A., and Papas, T. (1990). The *c-ets-1* proto-oncogene has oncogenic activity and is positively autoregulated. *Oncogene* **5**: 1761-1767.

Shimizu, K., H. Ichikawa, T. Tojo, Y. Kaneko, N. Maseki, Y. Hayashi, M. Ohira, S. Asano, and M. Ohki. (1993). An *ets*-related gene, *ERG*, is rearranged in human myeloid leukemia with t(16;21) chromosomal translocation. *Proc. Natl. Acad. Sci. USA.* **90**: 10280-10284.

Shyam, E., P. Reddy, V.N. Rao, and T.S. Papas. (1987). The *erg* gene: A human gene related to the *ets* oncogene. *Proc. Natl. Acad. Sci. USA.* **84**: 6131-6135.

Shyam, E., P. Reddy, and V. Rao. (1990). Localization and Modulation of the DNA-binding Activity of the Human *c-ets-1* Protooncogene. *Cancer Res* **50**: 5013-5016.

Silberstein, G.B., K.C. Flanders, A.B. Roberts, and C.W. Daniel. (1992). Regulation of mammary morphogenesis: evidence for extracellular matrix-mediated inhibition of ductal budding by transforming growth factor beta-1. *Dev. Biol.* **152**: 354-362.

Smillie, D. (1993). Molecular analysis of the mouse PEA3 gene. M.Sc. Thesis. McMaster University, Dept. of Biology. Hamilton, Canada. Copyright 1993, David Smillie.

Snell, W.J., and J.M. White. (1996). The Molecules of Mammalian Fertilization. *Cell* **85**: 629-637.

Sonnenberg-Reithmacher, E., B. Walter, D. Riethmacher, S. Godecke, and C. Birchmeier. (1996). The *c-ros* tyrosine kinase receptor controls regionalization and differentiation of epithelial cells in the epididymis. *Genes & Dev.* **10**: 1184-1193.

Sorensen, P.H.B., L.S. Lessnick, D. Lopez-Terrada, X.F. Liu, T.J. Triche, and C.T. Denny. (1994). A second Ewing's sarcoma translocation, t(21;22), fuses the EWS gene to another ETS-family transcription factor, ERG. *Nature Genetics* **6**: 146-151.

Southern, E.M. (1975). Detection of specific sequences among DNA fragments separated by gel electrophoresis. *J. Mol. Biol.* **98**: 503.

St. Johnston, D., and C. Nusslein-Volhard. (1992). The origin of pattern and polarity in the *Drosophila* embryo. *Cell* **68**: 201-219.

Stacey, K., Fowles, L., Colman, M., Ostrowski, M., and Hume, D. (1995). Regulation of urokinase-type plasminogen activator gene transcription by macrophage colony stimulating factor. *Mol. Cell. Biol.* **15**: 3430-3441.

Stringer, K.F., C.J. Ingles, and J. Greenblatt. (1990). Direct and selective binding of an acidic transcriptional activation domain to the TATA-box factor TFIID. *Nature* **345**: 783-786.

Struhl, K. (1985). A Rapid Method for Creating Recombinant DNA Molecules. *BioTechniques* **3(6)**: 452-453.

Sumarsono, S.H., T.J. Wilson, M.J. Tymms, D.J. Venter, C.M. Crrick, R. Kola, M.H. Lahoud, T.S. Papas, A. Seth, and I. Kola. (1996). Down's syndrome-like skeletal abnormalities in *Ets2* transgenic mice. *Nature* **379**: 534-537.

Sun, E.L., and C.J. Flickinger. (1979). Development of Cell Types and of Regional Differences in the Postnatal Rat Epididymis. *Am. J. Anat.* **154(1)**: 27-55.

Sun, E.L., and C.J. Flickinger. (1980). Morphological Characteristics of Cells With Apical Nuclei in the Initial Segment of the Adult Rat Epididymis. *Anat. Rec.* **196**: 285-293.

Takeichi, M. (1988). The cadherins: cell-cell adhesion molecules controlling animal morphogenesis. *Development* **102**: 639-655.

Tam, P.P.L., and P.A. Trainor. (1994). Specification and segmentation of the paraxial mesoderm. *Anat. Embryol.* **189**: 275-305.

Tam, P.P.L., and R.R. Behringer. (1997). Mouse Gastrulation: the formation of a mammalian body plan. *Mech. of Dev.* **68**: 3-25.

Tanaka, E.M., and A.A.F. Gann. (1995). The budding role of fgf. *Curr. Biol.* **5(6)**: 594-597.

Taylor, J.M., E.E. Dupont-Versteegden, J.D. Davies, J.A. Hassell, J.D. Houle, C.M. Gurley, and C.A. Peterson. (1997). A Role for the ETS Domain Transcription Factor PEA3 in Myogenic Differentiation. *Mol. Cell. Biol.* **17(9)**: 5550-5558.

They, C., M.J. Sharpe, S.J. Batley, C.D. Stern, and E. Gherardi. (1995). Expression of HGF/SF, HGF1/MSP and c-met suggests new functions during early chick development. *Developmental Genetics* **17**: 90-101.

Thompson, C.B., C. Wang, , I. Ho, P.R. Bohjanen, B. Petryniak, C.H. June, S. Miesfeldt, L. Zhang, G.J. Nabel, B. Karpinski, and J.M. Lieden. (1992). *cis*-Acting Sequences for Inducible Interleukin-2 Enhancer Function Bind a Novel Ets-Related Protein, Elf-1. *Mol. Cell. Biol.* **12**: 1043-1053.

Tickle, C. (1995). Vertebrate limb development. *Curr. Opin. in Gen. & Dev.* **5**: 478-484.

Todaro, G.J., and H. Green. (1963). Quantitative Studies of the Growth of Mouse Embryo Cells in Culture and their Development into Established Lines. *J. Cell Biol.* **17**(2): 299-313.

Trimble, M.S., J. Xin, C.T. Guy, W.J. Muller, and J.A. Hassell. (1993). PEA3 is overexpressed in mouse metastatic mammary adenocarcinoma. *Oncogene* **8**: 3037-3042.

Tsang, S.S., X. Yin, C. Guzzo-Arkuran, V.S. Jones, and A.J. Davison. (1993). Loss of resolution in gel electrophoresis of RNA: a problem associated with the presence of formaldehyde gradients. *BioTechniques* **14**(3): 380-381.

Tsuchida, T., M. Ensini, S.B. Morton, M. Baldassare, T. Edlund, T.M. Jessell, and S.L. Plaff. (1994). Topographic organization of embryonic motor neurons defined by expression of LIM homeobox genes. *Cell* **79**: 957-970.

Tymms, M.J., A. Ng, R.S. Thomas, B.C. Schutte, J. Zhou, H.Y. Eyre, G.R. Sutherland, A. Seth, M. Rosenberg, T. Papas, C. Debouck, and I. Kola. (1997). A novel epithelial-expressed ETS gene, *ELF3*: human and murine cDNA sequences, murine genomic organization, human mapping to 1q32.2 and expression in tissues and cancer. *Oncogene* **15**: 2449-2463.

Umbhauer, M., C.J. Marshall, C.S. Mason, R.W. Old, and J.C. Smith. (1995). Mesoderm induction in *xenopus* caused by activation of MAP kinase. *Nature* **376**: 58-62.

Urano, F., A. Umezawa, W. Hong, H. Kikuchi, and J. Hata. (1996). A Novel Chimera Gene between *EWS* and *E1A-F*, Encoding the Adenovirus E1A Enhancer-Binding Protein, in Extrasosseous Ewing's Sarcoma. *Biochem. & Biophys. Res.* **219**: 608-612.

Valius, M., and A. Kazlaukas. (1993). Phospholipase C- γ 1 and phosphatidylinositol 3 kinase are the downstream mediators of the PDGF receptors mitogenic signal. *Cell* **73**: 321-334.

Vandenbunder, B., L. Pardanaud, T. Jaffredo, M.A. Mirabel, and D. Stehelin. (1989). Complementary patterns of expression of *c-ets-1*, *c-myb* and *c-myc* in the blood forming system of the chick embryo. *Development* **106**: 265-274.

Veldman, G.M., S. Lupton, and R. Kamen. (1985). Polyomavirus enhancer contains multiple redundant sequence elements that activate both DNA replication and gene expression. *Mol. Cell. Biol.* **5**: 649-658.

Vonderhaar, B.K., and A.E. Greco. (1979). Lobulo-alveolar development of mouse mammary glands is regulated by thyroid hormones. *Endocrinology* **2**: 409-418.

Voso, M.T., T.C. Burns, G. Wulf, B. Lim, G. Leone, and D.G. Tenen. (1994). Inhibition of hematopoiesis by competitive binding of transcription factor PU.1. *Proc. Natl. Acad. Sci. USA.* **91**: 7932-7936.

Vu, T.H., J.M. Shipley, G. Bergers, J.E. Berger, J.A. Helms, D. Hanahan, S.D. Shapiro, and Z. Werb. (1998). MMP-9/gelatinase B is a key regulator of growth plate angiogenesis and apoptosis of hypertrophic chondrocytes. *Cell* **93**: 411-422.

Wang, L.C., F. Kuo, Y. Fujiwara, D.G. Gilliland, T.R. Golub, and S.H. Orkin. (1997). Yolk sac angiogenic defect and intra-embryonic apoptosis in mice lacking the Ets-related factor TEL. *EMBO J.* **16(14)**: 4374-4383.

Wasylyk, B., S.L. Hahn, and A. Giovane. (1993). The Ets family of transcription factors. *Eur. J. Biochem.* **211**: 7-18.

Wasylyk, C., Gutman, A., Nicholson, R., and Wasylyk, B. (1991). The c-ets-1 oncoprotein activates the stromelysin promoter through the same elements as several non nuclear oncoproteins. *EMBO J.* **10**: 1127-1134.

Watanabe, H., J. Sawada, K. Yano, K. Yamaguchi, M. Goto, and H. Handa. (1993). cDNA Cloning of Transcription Factor E4TF1 Subunits with Ets and Notch Motifs. *Mol. Cell. Biol.* **13(3)**: 1385-1391.

Watson, D.K., M.J. McWilliams-Smith, M.F. Nunn, P.H. Duesberg, S.J. O'Brien, and T.S. Papas. (1985). The *ets* sequence from the transforming gene avian erythroblastosis virus, E26, has unique domains on human chromosomes 11 and 21: Both loci are transcriptionally active. *Proc. Natl. Acad. Sci. USA.* **82**: 7294-7298.

Watson, D.K., M.J. McWilliams, P. Lapis, J.A. Lautenberger, C.W. Schweinfest, and T.S. Papas. (1988). Mammalian *ets-1* and *ets-2* genes encode highly conserved proteins. *Proc. Natl. Acad. Sci. USA.* **85**: 7862-7866.

Watson, D.K., F.E. Smyth, D.M. Thompson, J.Q. Cheng, J.R. Testa, T.S. Papas, and A. Seth. (1992). The *ERGB/Fli-1* Gene: Isolation and Characterization of a New Member of the Family of Human *ETS* Transcription Factors. *Cell Growth and Diff.* **3**: 705-713.

Weismann, A. (1892). *Essays on heredity and kindred biological problems*. Translated by E.B. Poulton, S. Schoenland and A.E. Shipley. Clarendon, Oxford.

Weismann, A. (1893). *The germ-plasm: a theory of heredity*. Translated by W. Newton Parker and H. Ronnfeld. Walter Scott, Ltd., London.

Whitman, M., and D. Melton. (1992). Involvement of p21ras in *xenopus* mesoderm induction. *Nature* **357**: 252-254.

Wilkinson, M.G., and J.B.A. Millar. (1998). SAPKs and transcription factors do the nucleocytoplasmic tango. *Genes & Dev.* **12**: 1391-1398.

Wilson, R.I., J. Yanovsky, A. Godecke, D.R. Stevens, J. Schrader, and H.L. Haas. (1997). Endothelial nitric oxide synthase and LTP. *Nature* **386**: 338.

Xiao, H., A. Pearson, B. Coulombe, R. Truant, S. Zhang, J.L. Regier, S.J. Treizenberg, D. Reinberg, O. Flores, C.J. Ingles, and J. Greenblatt. Binding of basal transcription factor TFIID to the acidic activation domains of VP16 and p53. *Mol. Cell. Biol.* **14(10)**: 7013-7024.

Xin, J., A. Cowie, P. Lachance, and J. Hassell. (1992). Molecular cloning and characterization of PEA3, a new member of the *Ets* oncogene family that is differentially expressed in mouse embryonic cells. *Genes & Dev.* **6**: 481-496.

Yamaguchi, T.P., and J. Rossant. (1995). Fibroblast growth factors in mammalian development. *Curr. Opin. in Gen and Dev.* **5**: 485-491.

Yamaguchi, T.P., K. Harpal, M. Henkmeyer, and J. Rossant. (1994). *fgfr-1* is required for embryonic growth and mesodermal patterning during mouse gastrulation. *Genes & Dev.* **8**: 3032-3044.

Yamaguchi, T.P., R. Conlon, and J. Rossant. (1992). Expression of the fibroblast growth factor receptor FGFR-1/flg during gastrulation and segmentation in the mouse embryo. *Dev. Biol.* **152**: 75-88.

Yamamoto, H., M.L. Flannery, S. Kupriyanov, J. Pearce, S.R. McKercher, G.W. Henkel, R.A. Maki, Z. Werb, and R.G. Oshima. (1998). Defective trophoblast function in mice with a targeted mutation of *Ets-2*. *Genes & Dev.* **12**: 1315-1326.

Yang, B., C.A. Hauser, G. Henkel, M.S. Colman, C. Van Beveren, K.J. Stacey, D.A. Hume, R.A. Maki, and M.C. Ostrowski. (1996). Ras-Mediated Phosphorylation of a

Conserved Residue Enhances the Transactivation Activities of c-Ets-1 and c-Ets-2. *Mol. Cell. Biol.* **16(2)**: 538-547.

Zabel, U., T. Henkel, M. dos Santos Silva, and P.A. Baeuerle. (1993). Nuclear uptake control of NF- κ B by MAD3, an I κ B protein present in the nucleus. *EMBO J.* **12(1)**: 201-211.

Zhu, X., C. Lai, S. Thomas, and S.J. Burden. (1995). Neuregulin receptors, erbB3 and erbB4, are localized at neuromuscular synapses. *EMBO J.* **14(23)**: 5842-5848.

Zonszein, J. (1995). Diagnosis and management of endocrine disorders of erectile dysfunction. *Urol. Clin. of Nor. Am.* **22(4)**: 789-802.